8-AJ

PRESSURE DROP – FLOW RATE CHARACTERISTICS OF A SPHERICAL TYPE BLOWOUT PREVENTER DURING CLOSURE

A Thesis

Submitted to the Graduate Faculty of the
Louisiana State University and
Agricultural and Mechanical College
in partial fulfillment of the
requirements for the degree of
Master of Science

in

The Department of Petroleum Engineering

by
Raymond Scott Doyle
B.S., Louisiana State University, 1979
August, 1981

LIST OF TABLES

LIST OF FIGURES

ABSTRACT

When formation fluid flows into a well bore during drilling operations, the well is said to "kick". To avoid a blowout, rig personnel must watch for warning signs of kicks and quickly shut in the well if a kick occurs.

There are two procedures commonly used to shut in wells. The "hard shut-in" is used to minimize the volume of the kick while the "soft shut-in" is used to reduce the pressure surges caused by closing the blowout preventer. In order to evaluate shut-in procedures and develop improved procedures, a computer model of the transient behavior of the well bore is needed.

Previous researchers have studied water hammer, which is analogous to pressure surges in a well due to shut-in. The magnitude and propagation of the water hammer produced by valve closure is reviewed for a simple pipe network. To obtain an accurate description of complex systems, the basic differential equations of water hammer must be solved using the Method of Characteristics. This study examines the downstream boundary conditions imposed on the well by closure of a spherical blowout preventer.

Using experimental pressure drop - flow rate data for flow of various drilling fluids through a 7/16 in.

spherical blowout preventer, it was determined that flow through the blowout preventer is unrestricted until it is almost completely closed. The initial restriction occurs at different piston positions, (degrees of closure) for different sizes of pipe in the hole. The effects of viscosity were found to be negligible compared to the effects of the varying deformation characteristics of the rubber element.

A series of curves describes the pressure drop - flow rate characteristics of the blowout preventer in terms of a valve coefficient, C_v. This parameter was found to be a function of both piston position and flow rate.

space between the outside of the protective casing and the weak formations above the casing shoe.

Since it is confined to a subsurface stratum, an underground blowout is not immediately as dangerous as a surface blowout. However, this type of blowout is more difficult to control because of the additional complication of lost returns to the fractured formation.

Since a blowout is such a dangerous problem, and since human error is a significant factor in many blowouts, it is only natural that the petroleum industry has invested tremendous amounts of time and effort in the training of rig personnel in blowout prevention procedures in an effort to reduce the chance of human error. There have also been extensive studies within the industry to develop improved well control procedures.

The major thrust of published industry studies on blowout prevention has been in the development of:

1. Improved techniques for abnormal pressure prediction.
2. Improved well control equipment such as blowout preventers and chokes, to provide increased reliability and pressure handling capabilities.
3. Improved procedures for circulating out kicks and killing wells under various conditions.

Probably the most significant advance in well

CHAPTER I

INTRODUCTION

One of the most costly and dangerous problems in the petroleum industry is an oil or gas well blowout. There are basically two types of blowouts, each presenting its own characteristics and problems, as explained below.

A surface blowout is the uncontrolled flow of formation fluid at the surface. It is particularly dangerous in that it presents an immediate threat to the safety of rig personnel. It can also destroy expensive rig equipment, as well as cause considerable damage to the environment. A surface blowout can occur as a result of equipment failure, or because of human error such as failure to recognize the warning signs of a kick.

An underground blowout is the uncontrolled flow of fluid within the wellbore from one formation, usually the most recently penetrated zone, into another weaker, lower-pressured formation. Shallow, weak formations are normally protected by casing and cement to prevent their being subjected to excessive pressure. An underground blowout is often the result of a failure of the cement at the casing shoe, allowing wellbore fluid to leak into the annular

control was the development of the "constant bottom hole pressure method" proposed by O'Brien and Goins[17]. Previously, it was common practice to use the "constant pit level method" for circulating out kicks[3]. The constant pit level method calls for circulating the well such that the rate of flow from the pump into the well is maintained equal to the rate of flow out of the well. Thus, the kick volume remains constant as it moves up the wellbore annulus. For the case of a gas kick, the pressure within the kick remains equal to the initial bottom hole pressure so that as the kick nears the surface the casing seat and the surface blowout preventer equipment are exposed to possibly excessive pressures. The casing seat or adjacent formations could be fractured by this excessive pressure, resulting in an underground blowout, or the surface equipment may fail, resulting in a surface blowout.

The constant bottom hole pressure method of well control, which is most commonly used today, allows the kick fluid to expand as it moves up the wellbore. This reduces the ultimate pressure which a gas kick would exert on any portion of the wellbore as it passes up the hole. At the same time the wellbore pressure adjacent to the formation which supplied the kick fluid is maintained at a value equal to or greater than the formation pressure, thus preventing

the entry of additional formation fluid into the wellbore. This method represents the state of the art for the circulating phase of all well control procedures.

Another very important phase of any well control operation is the early detection of a kick and subsequent shut-in of the well to minimize the volume of formation fluid which enters the well. The shut-in procedure used varies from one operator to the next but there are two basic philosophies within the industry. Both philosophies are based on intuitive explanations of the transient behavior of the well during shut-in.

The "hard shut-in" procedure is followed by many operators in an attempt to minimize the kick volume and is accomplished by simply closing the blowout preventer immediately after shutting the rig pump down and verifying that the well is flowing. The blowout preventer is the ultimate closing mechanism in this procedure.

An alternate procedure, the "soft shut-in," is used by some operators in an attempt to avoid the surge pressures that they believe are created by the sudden closure of a valve or blowout preventer.

The soft shut-in procedure calls for a less abrupt termination of flow to reduce the magnitude of the surges produced. When a kick is taken the HCR

valve and the remote adjustable choke are placed in the open position and then the blowout preventer is closed. After the blowout preventer has been closed, then the choke is slowly closed to achieve a gradual shut-in of the well.

The surge pressure produced by the closure of the blowout preventer could, conceivably, cause the blowout preventer to fail or a down-hole failure such as a fracture at the casing seat. The presence of surge pressures is particularly undesirable in subsea operations since the additional hydrostatic pressure induced by a long vertical choke line and riser from the seafloor to drilling vessel causes a reduction in the mud weight which can be tolerated at any depth within the well. The surges are analogous to the surges created by the water hammer phenomenon characteristic of transient pipeline flow.

One obvious disadvantage of the soft shut-in is the longer time period required to achieve shut-in. This extra time allows more formation fluid to enter the well resulting in a larger initial kick volume. In the case of a gas kick, the ultimate casing pressure encountered in kick circulation is a direct function of the initial volume of the kick as shown in Fig.1.1[13]. Thus the ultimate casing pressure during kick circulation is higher when the soft shut-in procedure is used, possibly high enough to cause fracture of the

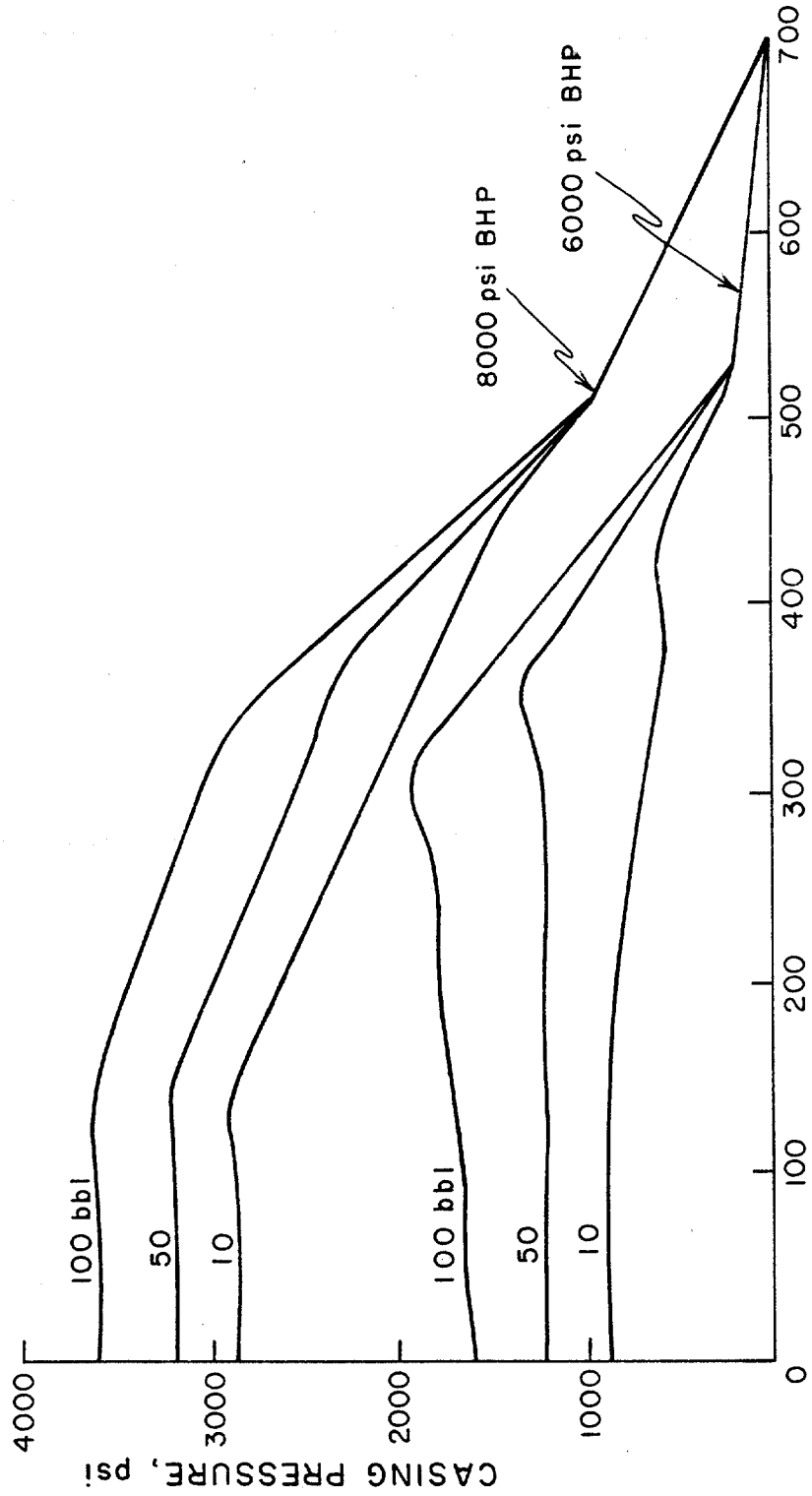

FIGURE 1.1. EFFECT OF INITIAL VOLUME OF GAS KICK ON ULTIMATE CASING PRESSURE. (AFTER McKENZIE[13])

casing seat or surface equipment failure.

It appears that each method of shut-in has its own advantages and disadvantages which could be considered in choosing an optimum shut-in procedure. The hard shut-in, while assuring a minimal influx of formation fluid, can conceivably produce pressure surges which might damage surface equipment or subsurface strata. On the other hand, the soft shut-in theoretically reduces the magnitude of the pressure surges due to shut-in, but at the same time, allows a larger kick volume to enter the well, which could produce higher casing pressures during subsequent operations to circulate the kick from the well.

There is much disagreement within the industry as to which method of well closure is most appropriate. This disagreement is due, in part, to the fact that the surge pressure (water hammer) phenomenon is not well understood, as applied to the well bore. The soft shut-in procedure is based on an intuitive explanation of the transient behavior of the well system during shut-in. Proponents of the soft shut-in argue that the closure of the blowout preventer constitutes a rapid termination of flow, while the choke can be closed at any desired rate. Proponents of the hard shut-in have various reasons for supporting this method. Some feel that the surges produced, if any, are not of a magnitude which would constitute a threat to the

operation, or that although surges may be produced at the surface they are not propagated down-hole and so only the surface equipment needs to resist the surges. Still others argue that a conventional hard shut-in with a bag type annular blowout preventer is, in effect, a soft shut-in due to the time (typically about 20 - 30 seconds) that is required for the preventer to be hydraulically activated by the accumulator and effect a complete closure.

As was mentioned previously, the arguments frequently heard supporting either method of well closure are based primarily on intuition. The author is unaware of any published research, either experimental or theoretical, on the transient behavior of the well system during shut-in. Considering the importance of the initial shut-in phase in any well control procedure used, it seems that an investigation of shut-in procedures is long overdue. The study presented here is one phase of an extensive research program, funded in part by the United States Geological Survey, to develop improved procedures for blowout prevention in deep-water drilling operations.

In order to evaluate present and alternative procedures for well shut-in, an accurate mathematical model of the well system and its behavior during shut-in is needed. This study represents one phase in the development of such a model. Specifically,

it is an examination of the pressure losses occuring during steady-state flow through a spherical-type, annular blowout preventer at various degrees of closure. Three types of fluids were examined to determine the effects of viscosity and four pipe sizes were used to examine the effects of annular geometry on the closing characteristics of the blowout preventer.

The blowout preventer prescribes the downstream boundary condition of a well system during a hard shut-in. The pressure drop - flow rate characteristics of drilling chokes, which prescribe the boundary condition for a soft shut-in, is being investigated in yet another phase of the overall well control research project. These closing characteristics can ultimately be incorporated into the mathematical model of the well system. The evaluation of shut-in procedures using the model could then include the effects of the response time of the control equipment, along with the reaction time of the rig crew, to give more realistic results.

CHAPTER II

LITERATURE REVIEW

The success of any well control operation depends heavily on the early detection of a kick and subsequent shut-in of the well. These factors assure that the volume of the kick taken will be minimized. McKenzie[13] has shown that, for a gas kick, the ultimate casing pressure encountered during the well control operation is directly proportional to the initial volume of the kick, (See Figure 1.1). This is especially important in deep water drilling since the long underwater riser and choke lines exert additional hydrostatic pressure on the annulus. Consider for example a rig drilling in 4000 ft of water with 3000 ft of casing set through the sediments below the sea floor. The hydrostatic pressure at the casing seat would be that created by a 7000 ft column of mud in the annulus. For the same casing setting depth on a land rig operation, the casing seat pressure would be that of only a 3000 ft column of mud. The additional hydrostatic pressure in the deep water operation effectively lowers the tolerance of subsea formations to additional pressures that would accompany a well kick. In other words, formation fracture or on-bottom equipment failure can occur at much lower surface annular pressures than those that would be considered dangerous on a land operation.

Many operators use a "hard shut-in" procedure in an effort to minimize the volume of the kick taken.[11] When the warning signs of a kick are noticed, the driller first picks up the kelly to clear the bit from the bottom of the hole. The pump is then shut down and the well is checked for flow. If the well is flowing, then the annular blowout preventer is closed. Since the remote operated choke line valve (HCR valve) is kept closed during drilling, closing the blowout preventer achieves shut-in of the well. The HCR valve is then opened and the shut-in drill pipe and casing pressures are recorded. Before opening the HCR valve the remote operated choke must be checked to be sure it is in the closed position. Otherwise, additional flow into the wellbore will occur.

Opponents of the hard shut-in procedure argue that the sudden deceleration of the fluid in the annulus during rapid shut-in produces a high-pressure shock wave which can fail surface BOP equipment or fracture the formations below the casing seat. The situation is even more complicated for deepwater drilling due to the reduced tolerances of the formations to additional pressures. From an operators standpoint, it is also conceivably possible that once the well is shut in, the HCR valve could be difficult or impossible to open due to the differential pressure across the valve. In this case the choke line would have to be pressured

up in order to open the valve. Finally, some operators argue that when the valve is opened with a large differential pressure across it, the choke manifold could experience a large pressure surge, especially if the choke manifold were filled with air as is sometimes the case in artic drilling operations.

An alternative way to close in a well is the so-called "soft shut-in" procedure. Once flow from the well has been verified the HCR valve is opened, the remote adjustable choke is checked to make sure it is open and the annular blowout preventer is closed. Once the blowout preventer has sealed, then the choke is slowly closed to achieve shut-in. The shut-in drill pipe and casing pressures are then recorded.

The most obvious disadvantage of the soft shut-in is the additional time needed to achieve closure. This allows a larger kick to be taken which results in a higher ultimate casing pressure. Figure 2.1 compares the theoretical casing pressure profiles which might result from either a hard shut-in or a soft shut-in. Notice the sharp pressure peak at well closure for the hard shut-in (point 3), but also notice the higher ultimate pressure during circulation for the soft shut-in (points 4 through 8). Operators who use the hard shut-in may be more concerned with the ultimate casing pressure as the gas nears the surface than with the surge pressures which may be produced when closing

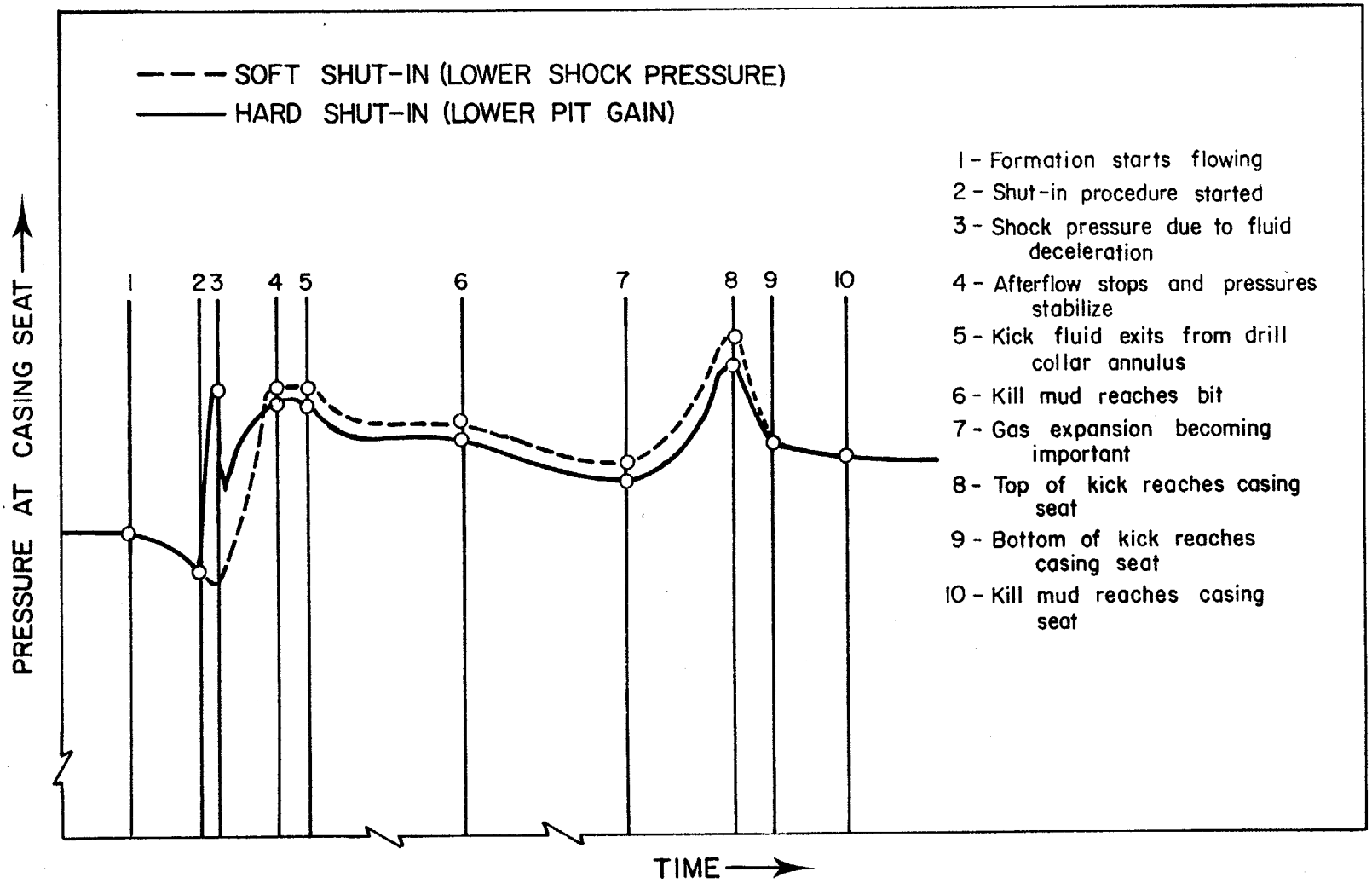

FIGURE 2.1. POSSIBLE PRESSURE PEAKS AT CASING SEAT DURING WELL CONTROL OPERATIONS. (AFTER BOURGOYNE[5])

the blowout preventer. Proponents of the soft shut-in, on the other hand, feel just the opposite about the significance of the two pressure peaks.[5]

There is much disagreement among drilling engineers over which shut-in procedure is most appropriate. The issue is clouded by a lack of any actual data concerned with the magnitude and propagation characteristics of surge pressures produced by well closure. While the problem has not been addressed in the petroleum literature, the basic phenomenon, water hammer, has been extensively researched for applications in the design of water works and pipe lines. A review of the literature dealing with water hammer is presented below to provide a better understanding of this phenomenon, since any attempt at mathematical simulation of well behavior during the shut-in phase would require such a basic understanding.

2.1 Fundamentals of Water Hammer

Water hammer refers to the pressure surge which occurs in a pipe carrying a flowing liquid when a valve is abruptly closed. This is the phenomenon which causes water pipes to rattle when a kitchen faucet is shut off quickly. It occurs in large industrial pipe lines and, depending on the magnitude of the pressure surges, can present rather difficult design problems. In recent years, much attention

has been given to the postulated double-ended line rupture problem in feedwater lines in nuclear power plants. Damaging surge pressure (water hammer) can result from the rapid closure of conventional check-valves in such a line.

The magnitude of this surge pressure is a function of the change in velocity of the flowing fluid. Valves designed to stop the flow of fluids very quickly, for instance subsurface safety valves installed in oil and gas wells, must be able to withstand the water hammer effects that such a closure will induce.

Analytical studies in the area of water hammer during the last century are quite extensive. Many of the ideas and equations developed in these works are quite helpful in analyzing the behavior of a well during shut-in operations.

2.1.1 The Mechanism of Water Hammer

Virtually every published reference concerning water hammer [7, 12, 18, 20, 22, 23, 24] provides a brief description of the sequence of events which produces the water hammer effect when a valve in a pipe line is abruptly closed. Basically, the phenomenon is a series of cyclic loadings in which the kinetic energy of the system is converted into potential energy and then reconverted to kinetic energy through four mechanical processes, illustrated in Figures 2.2 through 2.5.

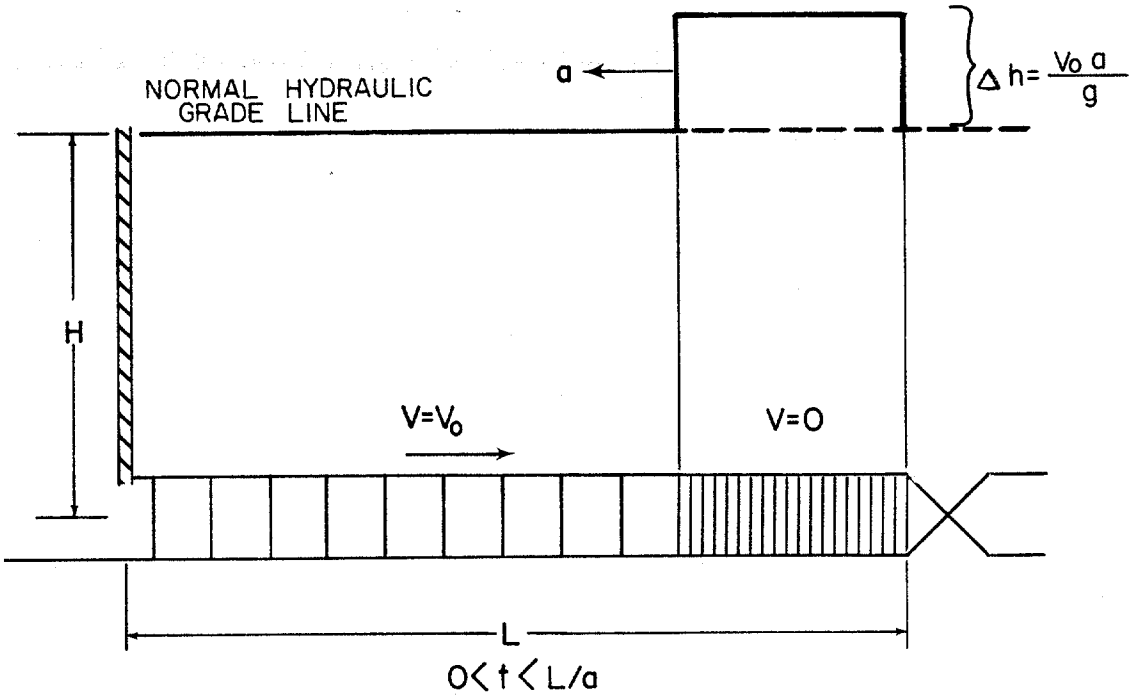

(a)

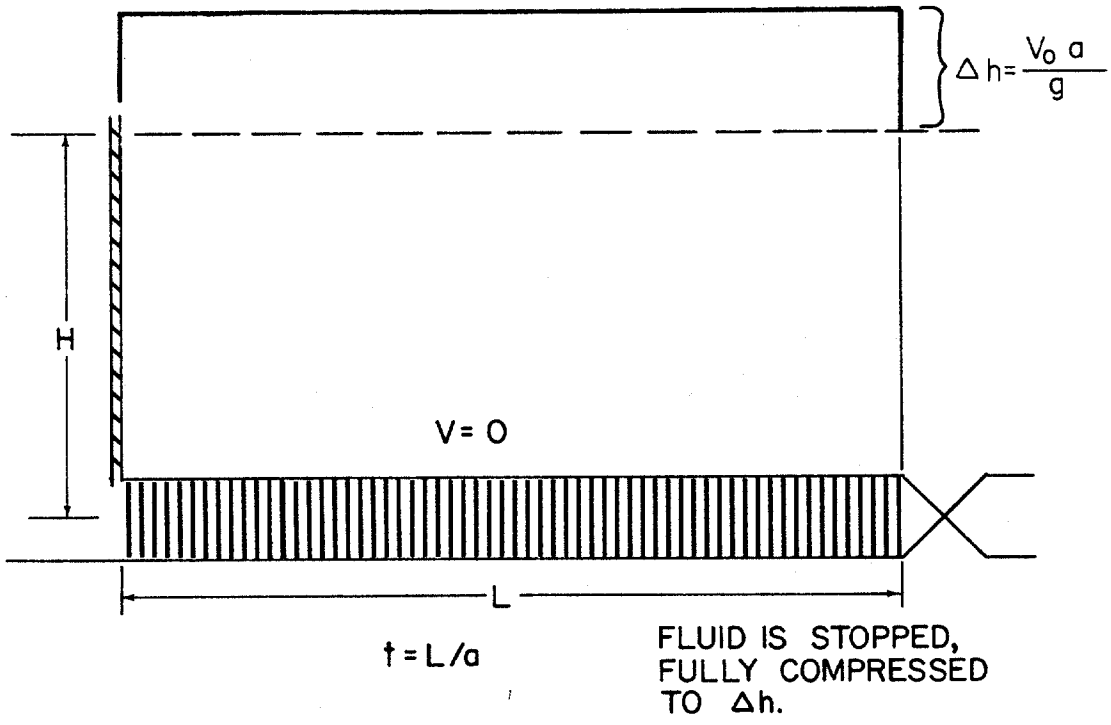

(b)

FIGURE 2.2. TRANSIENT RESPONSE OF FRICTIONLESS PIPE AT TIME, t, AFTER INSTANTANEOUS VALVE CLOSURE.

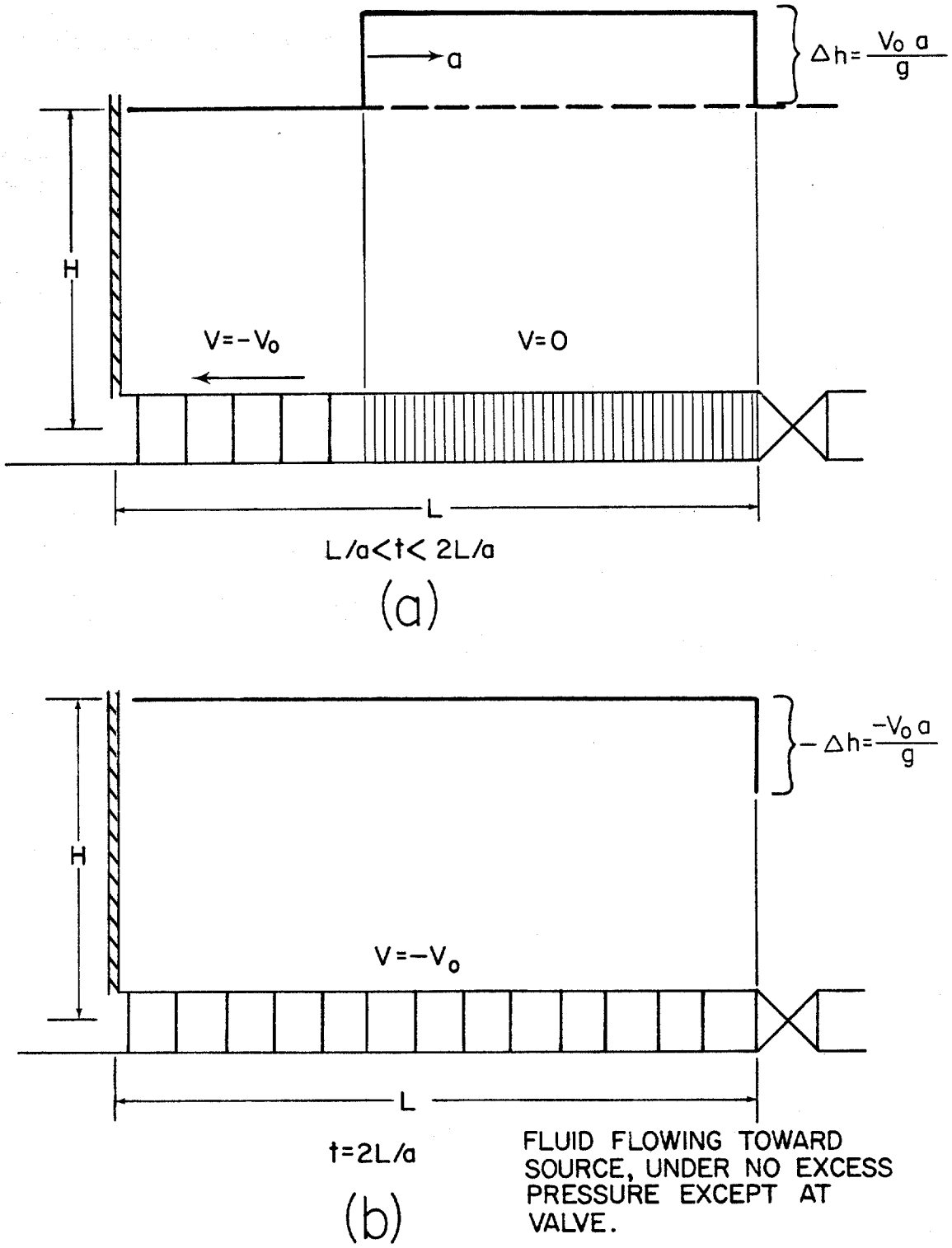

FIGURE 2.3. TRANSIENT RESPONSE OF FRICTIONLESS PIPE AT TIME, t, AFTER INSTANTANEOUS VALVE CLOSURE.

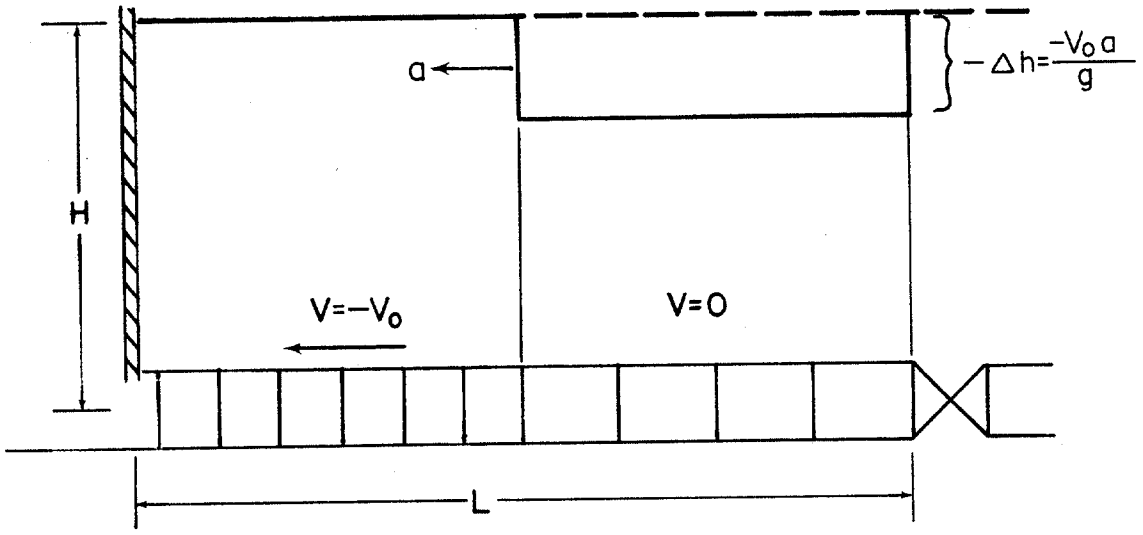

$2L/a < t < 3L/a$

(a)

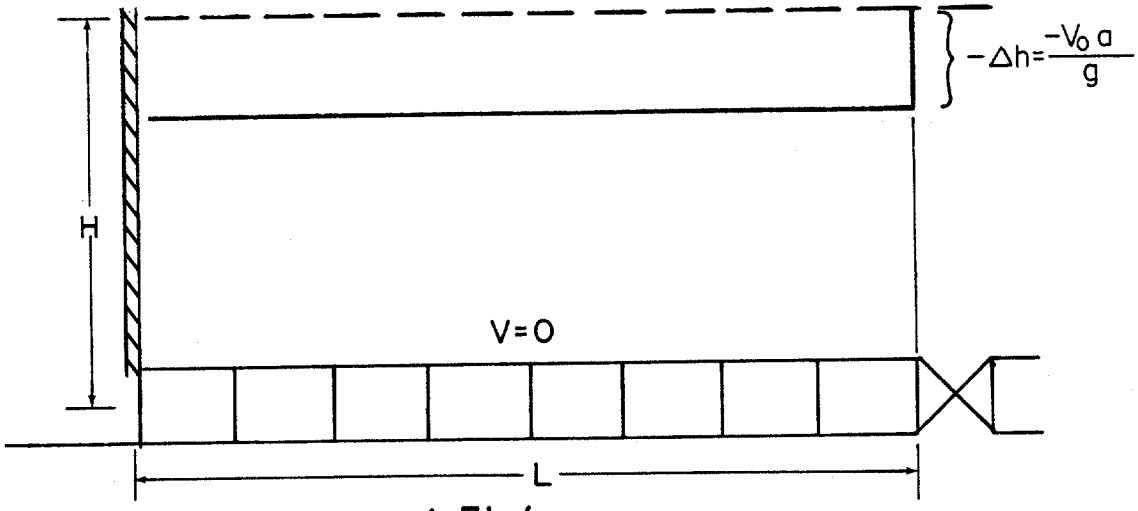

$t=3L/a$

FLUID AT REST, MAXIMUM EXPANSION OF FLUID.

(b)

FIGURE 2.4. TRANSIENT RESPONSE OF FRICTIONLESS PIPE AT TIME, t, AFTER INSTANTANEOUS VALVE CLOSURE.

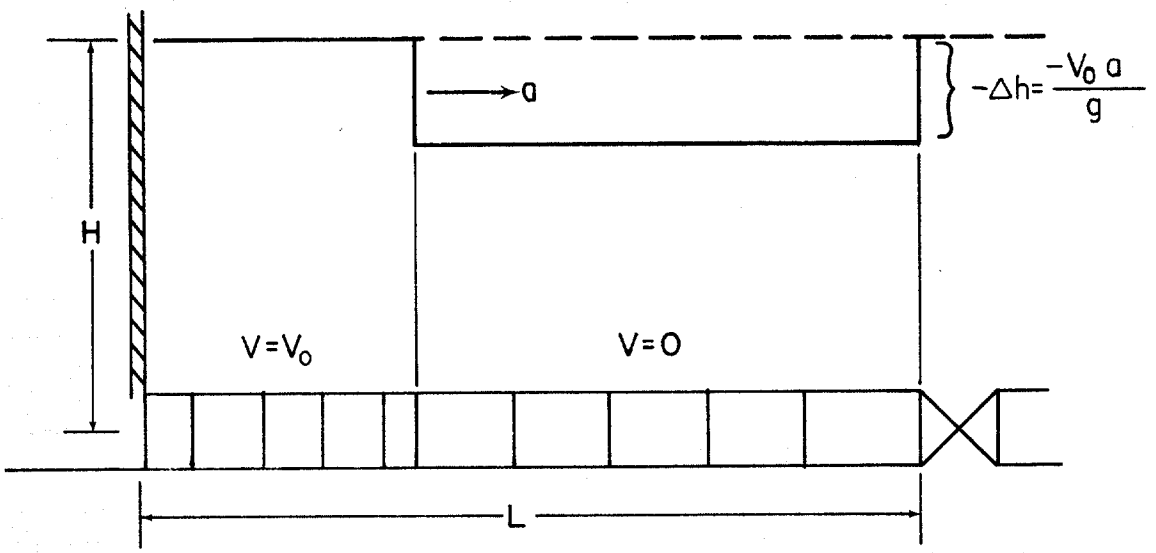

$3L/a < t < 4L/a$

(a)

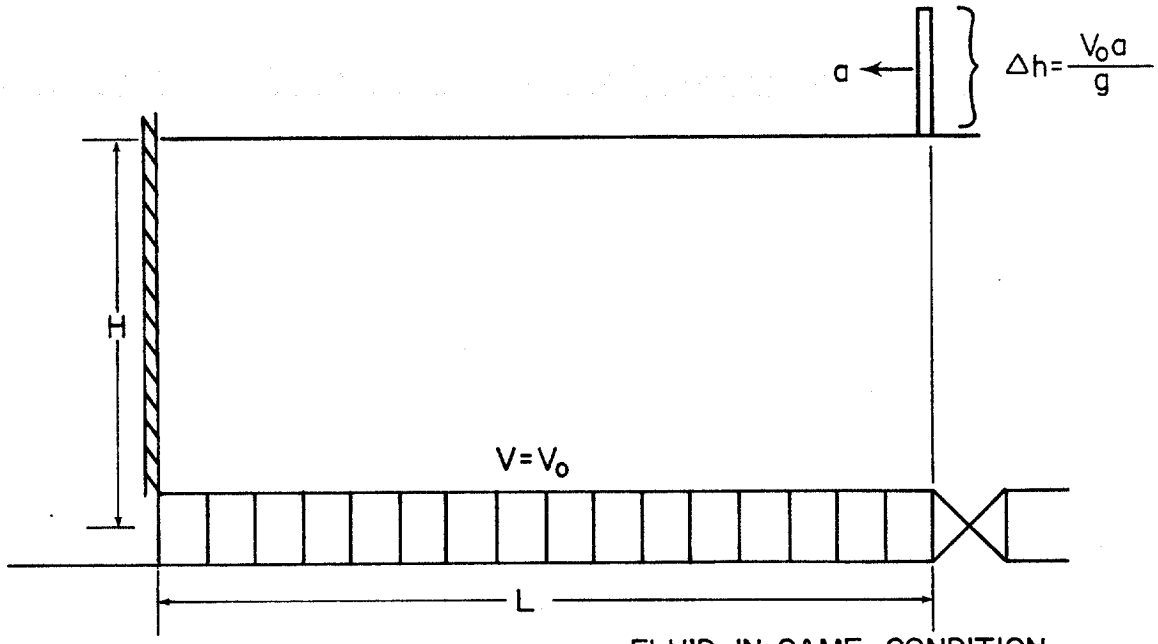

$t = 4L/a$

FLUID IN SAME CONDITION AS FOR TIME 0. SEQUENCE BEGINS AGAIN

(b)

FIGURE 2.5. TRANSIENT RESPONSE OF FRICTIONLESS PIPE AT TIME, t, AFTER INSTANTANEOUS VALVE CLOSURE.

The description below assumes instantaneous closure of the valve at the downstream end of a frictionless system. This idealized case of water hammer provides the clearest explanation of the basic mechanisms involved. The water in the pipe of Figure 2.2a is originally flowing under steady state conditions with velocity $V = V_o$. The valve at the downstream end of the system is closed instantaneously at time $t = 0$. The water in most of the pipe continues to flow at velocity, V_o. However, the lamina of water nearest the valve is compressed and the wall of the pipe is stretched. The kinetic energy of the water in this lamina is converted to potential energy as the velocity of the lamina drops to zero and the hydraulic head (pressure) within the lamina increases by a value Δh. Each lamina in turn undergoes the same energy conversion process as the pressure wave moves toward the origin at the velocity of propagation, a, (Figure 2.2a). At time $t = L/a$ the pressure wave has reached the upstream end of the system as shown in Figure 2.2b. The entire water column is now at rest but is under an excess pressure, Δh.

In Figure 2.3a the water in the pipe has begun to flow back into the reservoir at velocity $V = -V_o$ due to the pressure difference between the pipe and the reservoir. The pressure in the system drops to the normal, static value as the rarefactive wave travels

toward the valve at velocity a. Successive laminae of water expand and the pipe walls relax, beginning at the reservoir. Figure 2.3b shows the system at time t = 2L/a. The unloading wave has now reached the valve and the pressure throughout the pipe is the normal static pressure. However, since the valve is closed, the flow at velocity $V = -V_o$ cannot be maintained.

The fluid near the valve expands beyond its normal volume as it continues to flow away from the valve, inducing a pressure drop at the valve which is as far below the static pressure as the initial pressure rise was above it. This negative pressure drop now travels as a wave toward the source as successive layers of water expand and are brought to a halt (Figure 2.4a). At time t = 3L/a, in Figure 2.4b, all the water in the pipeline is at rest but the pressure level in the pipe is below the pressure in the reservoir by $-\Delta h$ feet of hydraulic head.

As seen from Figure 2.5a, the pressure differential between the pipe and the reservoir induces flow of water in the positive sense at a velocity $V = V_o$. The pressure returns to the normal static level again as the unloading wave travels with velocity, a, toward the valve. At time t = 4L/a, (Figure 2.5b), the velocity of the water is $V = V_o$ everywhere in the pipe and the pressure is also at the normal level throughout the pipe. The conditions in the pipe are now the same as

at the moment of closure. The entire cycle will continue until friction, which has been neglected up to this point, reduces the pressure vibrations to zero and the fluid in the pipe comes to rest.

The same type of analysis used for the case of instantaneous closure can also be used to examine cases of water hammer due to the closure of a valve in a finite element of time. For less than instantaneous closure, the closure is treated as a series of instantaneous partial closures and the effects of each partial closure are superimposed to obtain the net effect of the total closure. Joukovsky[12] was one of the first to recognize this method of analysis.

2.1.2 Velocity of Propagation and the Magnitude of the Water Hammer

As previously shown, the pressure surge created as the result of valve closure is propagated as a wave through the system. In 1898, Joukovsky[12] developed an accurate equation for calculating the velocity of propagation, a, which he later verified experimentally using long runs of various diameter pipes. The same basic formula was also derived independently by Allievi[1] in 1902. The equation, written in a more modern form, for the velocity of propagation is:

$$a = \frac{\sqrt{g_c(K/\rho_o)}}{\sqrt{1+(K/E)(D/t')}} \quad \ldots\ldots\ldots\ldots\ldots\ldots \quad (2.1)$$

where a = velocity of propagation, ft/sec

k = Bulk modulus of elasticity of fluid, lb/ft^2

E = Young's modulus of elasticity of pipe material, lb/ft^2

ρ_o = fluid density, lbm/ft^3

t' = wall thickness of pipe, ft

g_c = 32.17 lbm · ft/lbm · sec^2

The above equation agrees with that previously developed by Korteveg[12] for the velocity of sound in an elastic pipe filled with a compressible liquid. This would be expected since both water hammer and sound are special cases of pressure waves being propagated through a medium.

Joukousky[12] also pointed out that the velocity of propagation is independent of pressure intensity and the length of the system. Rather, the velocity of propagation is a function of only the compressibility of the fluid (which is the reciprocal of bulk modulus of elasticity) and the elasticity of the conduit.

More recent authors[18, 24] include a dimensionless constant C_1 in the previous equation for the velocity of propagation:

$$a = \frac{\sqrt{g_c(K/\rho_o)}}{\sqrt{1+(K/E)(D/t')c_1}} \quad \ldots\ldots\ldots\ldots\ldots \quad (2.2)$$

The coefficient, C_1, is calculated using the equations given by Streeter and Wylie[24] to accomodate

various assumptions made in developing the continuity equation for the system. The stress distribution is different in thick-walled vessels than in thin-walled vessels. Therefore, the value of C_1 is partly determined by the relative thickness of the pipe walls, (D/t'). The force balance on the pipe is also affected by the restraining forces which oppose pipe movement, so C_1 is also controlled by type of anchoring system used and by the presence or absence of expansion joints. Streeter and Wylie also give values for C_1 for the special cases of circular tunnels and lined tunnels, which might be used in analyzing cased and uncased boreholes.

Joukovsky was apparently the first to develop an analytical expression for the maximum pressure rise caused by instantaneous valve closure in a simple pipe system. The rigorous mathematical development of his equation is quite complicated. However, in 1933, Moody[14] proposed a simplified development of the same equation for water hammer in a single, uniform pipe.

Joukousk's experimental work, originally commissioned to determine the maximum safe velocity for use in the new Moscow water works, verified his equation. The equation is given by:

$$P = \frac{V_o \, a \, \rho_o}{g_c} \quad . . . . . \quad (2.3)$$

where P = pressure rise due to valve closure, lbf/ft^2

V_o = velocity of fluid prior to valve closure, ft/sec

a = velocity of propagation, ft/sec

ρ_o = density of flowing fluid, lbm/ft^3

g_c = 32.174 $(lbm \cdot ft)/(lbf \cdot sec^2)$

In terms of feet of hydraulic head we have:

$$h = \frac{V_o \, a}{g} \qquad (2.4)$$

where h = hydraulic head increase due to valve closure, ft

V_o = velocity of fluid prior to valve closure, ft/sec

a = velocity of propagation, ft/sec

g = local acceleration of gravity, ft/sec^2

Equations (2.3) and (2.4) are also applicable to the partial closure of a valve, resulting in a change in the velocity of the fluid and producing a pressure rise. For partial closure we have:

$$\Delta P = \frac{\Delta V \, a \, \rho_o}{g_c} \qquad (2.5)$$

or

$$\Delta h = \frac{\Delta V \, a}{g} \qquad (2.6)$$

As previously mentioned, the non-instantaneous

closure of a valve can be represented as a series of instantaneous partial closures. The pressure rise due to each partial closure is then calculated using Equation (2.5) or (2.6) and the total pressure rise is calculated using superposition. In using this method of analysis, the effects of rarefactive waves reflected from the reservoir end of the pipe must be included in the calculation of the total pressure change. The extent that reflected waves affect the total pressure rise produced by valve closure is determined by the time of closure, t_c, for the valve.

2.1.3 Effect of Speed of Valve Closure on the Water Hammer

Valve closure in the real world can never be instantaneous, but is achieved over a finite length of time called time of closure, t_c. In water hammer analysis there are two cases of closure time which are usually considered. "Rapid closure" refers to closure for which $t_c < 2L/a$ while "slow closure" refers to closure where $t_c > 2L/a$. This critical time, $t_c = 2L/a$, is the time required for a pressure wave to travel from the valve to the source of flow and then return to the valve as a rarefactive wave.

Joukovsky concluded from his work that if the valve were closed completely in a time interval less than $2L/a$, then all or part of the pipe would experience a

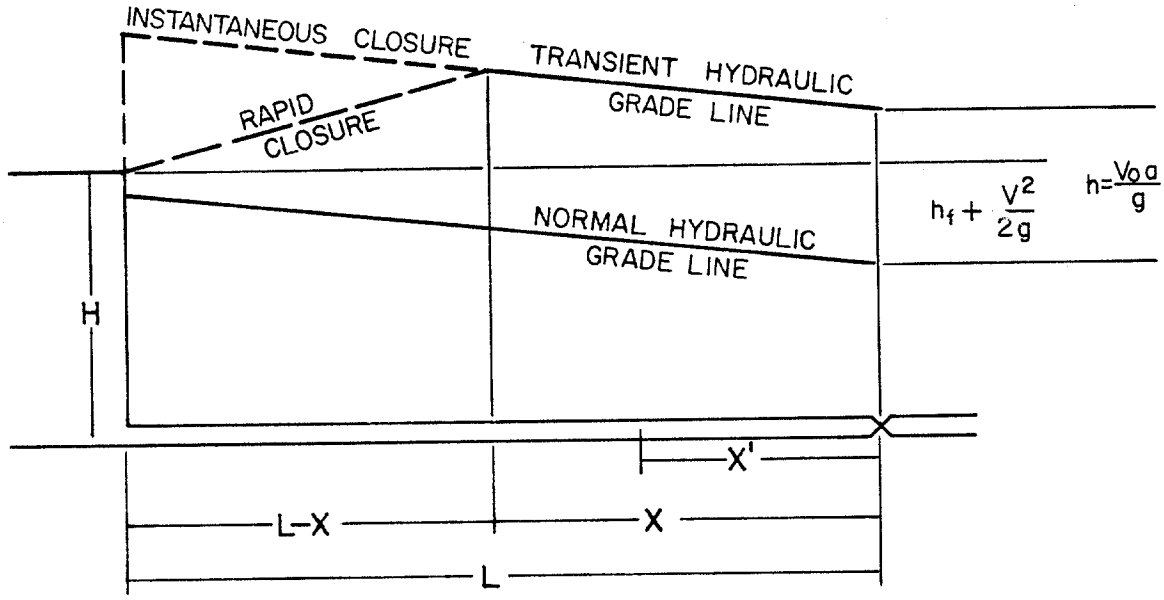

FIGURE 2.6. MAXIMUM PRESSURE PEAK PROFILE FOR INSTANTANEOUS CLOSURE AND RAPID CLOSURE. (AFTER DAUGHERTY AND INGERSOLL[4])

pressure increase the same as that for instantaneous closure, as given by Equation (2.3).

Consider, for example, the comparison of the maximum pressure peaks along the pipe for instantaneous closure and rapid closure shown in Figure 2.6. Friction is included in the normal grade line for the pipe, but it is assumed that it has no effect on the magnitude of the pressure surge caused by water hammer. For instantaneous closure the maximum pressure peak extends along the entire system from the valve to the reservoir. However, for the case of rapid closure, the maximum pressure peak extends from the valve to a distance x. Upstream of this point, the pressure surge decreases uniformly from the maximum valve at x to zero at the reservoir.

Streeter[22] gives Equation 2.7 below for calculating the length of pipe, x, which is exposed to the full pressure increase, as shown in Figure 2.6.

$$x = L - \frac{a\, t_c}{2} \quad \ldots\ldots\ldots\ldots\ldots \quad (2.7)$$

where x = length of pipe exposed to full pressure peak, ft

L = total length of pipe, ft

a = velocity of propagation, ft/sec

t_c = time of closure, sec

The time of duration of the maximum pressure surge

is also affected by the speed of closure. For any point, x', in the region of full pressure rise of Figure 2.6, the maximum pressure surge lasts only for a time equal to the difference between the closing time of the valve and the time for the pressure wave to travel from x' to the reservoir and be reflected back to x'. Equation 2.8 below can be used to calculate the time of duration.

$$t_d = \frac{2\ (L - x')}{a} - t_c \quad \ldots\ldots\ldots\ldots\ (2.8)$$

where t_d = time of duration of maximum pressure peak at x', sec

t_c = time of closure, sec

L = total length of pipe, ft

x' = distance from valve to point of interest, ft

a = velocity of propagation, ft/sec

For the special case where the time of closure, t_c, is 2L/c, Equation (2.7) gives x = 0. This means that the pressure peak attains the maximum possible value only at the valve, and that the pressure peak falls uniformly from this value at x = 0 to zero at the reservoir. Also, Equation (2.8) gives the time of duration of the maximum pressure peak at the valve, $t_d = 0$. The pressure at the valve begins to fall as soon as the maximum peak is reached.

To summarize the effects of rapid closure, where $0 < t_c < 2L/c$, two points should be made. First, the maximum pressure peak for all or part of the pipe is equal to the maximum peak for instantaneous closure. The length of pipe which is exposed to the maximum pressure peak depends on the total length of the system and on the time required to close the valve. Secondly, the time of duration of this pressure peak is not as long as for instantaneous closure and is also a function of the time of closure.

The effect of closure of the valve in times greater than $2L/a$ is to reduce the magnitude of the maximum pressure peak produced in the system. This is due to the fact that for $t_c > 2L/c$, the pressure waves produced by the initial action of the valve have time to reach the source and be reflected as rarefactive waves back to the valve before closure has been completed.[7] Assuming that the closure of the valve is linear, these rarefactive waves prevent the pressure from increasing further due to subsequent valve movement. The maximum pressure peak occurs at the valve and is somewhat less than the maximum pressure peak for the case of instantaneous closure. The pressure rise along the pipe decreases uniformly from the value at the valve to zero at the reservoir.

2.1.4 Effect of Branching Pipes and Changing Pipe Geometries on the Water Hammer

Complexities in the pipe network, such as a change in the pipe diameter, have significant effects on the water hammer propagation through a given system. These effects have been examined by various authors and will be discussed below.

Branching pipes and their effects on water hammer were studied by Joukousky.[12] He examined both open-ended and closed-ended branch pipes. He found that the pressure intensity within a branching pipe was doubled as the pressure wave reflects undiminished from the dead-end of the pipe. This behavior is also explained by Parmakian.[18] Joukousky goes on to conclude that the pressure in the main pipe, while not doubled, is increased by the reflected pressure wave in the branch pipe.

The case of an open-ended or discharging branch pipe shows quite a different effect on the water hammer pressure wave. As the pressure wave reaches the discharge of the branch pipe it is reflected as it would be from a reservoir at atmospheric pressure. A rarefactive wave is reflected and the pressure rise in the branch pipe is diminished rather than doubled. The overall effect of a discharging branch pipe is to lower the intensity of the pressure wave in the main

pipe.

Various authors [8, 18, 20] have treated also the problem of changes in cross sectional area. However, Parmakian[18] gives the simplest explanation of the effects of changes in pipe geometry or material on the water hammer. When the pressure wave encounters a change in pipe diameter from D_1 to D_2, the velocity of the wave is changed from a_1 to a_2 as predicted by Equation (2.1). Likewise the intensity of the pressure rise is also altered in the new section of pipe in accordance with Equation (2.3). The pressure wave is also partly reflected back toward the valve. According to Equation (2.1) the velocity of propagation is a function not only of pipe diameter, D, but also wall thickness, t', and shear modulus, E.

Therefore, similar behavior to that explained above should be expected for changes in pipe wall thickness and/or pipe material.

2.2 Methods of Analysis for Water Hammer

Streeter[24] presents a review of the various methods which have been used to analyze water hammer. Each method is based on an equation of motion and some particular form of the continuity equation, and is limited by the restrictive assumptions inherent in its development. Two of these methods of analysis are discussed below.

2.2.1 Arithmetic Integration Method

The Arithmetic Integration Method[18, 20, 22, 24] of analysis was discussed briefly in a previous section. Its primary application is in the analysis of water hammer in cases of gradual valve closure.

The closure of a valve is represented as a series of instantaneous partial closures. The water hammer due to each of these partial closures is computed using Equation (2.5) and total water hammer at any time, t, is taken to be the sum of all direct and reflected pressure waves up to that time.

Streeter[22], treats the valve as an orifice with variable area A_v, giving the equation below:

$$V \cdot A = C_d \cdot A_v \sqrt{2 \cdot g \cdot h} \quad \ldots\ldots\ldots\ldots \quad (2.9)$$

where V = velocity of fluid, ft/sec

A = cross-sectional area of pipe, ft^2

C_d = valve coefficient

A_v = area of orifice, ft

h = pressure head loss across the valve, ft

Just prior to closure, Equation (2.9) becomes:

$$V_o \cdot A = C_d \cdot A_{vo} \sqrt{2 \cdot g \cdot h_o} \quad \ldots\ldots\ldots\ldots \quad (2.10)$$

The velocity at any time is a function of the area of the orifice. In dimensionless terms, Streeter's equa- is written:

$$\frac{V}{V_o} = \frac{A_v}{A_{vo}} \sqrt{\frac{h}{h_o}} \quad \ldots\ldots\ldots\ldots\ldots \quad (2.11a)$$

or

$$\frac{V}{V_o} = \tau \sqrt{\frac{h}{h_o}} \quad \ldots\ldots\ldots\ldots\ldots \quad (2.11b)$$

where τ = dimensionless orifice area, A_v/A_{vo}

If the closure of the valve is represented as a series of partial closures we have, after one partial closure:

$$\frac{V - \Delta V_{t1}}{V_o} = \tau_{t1} \cdot \sqrt{\frac{h + h_{t1}}{h_o}} \quad \ldots\ldots\ldots \quad (2.12)$$

Equation (2.6) can be written in dimensionless terms as:

$$\frac{\Delta h}{h_o} = \frac{a\ v_o}{g\ h_o} \cdot \frac{\Delta V}{V_o} \quad \ldots\ldots\ldots\ldots\ldots \quad (2.13)$$

Equations (2.12) and (2.13) can be solved simultaneously for the conditions at the vlave at t_1 to obtain $\Delta h/h_o$ and $\Delta V/V_o$. Then the values of h and V are updated and Equations (2.12) and (2.13) are solved again for $\Delta h/h_o$ and $\Delta V/V_o$. An example problem presented by Streeter[22] is included below to illustrate the use of the analysis method.

Example 2.1

A 60 - inch diameter steel pipeline, 1.0 - in thick and 3730 ft long flows water at V_o = 2 ft/sec.

The valve at the downstream end has a head, h_o, of 200 ft across it prior to closure. The valve as a function of time is defined below:

t/t_c	0	0.2	0.4	0.6	0.8	1.0
$\tau = A_v/A_{vo}$	1.0	0.85	0.60	0.35	0.10	0.0

Calculate the pressure at the valve after 4 seconds for $t_c = 2.0$ sec.

The speed, a, of propagation is calculated using Equation (2.1):

$$a = \frac{\sqrt{\frac{32.17 \times (3 \times 10^5) \times 144}{62.4}}}{\sqrt{1 + \frac{3 \times 10^5 \times 60}{3 \times 10^7 \times 1}}} = 3730 \text{ ft/sec}$$

The time for each wave to be reflected back to the valve is:

$$\frac{2L}{a} = \frac{2 \times 3730}{3730} = 2 \text{ seconds}$$

Equation (2.13) is now written:

$$\frac{\Delta h}{h_o} = \frac{3730 \times 2}{32.17 \times 200} \cdot \frac{\Delta V}{V_o} = 1.16 \frac{\Delta V}{V_o}$$

Now for $t/t_c = 0.2$, Equation (2.12) gives:

$$1 - \frac{\Delta V}{V_o} = 0.85 \cdot \sqrt{1 + \frac{\Delta h}{h_o}}$$

Solving the two equations above we obtain $\Delta h/h_o = 0.12$

and $\Delta V/V_o = 0.101$. Using these values, $h/h_o = 1.12$ and $V/V_o = 0.899$ are computed, and the table of values presented below is updated.

For $t/t_c = 0.40$, Equation (2.12) gives:

$$0.899 - \frac{\Delta V}{V_o} = 0.60 \sqrt{1.12 + \frac{\Delta h}{h_o}}$$

which leads to $\Delta h/h_o = 0.23$ and $\Delta V/V_o = 0.202$. The calculations are repeated, as shown above, until $t/t_c = 1.0$. For $t/t_c = 1$, Equation (2.12) gives $\Delta V/V_o = 0.141$ and $\Delta h/h_o$ is found to be 0.16. At time $t/t_c = 1.2$, the initial pressure wave created at $t/t_c = 0.2$ has reached the valve as a reflected wave, producing a negative $\Delta h/h_o$ of twice the magnitude of the original pressure wave. So at $t/t_c = 1.2$, $\Delta h/h_o = -0.23$. Similarly, at $t/t_c = 1.4$, $\Delta h/h_o = -0.47$, since at t/t_c, the value of $\Delta h/h_o$ is 0.234. The reflected waves continue to arrive at the valve and reducing the head until $t/t_c = 2.0$ and $h/h_o = -0.32$. The results of the computations are shown in Table 2.1.[22]

It is evident from the above example problem that the calculations involved in the arithmetic integration method of water hammer analysis can be quite lengthy and tedious. The process becomes more complicated for slow closure of a valve or for analysis of points in the system other than at the valve. Also, the equations used in the analysis assume a frictionless,

t	$\frac{t}{t_c}$	$\frac{A_v}{A_{vo}}$	$\frac{\Delta V}{V_o}$	$\frac{\Delta h}{h_o}$	$\frac{V}{V_o}$	$\frac{h}{h_o}$	p,psi
0.0	0.0	1.00	.....	.....	1.00	1.00	87
0.4	0.2	0.85	0.101	0.12	0.899	1.12	97
0.8	0.4	0.60	0.202	0.23	0.697	1.35	118
1.2	0.6	0.35	0.249	0.29	0.448	1.64	143
1.6	0.8	0.10	0.307	0.36	0.141	2.00	174
2.0	1.0	0.00	0.141	0.16	0.00	2.16	188
2.4	1.2	0.00	.....	-0.23	0.00	1.93	168
2.8	1.4	0.00	.....	-0.47	0.00	1.46	127
3.2	1.6	0.00	.....	-0.58	0.00	0.88	77
3.6	1.8	0.00	.....	-0.72	0.00	0.16	14
4.0	2.0	0.00	.....	-0.32	0.00	-0.16	-14

Table 2.1 Results of Example 2.1
(After Streeter[22])

horizontal system, although corrections can be made to account for frictional losses in the system.

2.2.2 Method of Characteristics

The Method of Characteristics[23, 24] is presently the most practical method of analysis for water hammer. The assumptions made in developing this method are minimal, making it applicable to a large range of problems. The two partial differential equations of motion and continuity are converted to four total differential equations which can be solved using finite -

difference techniques using the digital computer.

Parmakian[18] presents a development of the differential equations governing water hammer. However, his development assumes that both frictional losses and velocity head are negligible. The continuity equation presented by Parmakian is:

$$\frac{a^2}{g} = \frac{\delta V}{\delta x} + \frac{\delta H}{\delta t} = 0 \quad \ldots\ldots\ldots\ldots \quad (2.14)$$

where a = velocity of propagation, ft/sec

V = velocity, ft/sec

H = hydraulic head, ft

t = time, sec

x = distance from reservoir, ft

g = acceleration of gravity, ft/sec^2

The equation of dynamic equilibrium, (motion) is written:

$$\frac{1}{g}\frac{\delta V}{\delta t} + \frac{\delta H}{\delta x} = 0 \quad \ldots\ldots\ldots\ldots \quad (2.15)$$

where V = velocity, ft/sec

H = hydraulic head, ft

t = time, sec

x = distance from reservoir, ft

g = acceleration of gravity, ft/sec^2

In Streeter's[23, 24] development of the continuity and motion equations, frictional losses and velocity

head are included. These terms, which were previously neglected in order to allow solution of the differential equations, can be included in the method of characteristics and thus provide improved accuracy in the results obtained. The equation of continuity,[23,24] including friction and velocity head, is:

$$L_1 = \frac{a^2}{g} \cdot \frac{\delta V}{\delta x} + V \frac{\delta H}{\delta x} + \frac{\delta H}{\delta t} + V \sin\theta = 0 \quad . \quad . \quad . \quad (2.16)$$

where a = velocity of propagation, ft/sec

g = acceleration of gravity, ft/sec^2

V = velocity, ft/sec

H = hydraulic head, ft

x = distance from reservoir, ft

t = time, sec

θ = angle of inclination of pipe, degrees

The equation of motion, L_2 including friction and velocity head, is given by:

$$L_2 = g \frac{\delta H}{\delta x} + V \frac{\delta V}{\delta x} + \frac{\delta V}{\delta t} + \frac{f V|V|}{2D} = 0 \quad . \quad . \quad . \quad (2.17)$$

where g = acceleration of gravity, ft/sec^2

V = velocity, ft/sec

H = hydraulic head, ft

x = distance from reservoir, ft

t = time, sec

f = Moody friction factor

D = pipe diameter, ft

As stated previously, the method of characteristics converts the two partial differential equations, L_1 and L_2, into four total differential equations. This is accomplished by combining L_1 and L_2 using an unknown multiplier λ to give:

$$L = L_1 + \lambda L_2 \quad . . . . . \quad (2.18)$$

Streeter showed that if $\lambda = \pm a/g$, then the following equations resulted:

$$\frac{dH}{dt} + \frac{a}{g}\frac{dV}{dt} + V \cdot \sin\theta + \frac{a \cdot f \cdot V|V|}{2 \cdot g \cdot D} = 0 \quad . . . . \quad (2.19)$$

for

$$\frac{dx}{dt} = V + a \quad . . . . . \quad (2.20)$$

and

$$\frac{dH}{dt} - \frac{a}{g}\frac{dV}{dt} + V \cdot \sin\theta - \frac{a \cdot f \cdot V|V|}{2 \cdot g \cdot D} = 0 \quad . . . \quad (2.21)$$

for

$$\frac{dx}{dt} = V - a \quad . . . . . \quad (2.22)$$

Equations (2.19) and (2.21) are total differential equations in V and H in terms of the independent variables x and t. The solution is carried out on an x-t plot as shown in Fig. 2.7. Equation (2.19) defines H and V along the C+ characteristic, Equation (2.20),

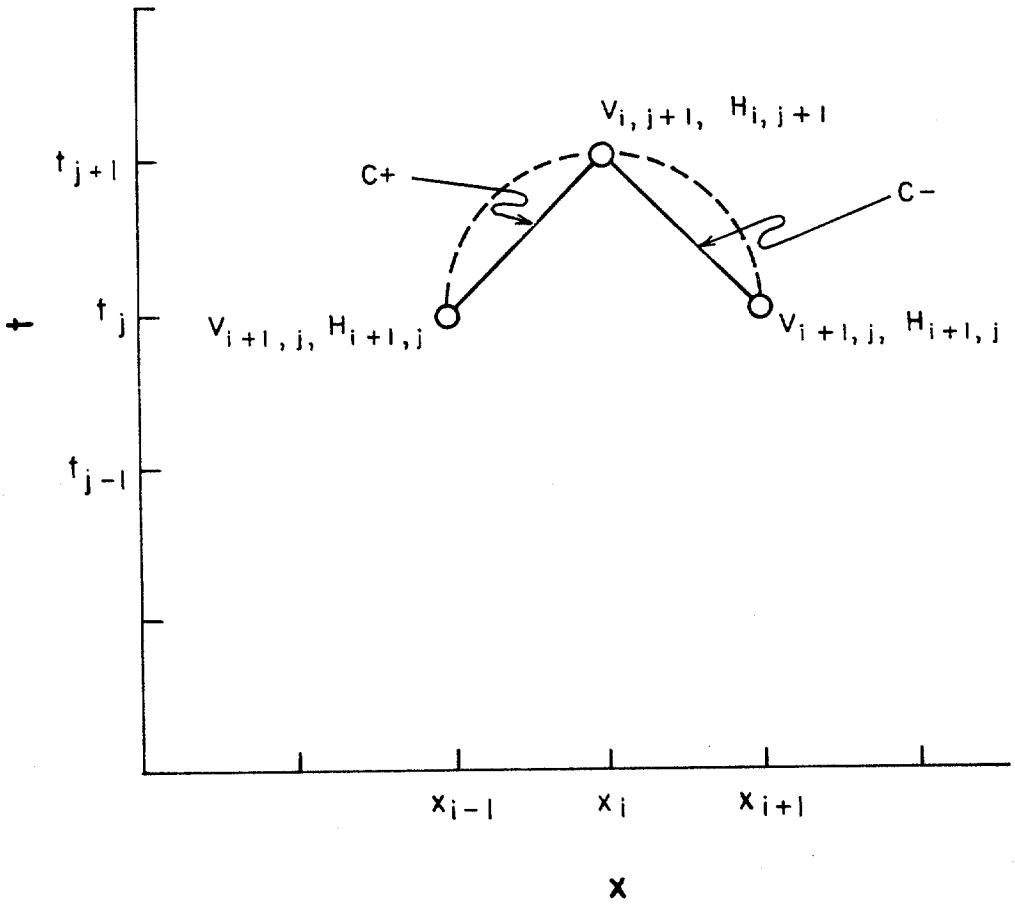

FIGURE 2.7. x−t GRID FOR METHOD OF CHARACTERISTICS. (AFTER STREETER[23,24])

and Equation (2.21) defines H and V along the C- characteristic, (Equation 2.22). Usually the characteristic equations are simplified by dropping the term V which is negligible compared to a. This produces the straight lines for the characteristic curves in Figure 2.7.

Equations (2.19) and (2.21) are expressed in finite difference form, and integrated along their respective characteristics. Then, by knowing H and V, (or Q if desirable) at two points, x_{i-1} and x_{i+1}, at the present time level, t_j, the two equations can be solved simultaneously to give H and V at the point, x_i, at the next time level t_{j+1} (See Figure 2.7). Obviously, this process can only be carried out over a limited range unless the boundary conditions of the system are known. The problem of defining the boundary conditions is the subject of the following section.

In summary, the method of characteristics of water hammer analysis seems to be the most up to date method of analysis. It includes the effects of friction and the effects of the pipes being nonhorizontal. It also easily accommodates boundary conditions and complex pipe networks, according to Streeter.[24] All of these considerations are important in regard to the analysis of the transient behavior of a wellbore during shut-in.

2.3 Boundary Conditions

As stated previously, in using the method of characteristics, the computations can only be carried out over a limited portion of the pipe unless the conditions at the ends of the system are known. The equations which are used to determine the pressure and velocity at a given point, x_i, at time level t_{j+1}, are expressed in terms of the pressures and velocities at the points to either side of that point, x_{i-1} and x_{i+1}, at the previous time level, t_j. Therefore, at each end of the system, only Equation (2.19) or (2.21) holds. Therefore, other equations must be used to define the conditions at each boundary as a function of time in order to be able to solve for both unknowns H and V.

Streeter[23, 24] describes methods of handling various boundary conditions which are applicable to pipe flow. Among these are:

1. Reservoir at upstream end
2. Valve at downstream end
3. Minor losses (due to sudden expansions of pipe)
4. Junctions of pipe segments
5. Restrictions, (orifices), in pipeline
6. Surge chambers

Some of the conditions listed above are directly applicable in the analysis of a well during shut-in. For

instance, the choke manifold is tied into the well head and can be treated in the same manner as the junction of two pipes. However, there are other conditions present in the well system which must be handled differently. For instance, the formation productivity must be included in any model of transient wellbore response in order to define the upstream boundary of the system.

The primary focus of this study is the boundary condition imposed on the wellbore by the closure of a blowout preventer. Therefore, the discussion below will be limited to downstream boundary conditions.

The closure of the blowout preventer in the hard shut-in procedure can be thought of as the rapid closure of a valve, a boundary condition which Streeter has considered. In fact, Streeter's method of handling valves at the downstream end of the system will accommodate both rapid closure and slow closure. Streeter's treatment of valves is the same for the method of characteristics as for the arithmetic integration method. Basically, he assumes that the area of the valve port varies as a known function of time. Then the dimensionless orifice equation, (2.11a), and Equation (2.21) are solved simultaneously to give the velocity, V, and hydraulic head, H. For convenience, Streeter's dimensionless orifice equation is restated here:

$$\frac{V}{V_o} = \frac{A_v}{A_{vo}} \sqrt{\frac{h}{h_o}} \quad \ldots\ldots\ldots\ldots\ldots \quad (2.11a)$$

When applied to a spherical blowout preventer, several difficulties arise in attempting to use this equation. The main problem is that the area open to flow in a spherical blowout preventer at various degrees of closure is not known. Measurement of these areas would not be practical since the rubber sealing element deforms differently each time it is closed. In order to avoid this problem, an alternative correlating parameter was used to describe the flow rate - pressure drop relation for the blowout preventer. The parameter chosen for this study, the valve coefficient, C_v, is often used in the valve industry to relate the pressure drop across valves or fittings to the flow rate through them.

By definition, C_v is the flow rate of water in gpm at 60°F through a valve, or fitting, for a 1 psi pressure drop across the valve.[6, 19] Experimentally determined, C_v is actually a correction factor used in place of certain terms in the Darcy - Weisbach equation to properly relate pressure drop and flow rate. The Darcy - Weisbach equation[2] can be written:

$$\Delta P = \frac{f\ L\ \rho\ V^2}{2\ g_c\ D} \quad \ldots\ldots\ldots\ldots\ldots \quad (2.23a)$$

or in terms of volume flow rate:

$$\Delta P = \frac{f\ L\ \rho\ Q^2}{1.234\ g_c\ D^5} \quad \ldots\ldots\ldots\ldots \quad (2.23b)$$

where ΔP = pressure drop across length L, lbf/ft^2

f = Moody friction factor, dimensionless

L = length of interest, ft

ρ = fluid density, lbm/ft^3

V = fluid velocity, ft/sec

D = internal diameter of pipe, ft

Q = fluid flow rate, ft^3/sec

In terms of more convenient units, the equation may be written:

$$\Delta P = \frac{1}{890.5}\ \frac{f\ L\ \rho\ Q^2}{D^5\ \rho_w} \quad \ldots\ldots\ldots \quad (2.24a)$$

or

$$\Delta P = \frac{1}{890.5}\ \frac{f\ L\ Q^2\ \gamma}{D^5} \quad \ldots\ldots\ldots \quad (2.24b)$$

where ΔP = psi

L = in.

ρ = lbm/ft^3

ρ_w = 62.4 lbm/ft^3

Q = gpm

D = in.

γ = specific gravity, dimensionless

The valve coefficient, C_v is now defined for a

pipe as:[6]

$$C_v = \frac{29.9\ D^2}{\sqrt{f\ L/D}} \quad \ldots\ldots\ldots\ldots\ldots \quad (2.25)$$

where C_v = valve coefficient, gal·in/min lbf

D = pipe diameter, in.

f = Moody friction factor

L = length of pipe, in.

and Equation (2.24b) can be written:

$$\Delta P = \frac{\gamma}{C_v^{\,2}} Q^2 \quad \ldots\ldots\ldots\ldots\ldots \quad (2.26)$$

where P = pressure drop, psi

C_v = valve coefficient

Q = flow rate, gpm

γ = specific weight of fluid

Notice that Equation (2.26) contains no length or diameter terms, which have no real significance for a valve, especially since the nominal size of a valve has little to do with the size of the port in the valve. If the value of C_v is known, the pressure drop through a valve for a given flow rate can be calculated using Equation (2.26). Usually the value of C_v for a valve is determined experimentally by actual flow rate and pressure drop measurements, and is back calculated from Equation (2.26) as shown in Example 2.2.

Example 2.2

The flow rate of water through a valve is measured to be 150 gpm with a total pressure drop across the valve of 60 psi.[6] Calculate the value of C_v.

Using Equation (2.26) we have:

$$C_v = Q\sqrt{\frac{\gamma}{\Delta P}} \quad \ldots\ldots\ldots\ldots\ldots\ldots \quad (2.27)$$

$$C_v = 150 \times \sqrt{\frac{1.0}{60}}$$

$$C_v = 19.4$$

One should be aware that the value of C_v for a valve is not constant, except in the range of complete turbulent flow. Since Equations (2.25) and (2.26) could be used to describe pipe flow, it is obvious that as the friction factor would necessarily change with flow rate, so also would the value of C_v change. Extending this theory to flow through valves, for laminar and transitional flow, the valve coefficient, C_v, will change with flow rate.

In order to properly describe the boundary condition induced by closure of a blowout preventer, the valve coefficient, C_v, must be defined as a function of time. A blowout preventer is closed by means of hydraulic fluid supplied by an accumulator.

The volume of hydraulic fluid pumped into the blowout preventer at a given time determines the value

of C_v. However, the rate at which the fluid can be supplied to the blowout preventer depends on a number of factors, such as frictional losses in the supply lines, and the power capacity of the accumulator. Therefore, defining C_v as a function of time is a two-step process. The value of C_v is a function of volume pumped, which in turn is a function of time. Once the boundary condition is defined, then the equation which describes it can be used with Equation (2.21) to determine the values of pressure head and velocity at the boundary for any time, t.

CHAPTER III

EXPERIMENTAL APPARATUS AND PROCEDURE

The surface equipment layout of the test facility used in this study, the L.S.U. Blowout Prevention Training and Research Well, is shown in Figure 3.1. The experimental apparatus used in this study was designed and constructed with the aid of the N.L. Shaffer Company specifically for studying the pressure drop - flow rate characteristics of a spherical blowout preventer. The test system consisted primarily of the Shaffer spherical blowout preventer test stump, the associated hydraulic fluid accumulator, a circulating system, and various data monitoring equipment as described in the following sections.

3.1 Circulating System

The circulating system is shown schematically in Figure 3.1. The diesel powered, Halliburton model T-10 cementing pump used in the study is equipped with 4.0-in. liners and has a stroke length of 10.0 in.[10] For 100% efficiency, the pump factor for the pump is 25.737 strokes per barrel. Flow tests with various fluids gave an actual pump factor of 26.1 strokes per barrel.

The main mud tanks cannot be used for experimental work with the Shaffer blowout preventer stump since return flow from the blowout preventer apparatus is routed

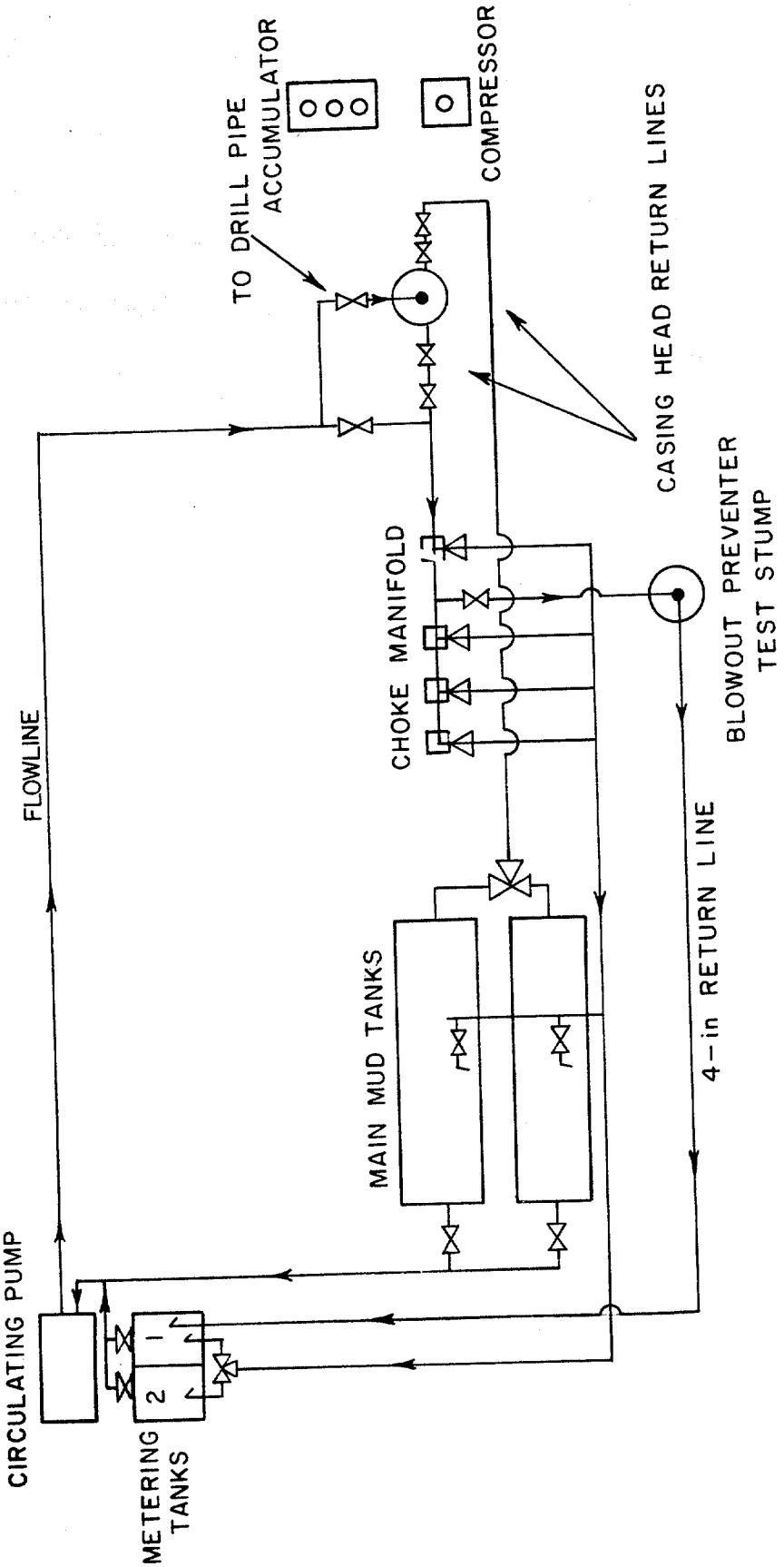

FIGURE 3.1. SURFACE LAYOUT OF LSU RESEARCH AND TRAINING WELL.

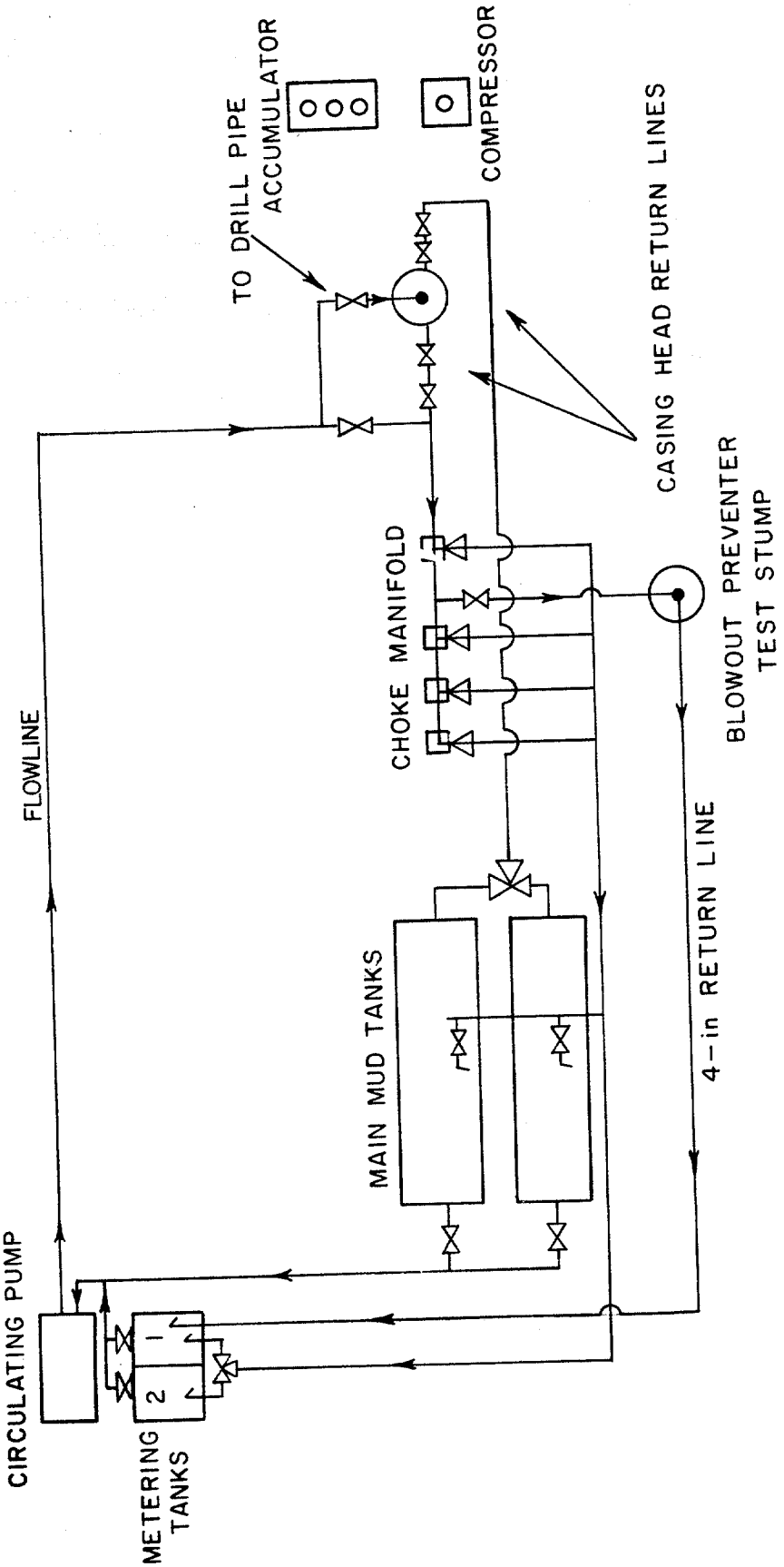

FIGURE 3.1. SURFACE LAYOUT OF LSU RESEARCH AND TRAINING WELL.

to the left hand metering tank (1). This piping complication also requires that the pump take suction from the two, 10-barrel metering tanks adjacent to the pump. The left tank (1) must be drawn from continuously, except when flow rates are being checked by metering flow through the preventer stack from the right tank (2) into the left tank (1).

The pump discharge is routed to the choke manifold where it can then be routed through any of four commercially available drilling chokes and/or through the blowout preventer stump. The valves on the manifold are set to allow flow through the blowout preventer stump and through the Swaco Super Choke only. With the Swaco choke kept in the closed position all flow is routed through the preventer stump. However, this choke provides a means for bleeding-off pressure in the system from the control house in the event that pressures become excessive as the blowout preventer ultimately seals to flow.

The training well was used as a large volume pulsation dampener in order to reduce the pressure fluctuations produced in the system by the stroking action of the pump. This was accomplished by opening the valves on the flow line and wellhead which would allow flow into the annulus of the well. With all other valves on the wellhead closed, the entire fluid volume in the well provided a pressurized surge chamber.

Although a small surge bottle was mounted on the flow-line the additional use of the well as a pulsation dampener proved to be quite effective.

The flow passes through the blowout preventer stump, which is discussed in detail in the following section, and is returned to the left hand tank (1) through a 4-in. return line. This large I.D. return line, fitted just above the blowout preventer, was used in order to assure that the preventer discharges to a downstream pressure as close to atmospheric pressure as possible. Pressure losses across the blowout preventer can then be easily derived from pressure readings made just upstream of the blowout preventer. For flow rates used in this study, it is a reasonable assumption that the frictional losses in the return line are negligible, and since the return line is fitted only 3-1/2 ft above the blowout preventer, only a small correction is needed for hydrostatic head. In fact, for most cases, the scatter of the data and the pressure fluctuations within the system make this 2-3 psi correction for hydrostatic head insignificant.

3.2 Spherical Blowout Preventer Test Stump

The test stump for the spherical blowout preventer is shown in Figure 3.2. A Shaffer 7-1/16 in. - 3000 psi spherical blowout preventer is mounted on a 9-1/2 ft joint of 7.921-in. I.D. casing sunken partially below ground level.[15] The casing joint is fitted with a

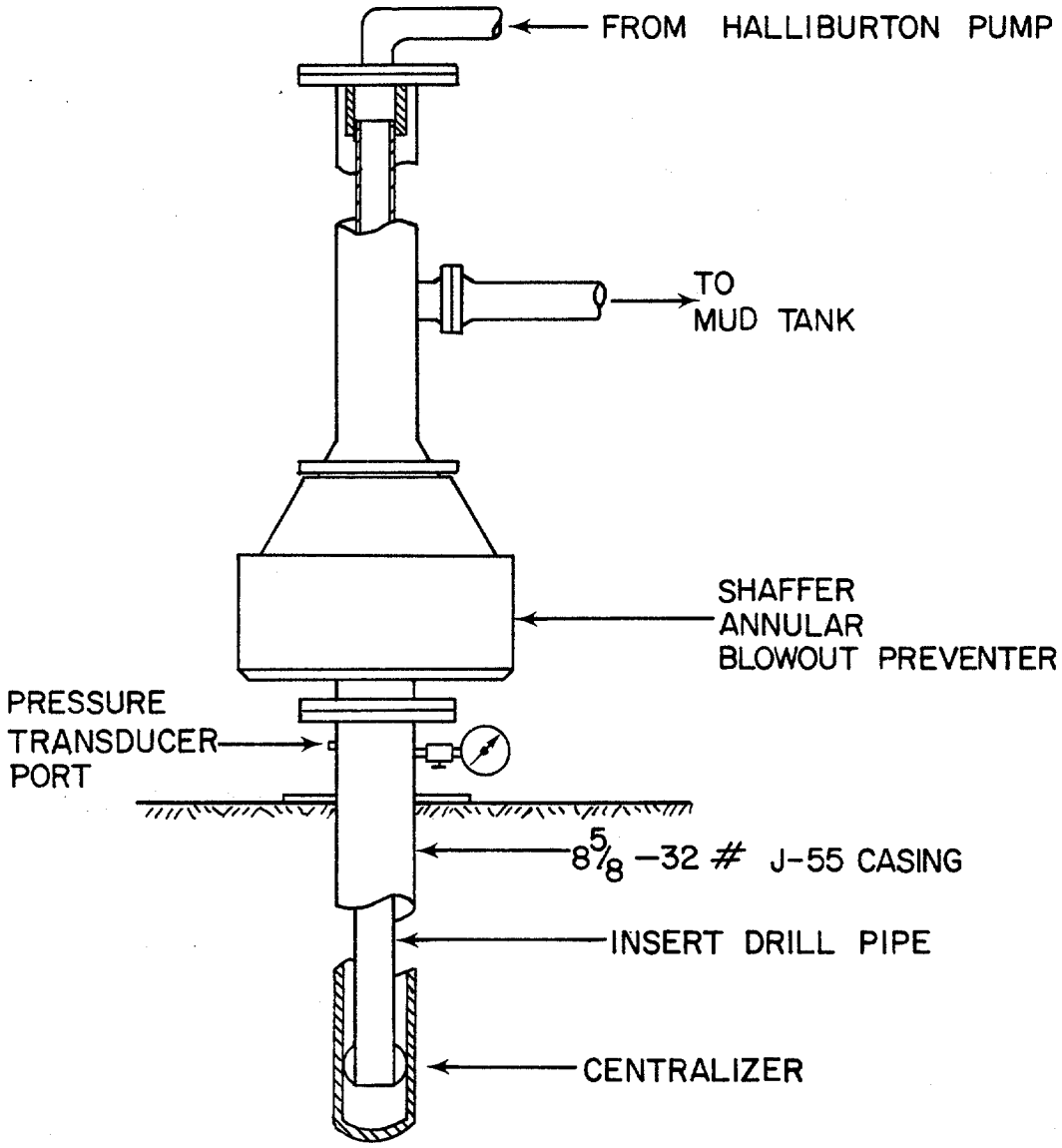

FIGURE 3.2. SPHERICAL BLOWOUT PREVENTER TEST STUMP.

and high pressure gate valves just below the blowout preventer. The pressure monitoring apparatus will be discussed in detail in a later section.

3.2.1 Shaffer Spherical Blowout Preventer

The 7-1/16 in. - 3000 psi Shaffer spherical blowout preventer is shown in Figure 3.3.[15] This particular design of annular blowout preventer derives its name from the shape of the inside of its upper housing, a design feature which plays an integral part in the closing mechanism of the preventer.

The main components of the blowout preventer are the upper and lower housings, the piston, the adapter ring, and the sealing element.[16, 21] The sealing element consists primarily of rubber with spherical steel inserts molded into the rubber to reinforce the rubber and to provide a low friction, metal-to-metal sliding contact between the sealing element and the spherical upper housing of the preventer. The element is designed to allow closure around any size or shape of pipe as well as on an open hole.

Figure 3.3 shows the preventer in the full open position, with the sealing element fully relaxed. To close the preventer, fluid is pumped in the closing chamber, forcing the piston upward as fluid is expelled from the opening chamber above the piston. The piston, in turn, drives the spherical sealing element upward as

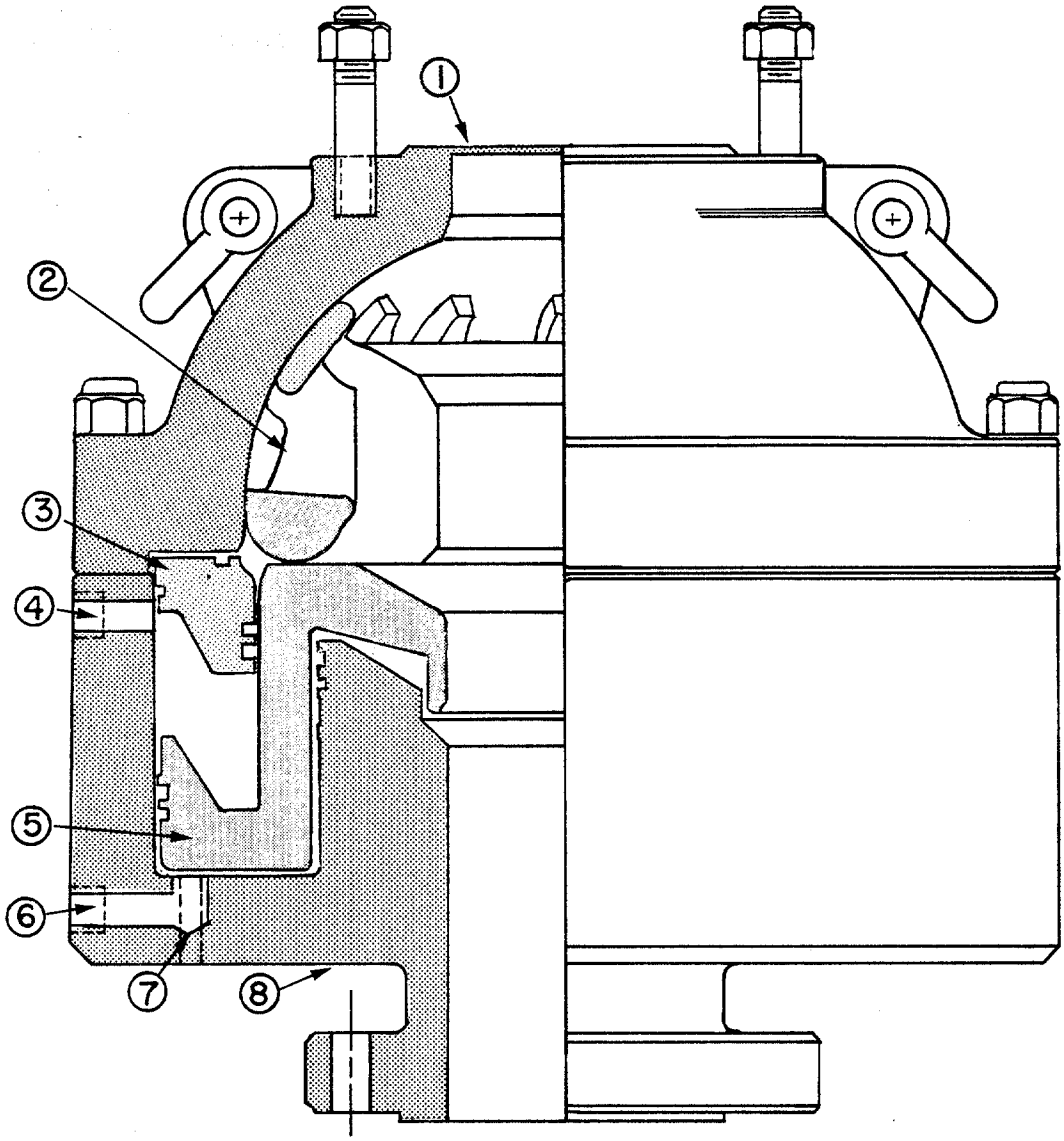

① UPPER HOUSING
② RUBBER SEALING ELEMENT
③ ADAPTER RING
④ OPENING CHAMBER PORT
⑤ PISTON
⑥ CLOSING CHAMBER PORT
⑦ PORT FOR POSITON INDICATOR ROD
⑧ LOWER HOUSING

FIGURE 3.3. CUTAWAY VIEW OF 7 1/16 INCH SHAFFER SPHERICAL BLOWOUT PREVENTER. (AFTER N.L. SHAFFER CO.[15])

it contacts the spherical-shaped, inside surface of the preventer's upper housing. A feature of the spherical design is the assist in closing the element that is obtained by well pressure exerted below the element. To open the preventer, fluid is pumped into the opening chamber displacing the piston downward and allowing the sealing element to relax and return to the full open position. It should be noted that the sales literature for the preventer specifies that in stripping operations, opening energy is provided by the tool joint forcing its way into the element. This fact, along with the design feature of well pressure assist, on closing, suggests that even with opening pressure applied to the piston, the well pressure may be adequate to maintain the sealing element in the fully closed position. In order to open the blowout preventer under a well pressure capable of maintaining element closure, either the pressure must be bled down to a level which would allow the element to relax, or movement of the pipe in the hole can provide the energy to open the element.

Hydraulic fluid to the opening and closing chambers is supplied through 1-in. high pressure lines tied into a hydraulic accumulator, according to the recommendations of the blowout preventer manufacturer. However, each line was also equipped with a high-pressure needle valve to regulate the flow of hydraulic fluid into each of the two chambers. Valves in the control lines are

not recommended for field use because inadvertent closure of a valve would put the blowout preventer out of service. A fitting is also provided on the closing chamber to allow the hook-up of a pressure gage for monitoring hydraulic pressure in the chamber.

The valve to the opening chamber is left fully open at all time to conform more accurately to actual field conditions. The needle valve on the closing control line is opened or closed as needed to regulate the flow of hydraulic fluid into the closing chamber when adjusting the position of the piston. With the piston in the desired position, the closing line valve is shut to prevent additional hydraulic fluid from flowing into the closing chamber and moving the piston.

3.2.2 Piston Position Indicator Assembly

The degree to which the blowout preventer is closed at any time is monitored by means of a 1/4-in. steel follower rod. The rod extends through a packed-off port bored through the lower housing of the blowout preventer specifically for this purpose. The rod, in contact with the steel piston, follows the piston's movement as the blowout preventer is closed or opened.

An external lever and weight mechanism was developed to apply a constant upward force to the end of the follower rod, keeping the rod in contact with the preventer piston at all times. This was necessary because

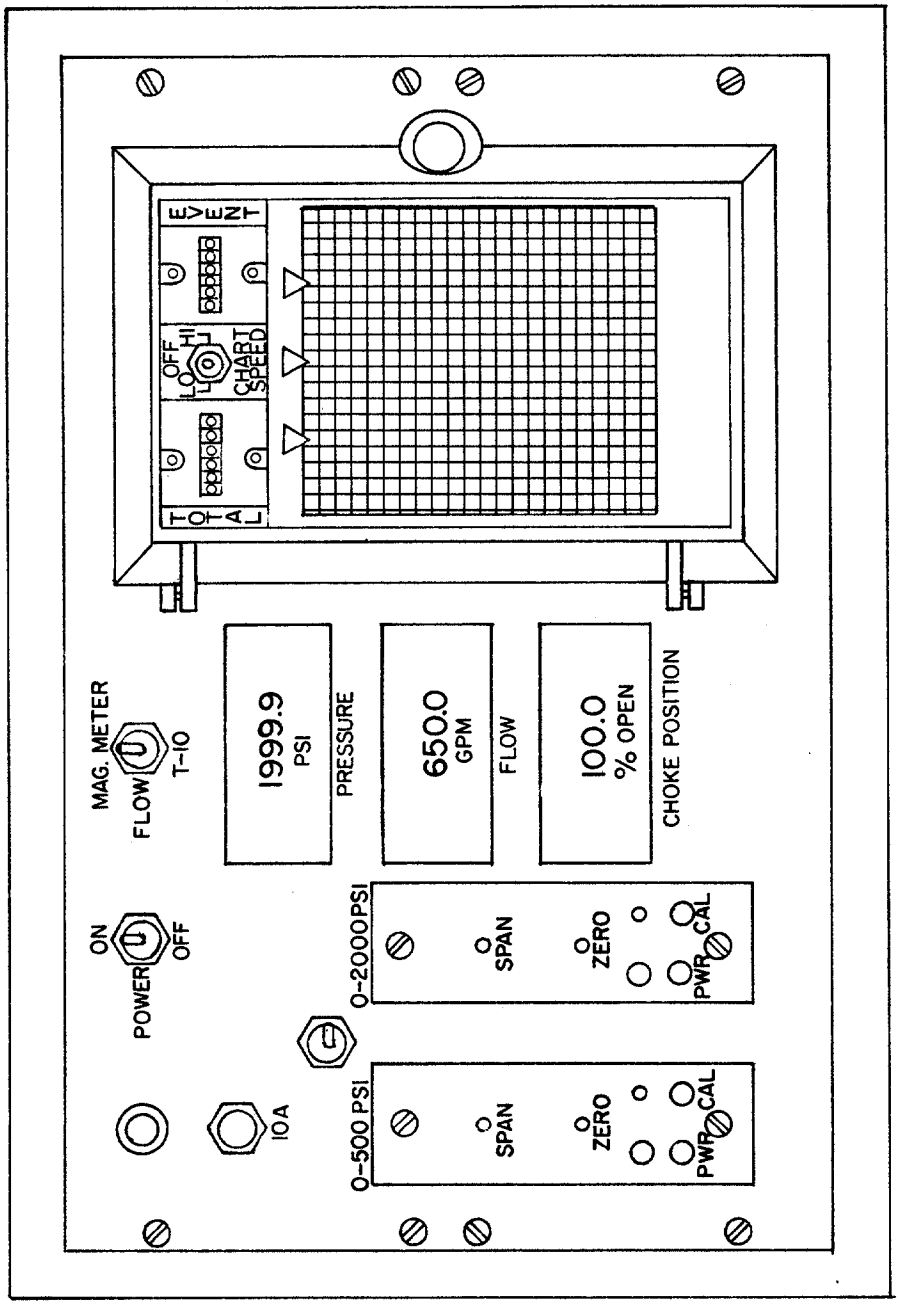

FIGURE 3.5. DISPLAY PANEL OF DATA MONITORING CONSOLE.
(AFTER HALLIBURTON SERVICES[10])

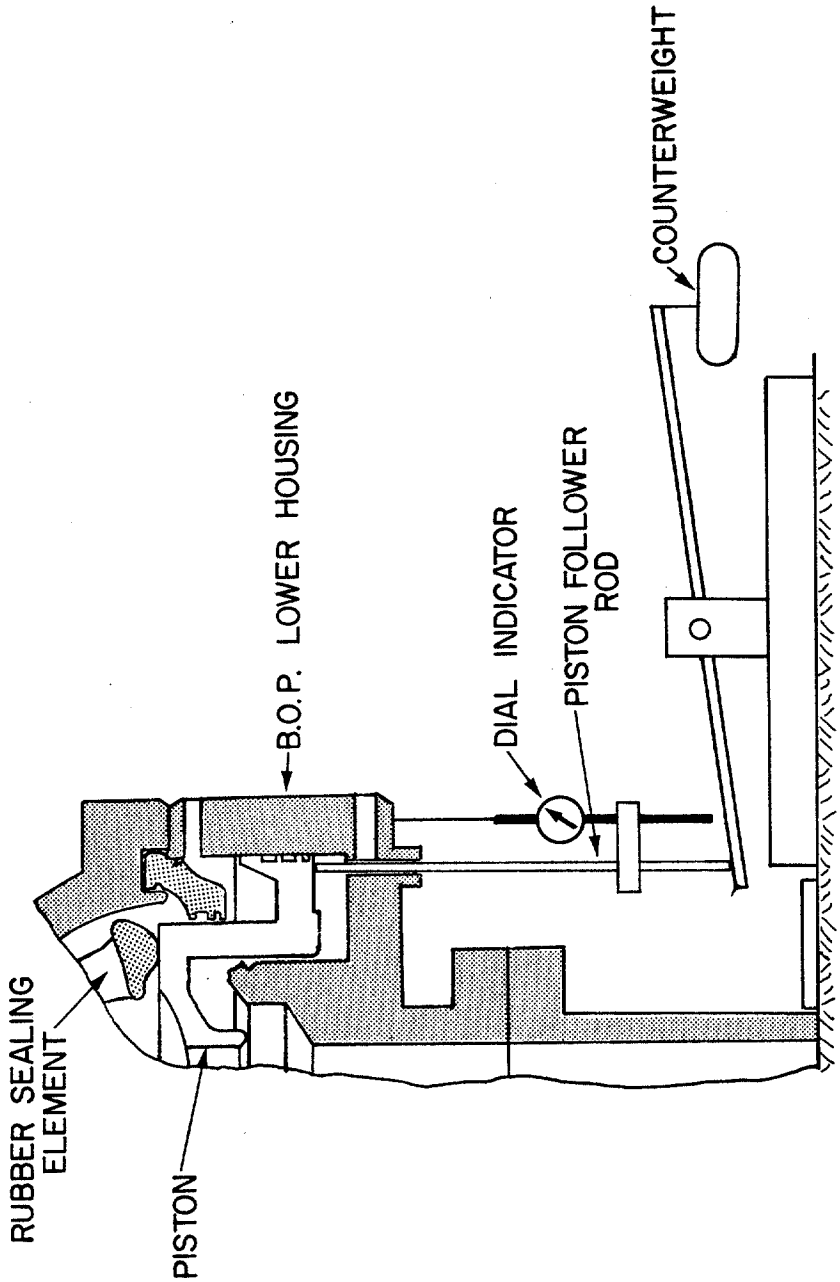

FIGURE 3.4. PISTON POSITION INDICATOR ASSEMBLY

Without extender block (dial indicator tip in contact with blowout preventer):

Travel = Present Dial Reading + (L - Full Open Dial Reading), inches. . . . . (3.2)

where: L = thickness of extender block, inches

As flow rate and pressure data were collected, the closing chamber pressure was monitored also in the control house in an effort to detect possible piston movement. It was found that at high differential pressures across the preventer, the closing pressure tends to rise, as the piston tends to back up slightly toward a more open position. This was an important observation in that with each set of pressure drop - flow rate data it was assumed that the piston remained in a fixed, preset position.

3.3 Flow Rate and Pressure Monitoring Equipment

A data monitoring console, specially designed and built by Halliburton Services for the L.S.U. Blowout Prevention Facility, is used to monitor pressure drops and flow rates across the blowout preventer. The unit combines various components having specific measuring or display capabilities into a semi-portable instrument console. A front view of the display panel is shown in Figure 3.5.[10]

The pressure and flow rate equipment only were used in this study. Also, since no permanent, continuous

record was needed for this study, and in order to simplify calibration of the monitoring systems, the L.E.D. data displays are used rather than the strip chart recorder. The calibration and operation of both the pressure monitoring system and the flow rate monitoring system and their corresponding displays are described below.

3.3.1 Pressure Monitoring System

The pressure sensing components of the Halliburton system are shown schematically in Figure 3.6. Annular pressures directly below the preventer are transmitted through a precharged gage protector and hydraulic line to a set of two pressure transducers. The Teledyne-Taber model 2204 pressure transducers with pressure ranges of 0 - 500 psi and 0 - 2000 psi are arranged in parallel in order to avoid the use of valves which would induce loss of the hydraulic precharge of the system, requiring recalibration.[10, 25]

The transducer signals are transmitted over electrical cable to signal conditioners (one for each transducer).[4] Depending on the position of the pressure range selector switch, the "conditioned" signal from either transducer is displayed on the L.E.D. digital meter, which reads directly in psi.

The pressure sensing system is calibrated using a dead-weight tester and the 0% - 80% calibration method

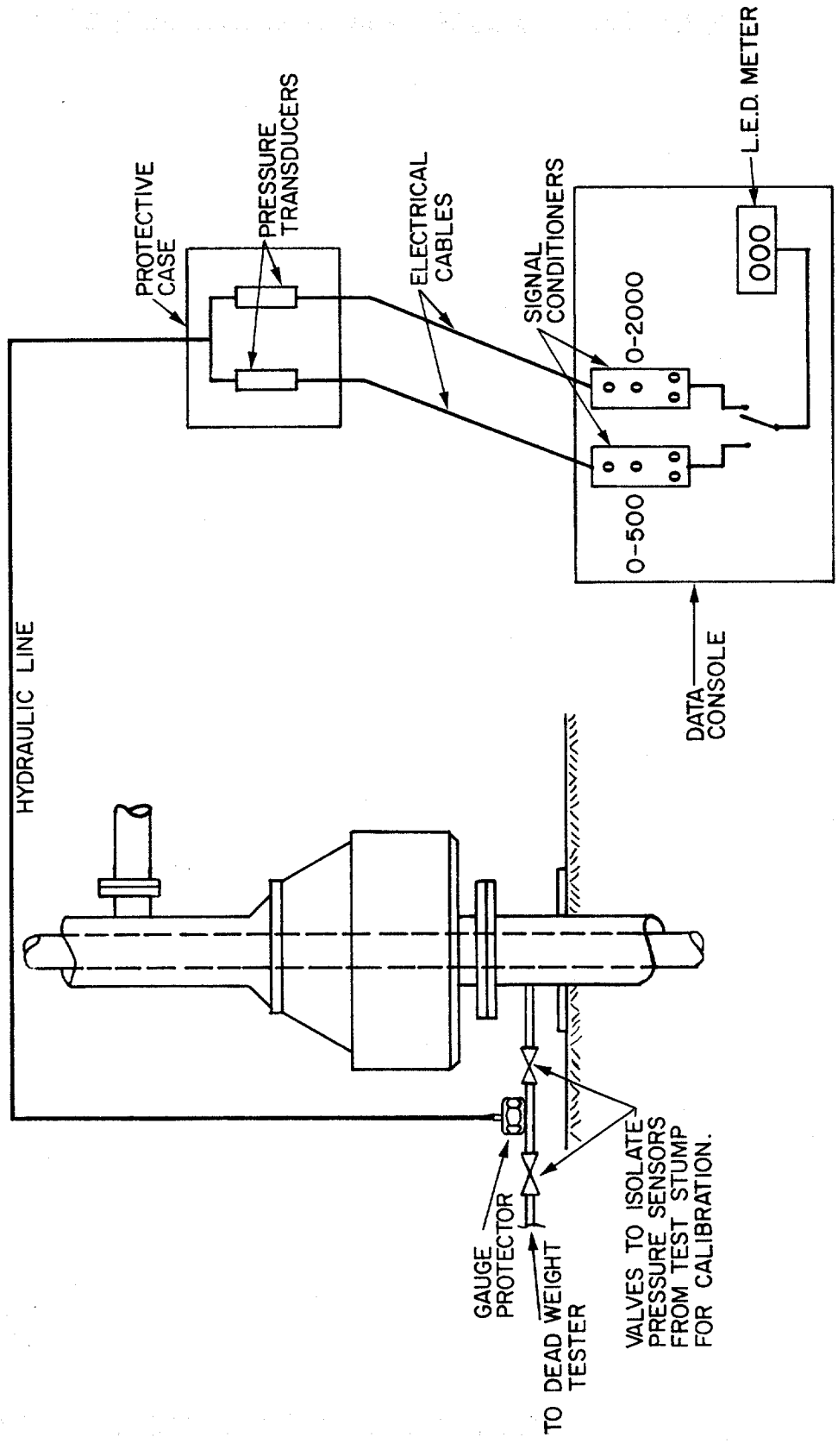

FIGURE 3.6. PRESSURE SENSING SYSTEM.

recommended by the manufacturer.[4] This method is a trial-and-error procedure to force a match of displayed pressures and those applied to the system by the dead-weight tester. The front panel of each signal conditioner contains a calibration switch and two adjustment screws as seen in Figure 3.7.[4]

To calibrate either pressure transducer, the gage protector manifold is first isolated from the blowout preventer test stump to provide a small volume system for dead-weight testing. With no pressure on the system, the ZERO screw is adjusted to force the meter to read 0000. Then 80% of the transducer's full scale is applied using the dead-weight tester and the hydraulic pump, and the meter is forced to read the proper value by adjusting the SPAN screw. For the 0 - 2000 psi transducer, 80% of full scale is 1600 psi. The applied pressure is then beld to 0000 and the meter reading is checked. This process of force matching the applied and displayed pressures is repeated until no further adjustment is needed. After the successful completion of the above calibration procedure, the CAL switch is pressed and the resulting value displayed on the L.E.D. meter is recorded as the Check Cal number for future reference. Once the system is dead-weight tested there should be no need to recalibrate unless the hydraulic precharge in the hose to the transducer is lost or altered.

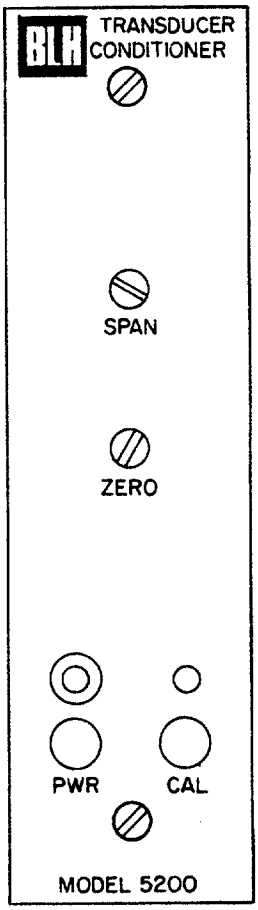

FIGURE 3.7. TRANSDUCER SIGNAL CONDITIONER–FRONT CONTROL PANEL.(AFTER BLH ELECTRONICS[4])

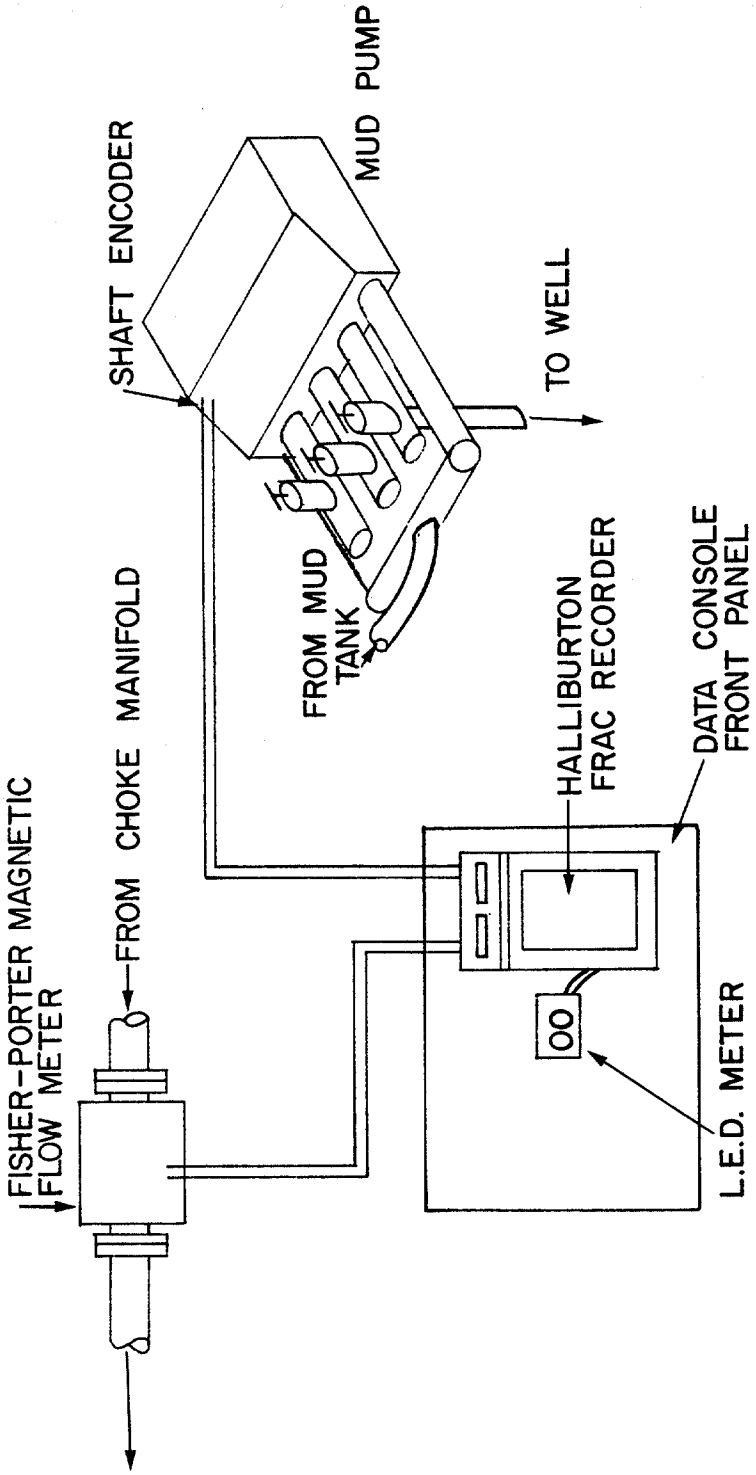

FIGURE 3.8. FLOW RATE SENSING SYSTEM.

The Check Cal number recorded previously can be used to check the electronic calibration of the system at any time. With zero pressure on the transducer and the CAL switch depressed, the displayed value should agree with the previously recorded Check Cal value. If it does not, the meter is forced to read the proper check value by adjusting the SPAN screw accordingly. The CAL switch is then released and the zero reading is checked. If the display does not read 0000 then the ZERO and SPAN settings until the proper Check Cal value and 0000 are obtained without further adjustment.

It should be noted that any large discrepency between the displayed and recorded values of Check Cal or a reading other than 0000 with zero pressure on the system may indicate a loss of the hydraulic precharge on the transducer. If this is encountered, the entire system should be checked using the dead-weight tester.

3.3.2 Flow Rate Monitoring System

The flow sensing components of the system are shown in Figure 3.8. A Halliburton model 73 Fracrecorder receives pulse signals from two sources - a shaft encoder mounted on the T-10 pump and a Fisher Porter magnetic flow meter mounted on the return line from the choke manifold.[9, 10] The flow selector switch on the front display console allows the user to monitor flow rate based on either source of the flow signal. The T-10

signal was used in this study because the return flow from the blowout preventer stack cannot be routed through the magnetic flow meter with the present piping network.

The flow rate section of the Fracrecorder circuitry converts the frequency of the input signal into voltage levels which drive the flow rate pen of the strip recorder and the external L.E.D. flow rate meter, both of which can be calibrated to read in barrels per minute or gallons per minute. The L.E.D. meter only was used since a continuous flow rate curve was not needed for the purpose of this study.

The flow rate meter is calibrated by applying an internal calibration signal to the meter and adjusting the meter to read the corresponding calibration flow rate as explained below.[9] With no flow signal applied to the system, the L.E.D. flow rate meter is set to 0000 using the ZERO adjust on the flow card, a circuit board within the Halliburton Fracrecorder. This adjustment should not be necessary after its initial adjustment which Halliburton provided during installation.

The flow rate switch on the back panel of the Fracrecorder, shown in Figure 3.9, is then switched to LO CAL which supplies the internal calibration signal to the flow rate circuitry. With the LO CAL signal applied, the SPAN potentiometer on the wire leading to the L.E.D. meter is adjusted, forcing the meter to read

the proper calibration flow rate. A similar procedure is used to calibrate the strip chart recorder but will not be discussed here since the recorder was not used in this study.

The calibration flow rate is calculated using Equation (3.3) below:

$$\text{Cal. Flow Rate} = \frac{\text{Cal. Freq. x 60 sec/min}}{\text{M.F. x Conv. Factor}} \qquad (3.3)$$

where:

Cal. Freq. = frequency of calibration signal applied to circuits.

LO CAL: Cal Freq. = 120 pulses/sec

HI CAL: Cal Freq. = 240 pulses/sec

M.F. = meter factor, pulses/gal

Conv. Factor = conversion factor, provides for display of flow rate in various units as shown in Table 3.1

The actual pump factor of the Halliburton T-10 pump has been measured for various pressures and flow rates and an average pump factor of 1.61 gal/stroke was found. The shaft encoder mounted on the pump produces 32 pulses per revolution or stroke of the pump. The meter factor, M.F., for calibrating the T-10 flow rate circuitry is then:

$$\text{M.F.} = \frac{32 \text{ pulses/stroke}}{1.61 \text{ gal/stroke}} = 19.9 \text{ pulses/gal}$$

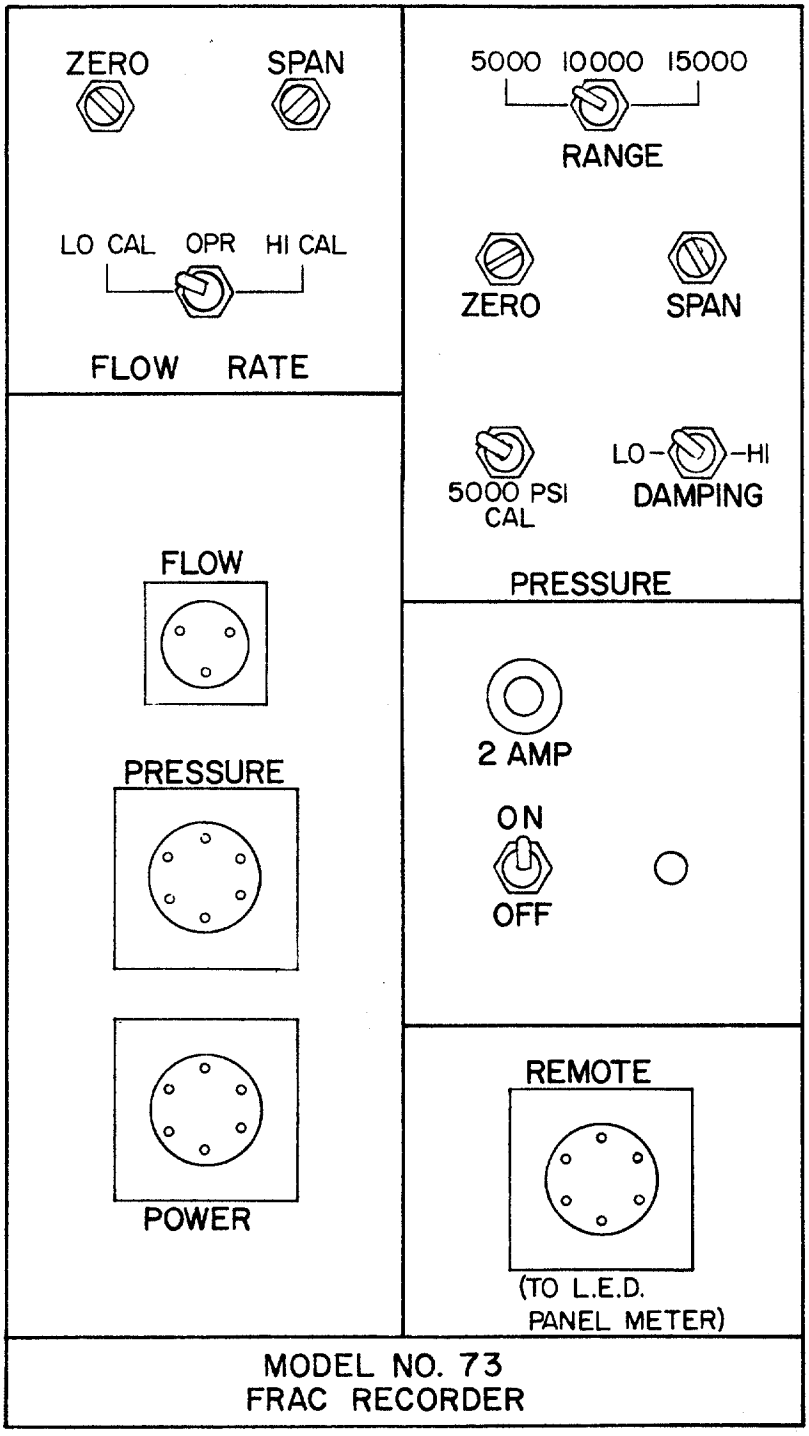

FIGURE 3.9. BACK PANEL OF HALLIBURTON FRAC RECORDER. (AFTER HALLIBURTON SERVICES[9])

Units	Conv. Factor
GPM	1.0
1/10 GPM	10.0
Bbl/min	42.0
1/10 Bbl/min	4.2

Table 3.1 - Conversion Factors For Flow Rate Calibration (After Halliburton Services[9])

Now, for output in gpm using the LO CAL Calibration signal, the calibration flow rate is given by:

$$\text{Cal. Flow Rate} = \frac{120 \text{ pulses/sec} \times 60 \text{ sec/min}}{19.9 \text{ pulses/gas} \times 1.0}$$

$$= 362 \text{ gpm}$$

Unless the pump factor changes, the flow rate meter should not need recalibration. However, occasional checks of the Cal. Flow Rate can be made to verify proper calibration of the meter.

3.4 Experimental Procedure

Pressure drop measurements were made for steady-state flow through the blowout preventer at various partial closures.

Since the well facility is also used for training purposes and for other research projects, before each data run the choke manifold and other valves must be set to accommodate flow through the blowout preventer

stump, as described in a previous section. The water or drilling mud is then circulated to allow the fluid properties to stabilize, and to assure a uniform fluid throughout the system.

Mud properties are checked before and after the pressure drop - flow rate data is taken in order to detect significant changes in the mud properties which might affect the quality of the data. The properties which are monitored are:

1. Density
2. Temperature
3. Six Fann Viscometer Readings
4. 10-sec. gel strength, 10-min. gel strength

Next, with the opening line valve open and the closing line valve closed on the blowout preventer supply lines, the accumulator blowout preventer control is activated, supplying hydraulic fluid to the closing line. Now, after recording the full open dial indicator reading, the procedure below is followed to obtain the needed pressure drop - flow rate data.

1. Piston position is set using closing line valve to supply fluid to closing chamber.
2. Dial indicator reading and hydraulic pressure are recorded for the desired piston position.
3. Flow rate is increased in incremental steps until the maximum possible rate is reached. Rate and resulting annular pressure are

recorded at each step.

4. The above operations are repeated until full closure of the blowout preventer is achieved.

There are several special notes which should be made concerning the steps above. First, the piston position should be set using closing pressure only. In the event that the desired piston position is passed, opening pressure should not be used to reverse the piston movement. Rather, the blowout preventer should be fully opened and then closing pressure used to obtain the appropriate setting. The rubber element seems to behave differently under closing pressure than under opening pressure. Therefore, the most obvious reason for using closing pressure only in adjusting piston position is that this procedure more accurately describes the physical experience of the blowout preventer during closure in an actual well control situation.

The well, or annular, pressure should be monitored as the closing pressure is applied to the blowout preventer, as a guide in choosing an appropriate piston position. In general, an increase in well pressure of 200 - 300 psi between one piston position and the next should provide reasonable results. However, the first piston position used should be chosen at the initial pressure response in order to identify the minimum piston movement which affects the flow rate - pressure drop response of the preventer.

Well pressures should always be recorded for an increasing sequence of flow rates in order to obtain more consistent data. Also, to provide a larger range of flow rates and pressures, the pump is shifted manually from second gear for low flow rates to third gear for high flow rates.

As the piston position approaches the full closed position, the rubber element has a tendency to close itself with the assist obtained from well pressure. Under these conditions, if the well pressure approaches 2500 psi, the pressure at which the pump's pop-off valve is set, then the pump is quickly throttled down and the Swaco Super Choke is opened to bleed off this excess pressure to avoid activating the pop-off valve.

The procedure is continued for various piston positions until the pressures and flow rates encountered indicate automatic closure of the blowout preventer. Closure of the blowout preventer can be induced by the well pressure assisting the hydraulic pressure and is apparent from a rapid and steady decrease in pump rate with a corresponding rise in well pressure. The piston position at which the element ultimately seals to all flow is determined by applying well pressure to the system by throttling the pump slightly. Then the closing line valve is opened slightly, to very slowly move the piston upward. When no flow through the blowout preventer can be heard, the preventer is assumed to

be fully closed to flow and the piston position (dial indicator reading) is noted.

CHAPTER IV

EXPERIMENTAL RESULTS

Using the apparatus and procedure described in Chapter 3, frictional pressure losses were recorded for various steady-state flow rates through a spherical blowout preventer as the device was closed in discrete steps. Graphical displays of the pressure drop - flow rate characteristics of the preventer were developed from this data to show the effects of:

1. Power piston travel, or degree of preventer closure,
2. Type and viscosity of flowing fluid,
3. Annular geometry, i.e., O.D. of pipe in preventer.

In order to study the effects of fluid viscosity on the blowout preventer pressure drop - flow rate characteristics, 3 fluids were examined for each pipe size. The fluid properties are shown in Table 4.1. Mud No. 1 is actually plain water. Muds 2 through 5 are low viscosity clay - water muds, while Muds 6 through 9 are high viscosity muds. The desired viscosity was obtained by adding bentonite clay to the mud in the tanks. Annular geometry effects were studied by using four pipe sizes of various diameters. The dimensions of the pipes are shown in Table 4.2.

Mud No.	Temp., °F	Density, lb/gal	Fann Viscometer Readings 600 rpm	300 rpm	200 rpm	100 rpm	6 rpm	3 rpm	10-sec gel, lb/100ft^2	10-min gel, lb/100ft^2	Plastic Viscosity, cp	Yield Point lb,100ft^2
1	70	8.33	2.0	1.0	.67	.33	-	-	0.0	0.0	1.0	0.0
2	86	8.59	20.0	17.0	14.0	6.0	1.0	0.5	0.0	2.0	3.0	14.0
	110+	8.57	21.0	15.0	12.0	8.0	2.0	1.5	1.5	14.0	6.0	9.0
3	-	-	-	-	-	-	-	-	-	-	-	-
4	78	8.61	21.0	13.0	10.0	8.0	3.5	2.0	1.0	1.0	8.0	5.0
	85	8.60	22.0	15.0	12.0	9.0	5.0	3.0	3.0	-	7.0	8.0
5	98	8.59	30.0	20.0	16.0	12.0	4.0	3.5	2.0	13.0	10.0	10.0
	109	8.59	38.0	27.0	21.0	14.5	5.0	4.0	3.0	24.0	11.0	16.0
6	94	8.63	125.0	88.0	73.0	55.0	30.0	29.0	43.0	75.0	37.0	51.0
	110+	-	161.0	118.0	102.0	80.0	48.0	47.0	69.0	90.0	43.0	75.0
7	90	8.64	143.0	98.0	79.0	57.0	27.0	25.0	34.0	64.0	45.0	53.0
	110+	-	148.0	110.0	95.0	75.0	47.0	46.0	50.0	90.0	38.0	72.0
8	94	8.60	155.0	109.0	92.0	69.0	37.0	36.0	47.0	74.0	46.0	63.0
	110+	8.62	166.0	120.0	103.0	79.0	48.0	47.0	58.0	90.0	46.0	74.0
9	100	8.67	225.0	160.0	136.0	104.0	57.0	56.0	70.0	105.0	65.0	95.0
	110+	8.65	245.0	176.0	152.0	119.0	69.0	69.0	88.0	110.0	69.0	107.0

Table 4.1 Summary of Fluid Properties

I.D., Inches	O.D., Inches
1.833	2 3/8
3.083	3 1/2
3.833	4 1/2
4.667	5 1/2

Table 4.2 Pipe Dimensions

Valve coefficients, used in the valve industry to characterize pressure losses through valves and fittings, were determined for the blowout preventer at each degree of closure (piston position). Curves of valve coefficients were developed to define the pressure drop - flow rate characteristics of the blowout preventer as a function of piston position.

The correlation between the piston position and the volume of hydraulic fluid pumped into the closing chamber of the blowout preventer was also determined. This relation was developed to allow the characteristics of the blowout preventer to be interfaced with the performance of the hydraulic accumulator in the ultimate analysis of shut-in procedures using a mathematical model.

4.1 Pressure Drop - Flow Rate Response of Blowout Preventer

Figures 4.1 through 4.12 show the experimental

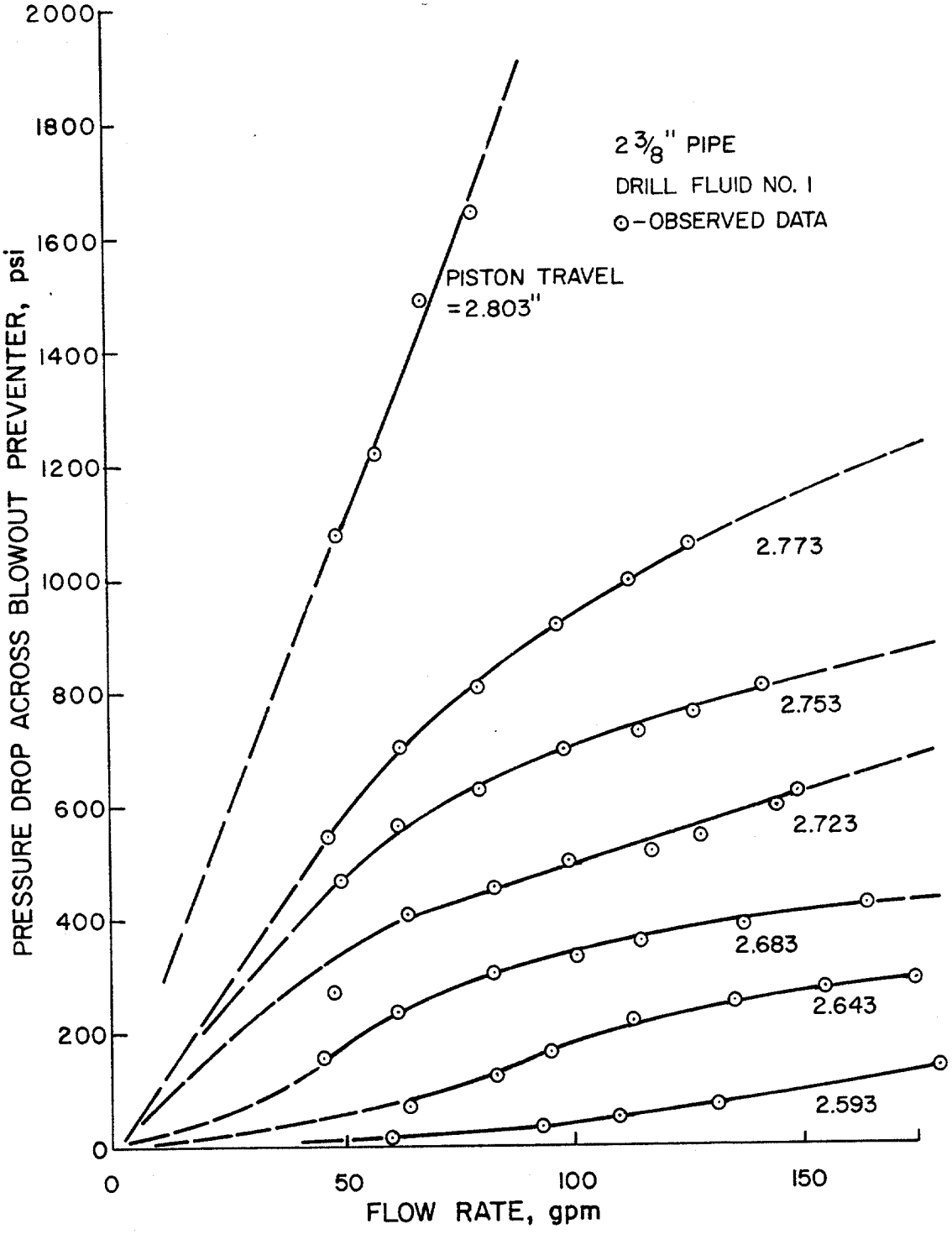

FIGURE 4.1. PRESSURE DROP THROUGH SPHERICAL BLOWOUT PREVENTER FOR VARIOUS POSITIONS OF THE CLOSING PISTON

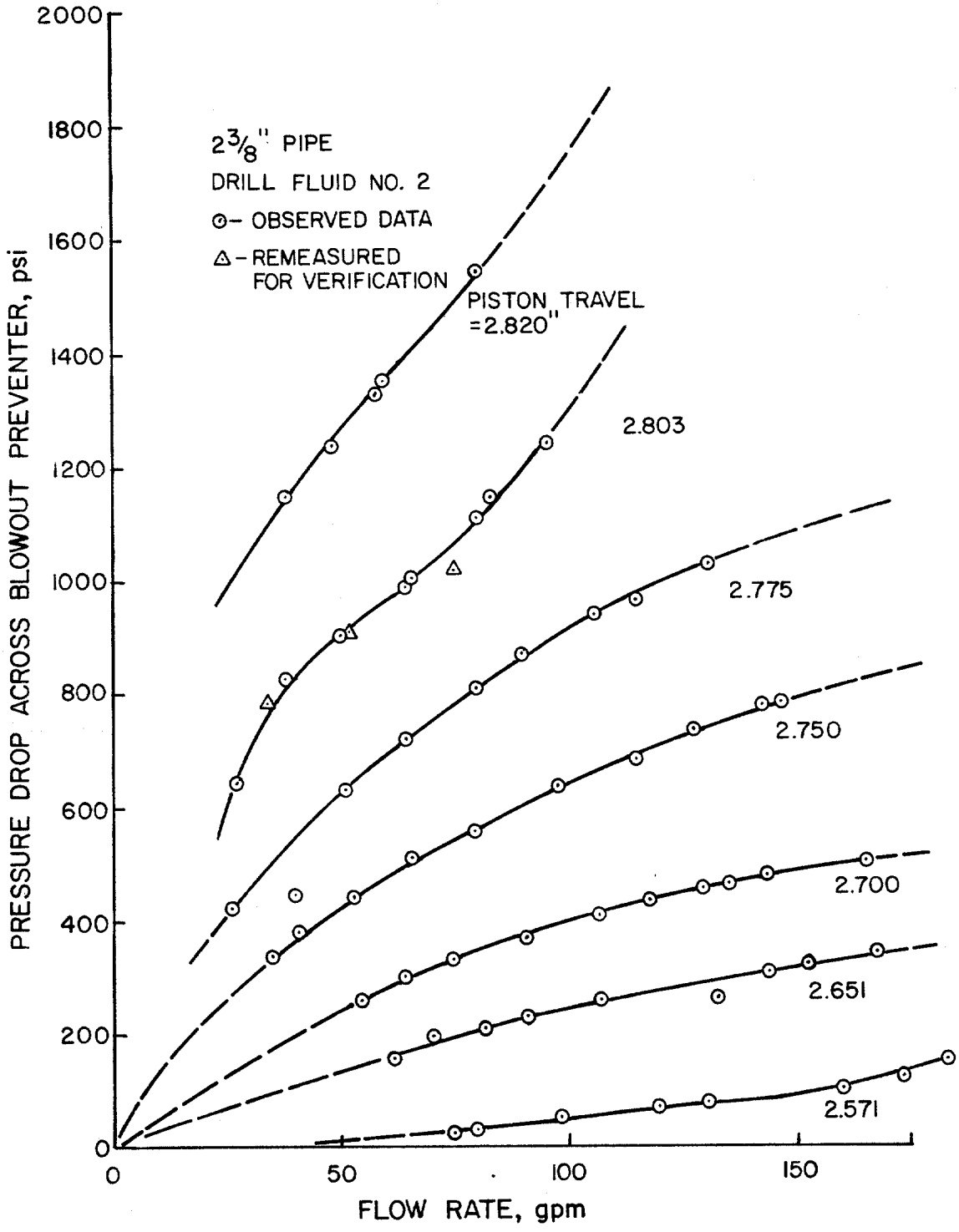

FIGURE 4.2. PRESSURE DROP THROUGH SPHERICAL BLOWOUT PREVENTER FOR VARIOUS POSITIONS OF THE CLOSING PISTON

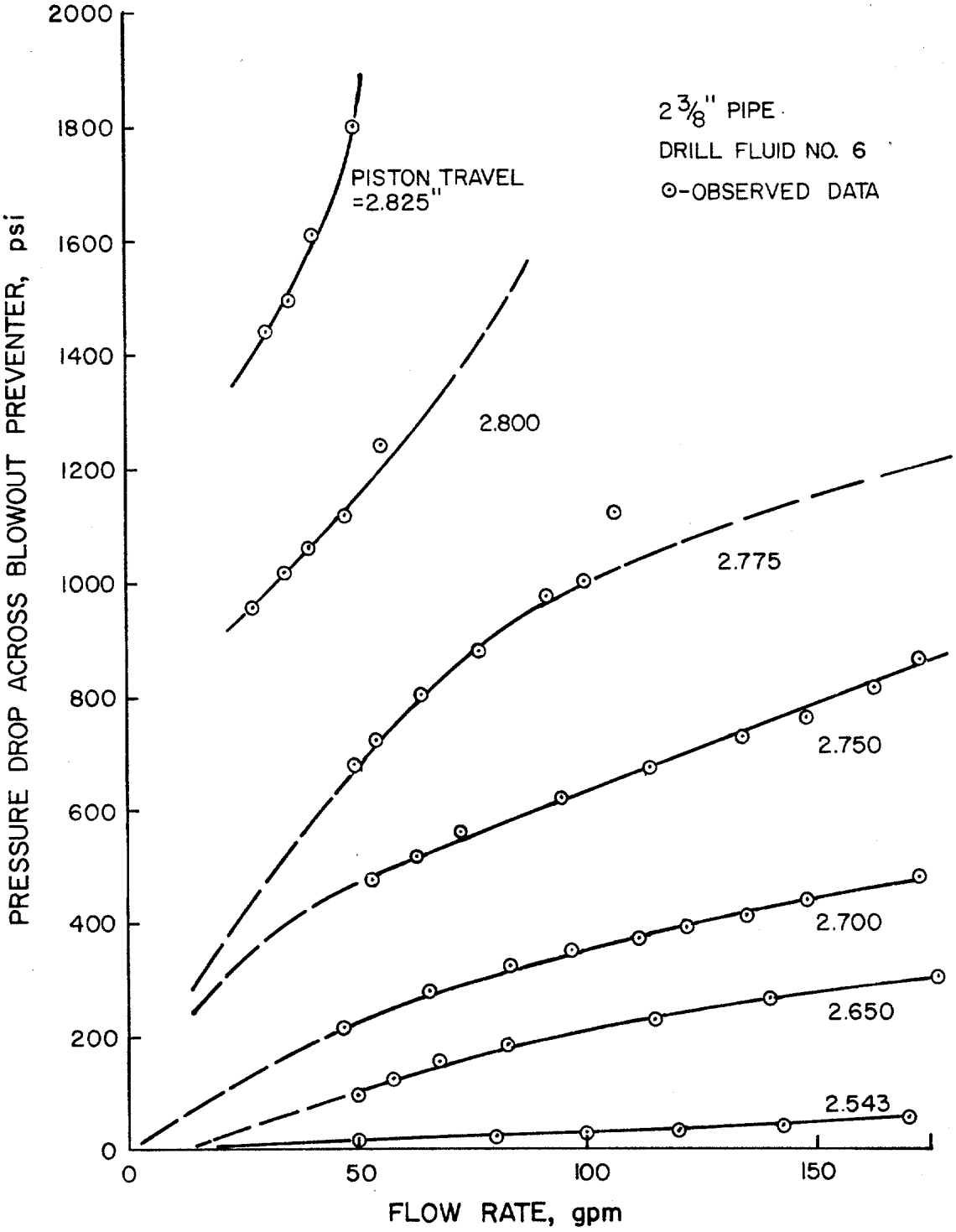

FIGURE 4.3. PRESSURE DROP THROUGH SPHERICAL BLOWOUT PREVENTERS FOR VARIOUS POSITIONS OF THE CLOSING PISTON

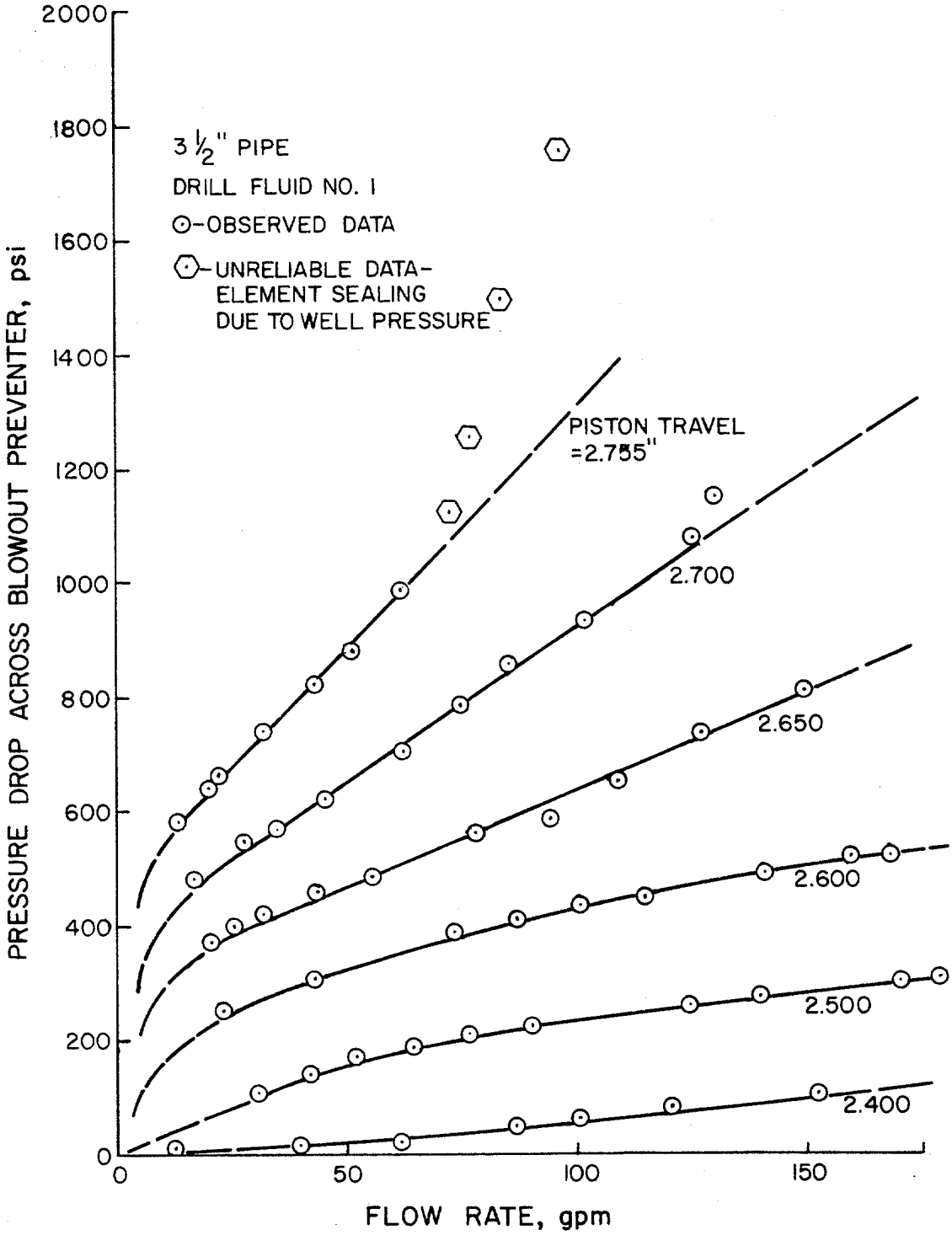

FIGURE 4.4. PRESSURE DROP THROUGH SPHERICAL BLOWOUT PREVENTER FOR VARIOUS POSITIONS OF THE CLOSING PISTON

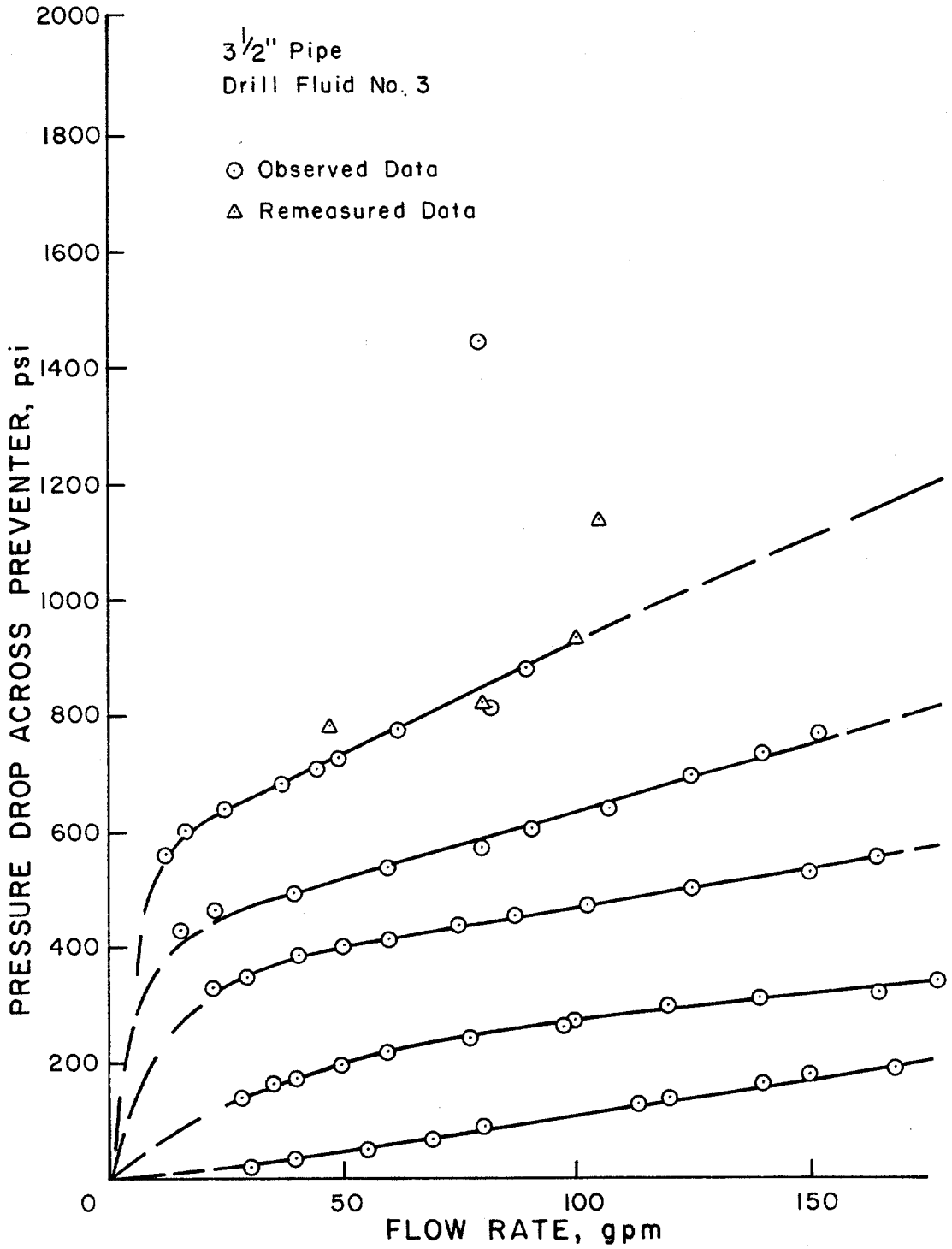

FIGURE 4.5. PRESSURE DROP THROUGH SPHERICAL BLOWOUT PREVENTER FOR VARIOUS POSITIONS OF THE CLOSING PISTON

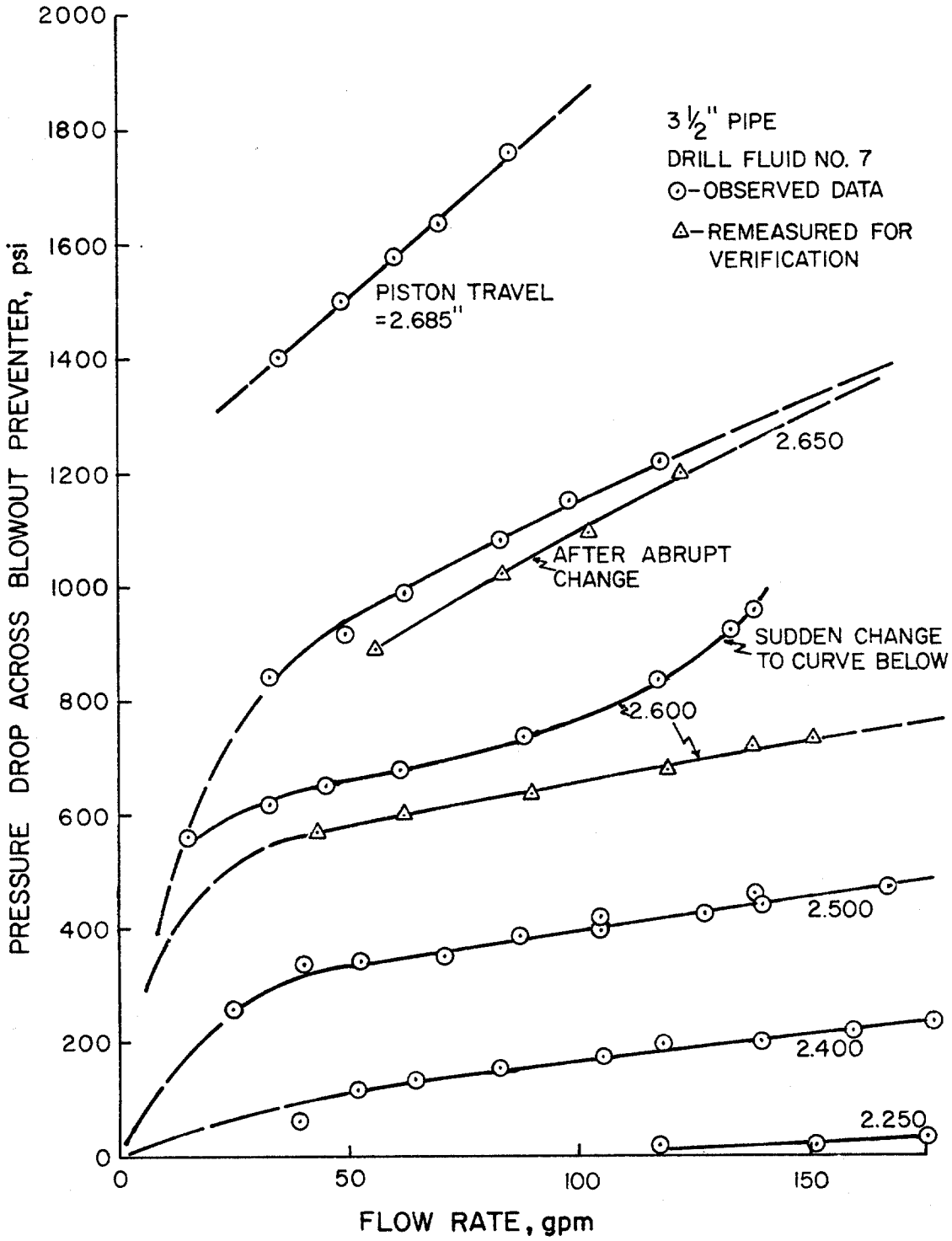

FIGURE 4.6. PRESSURE DROP THROUGH SPHERICAL BLOWOUT PREVENTER FOR VARIOUS POSITIONS OF THE CLOSING PISTON

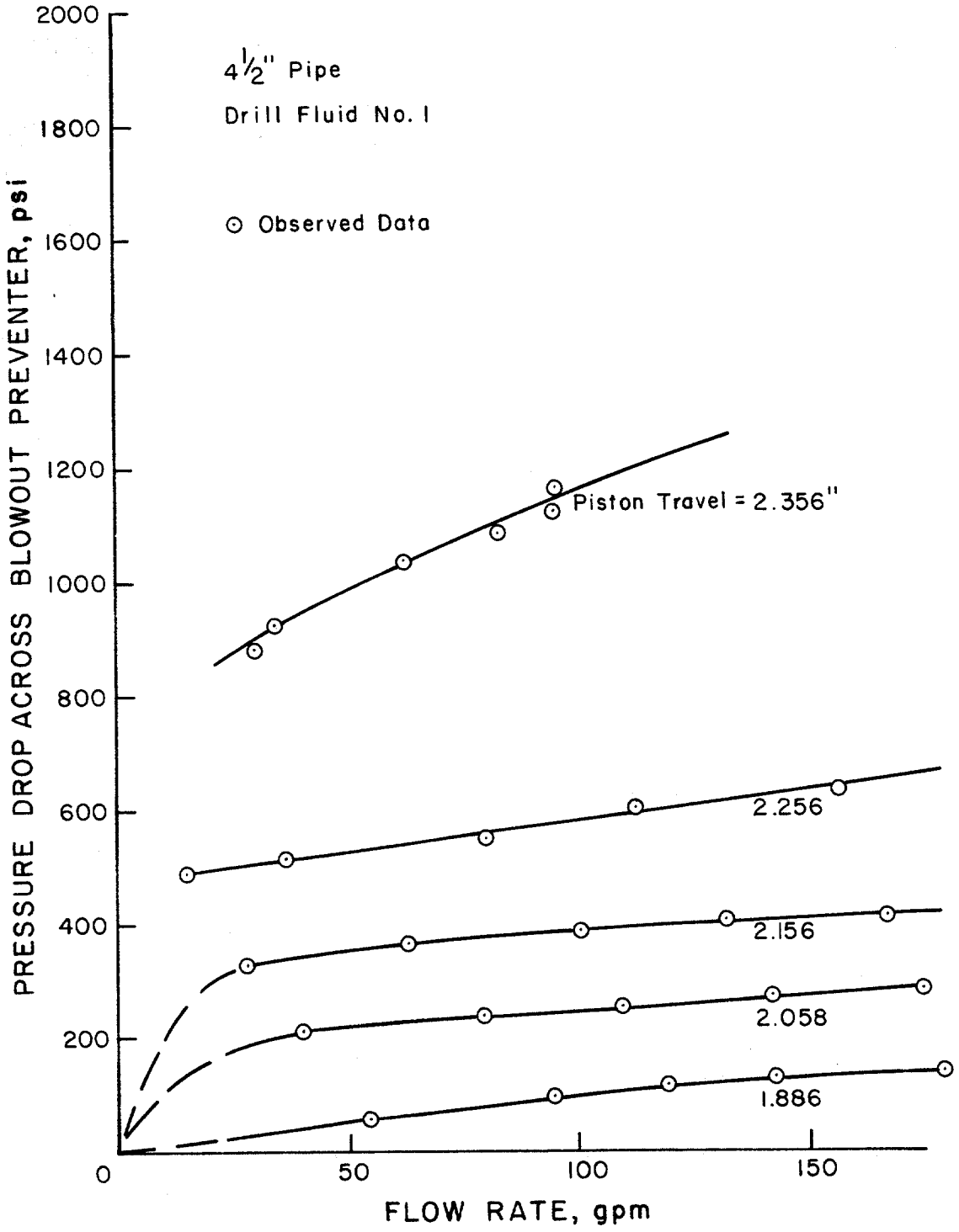

FIGURE 4.7. PRESSURE DROP THROUGH SPHERICAL BLOWOUT PREVENTER FOR VARIOUS POSITIONS OF THE CLOSING PISTON

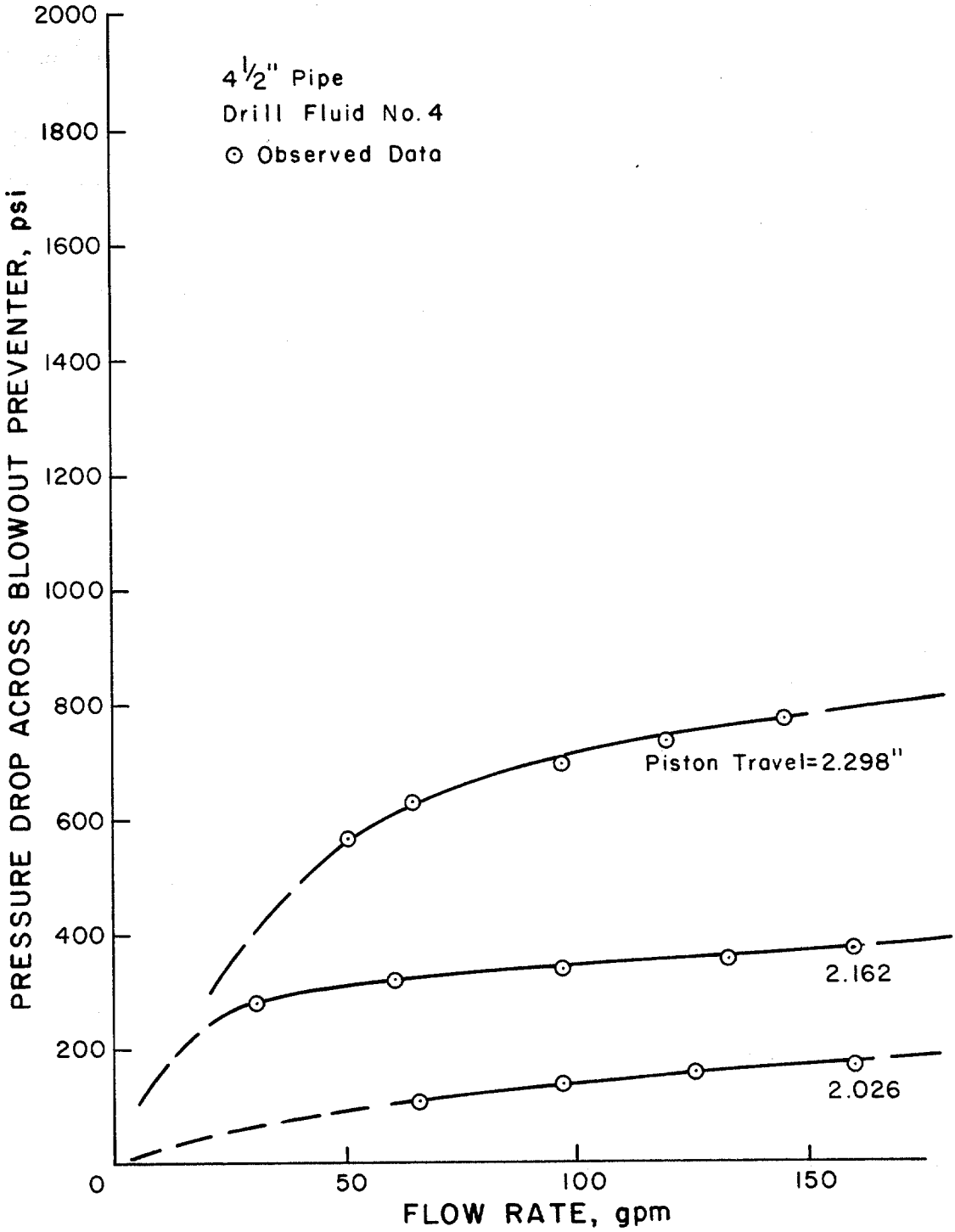

FIGURE 4.8. PRESSURE DROP THROUGH SPHERICAL BLOWOUT PREVENTER FOR VARIOUS POSITIONS OF THE CLOSING PISTON

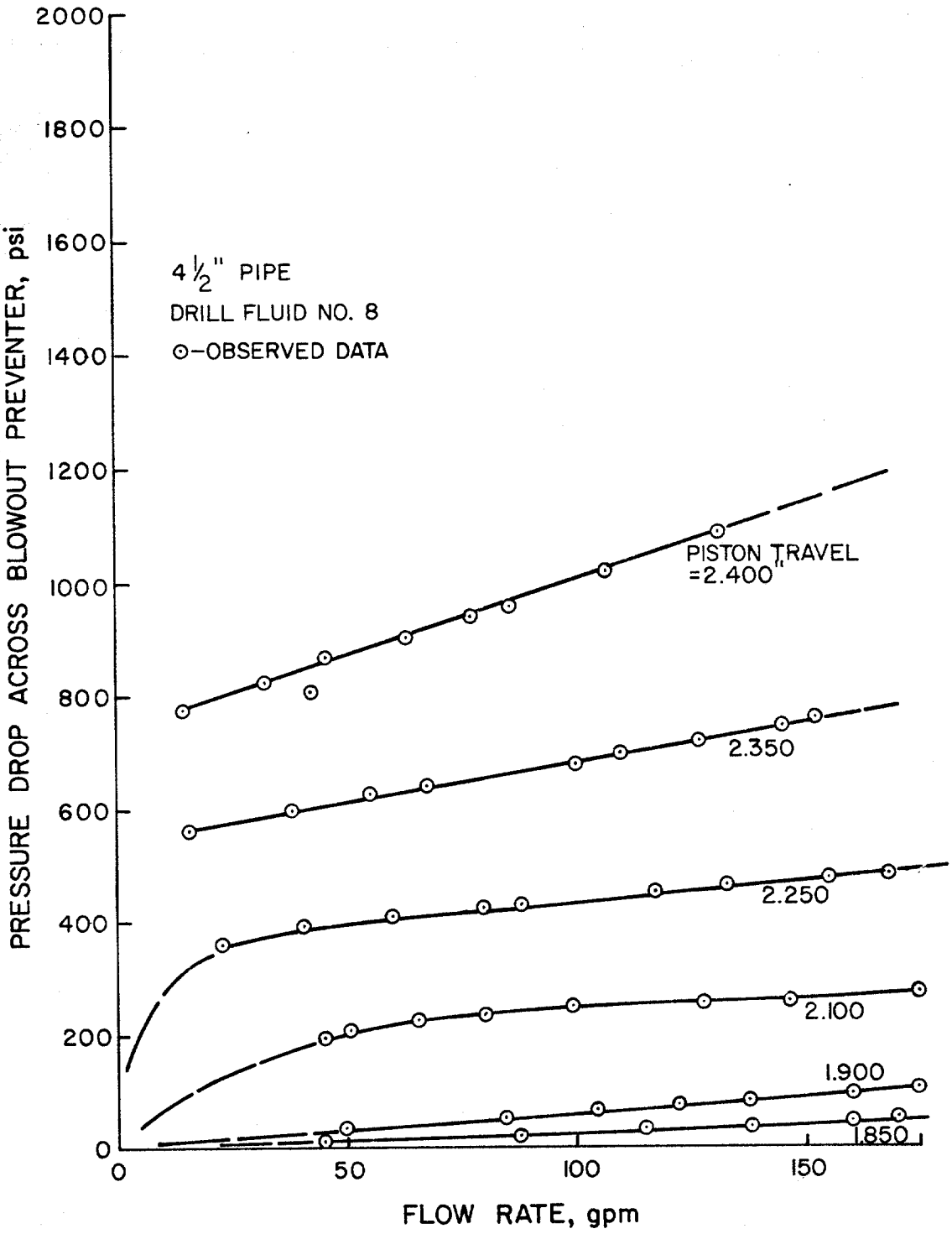

FIGURE 4.9. PRESSURE DROP THROUGH SPHERICAL BLOWOUT PREVENTER FOR VARIOUS POSITIONS OF THE CLOSING PISTON

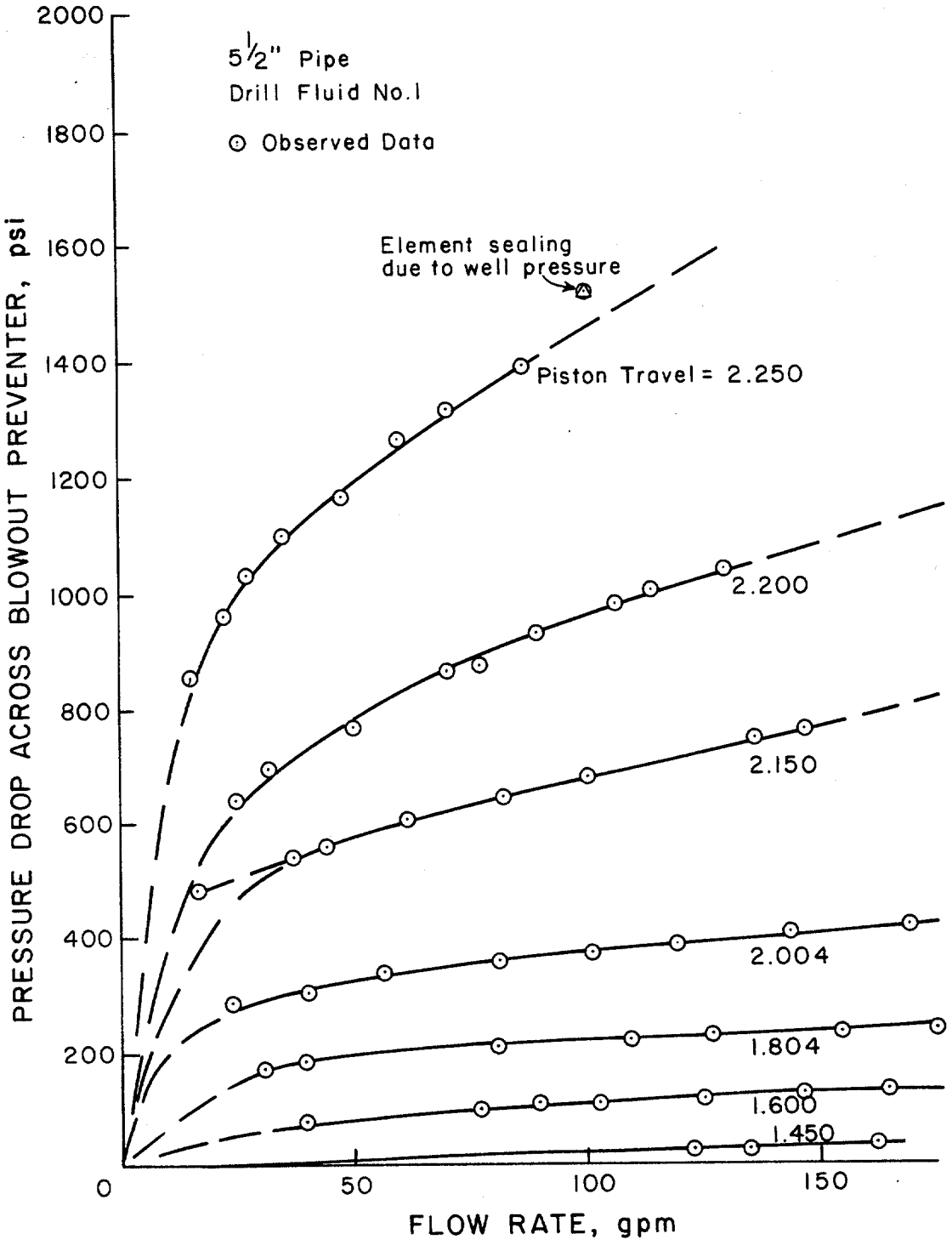

FIGURE 4.10. PRESSURE DROP THROUGH SPHERICAL BLOWOUT PREVENTER FOR VARIOUS POSITIONS OF THE CLOSING PISTON

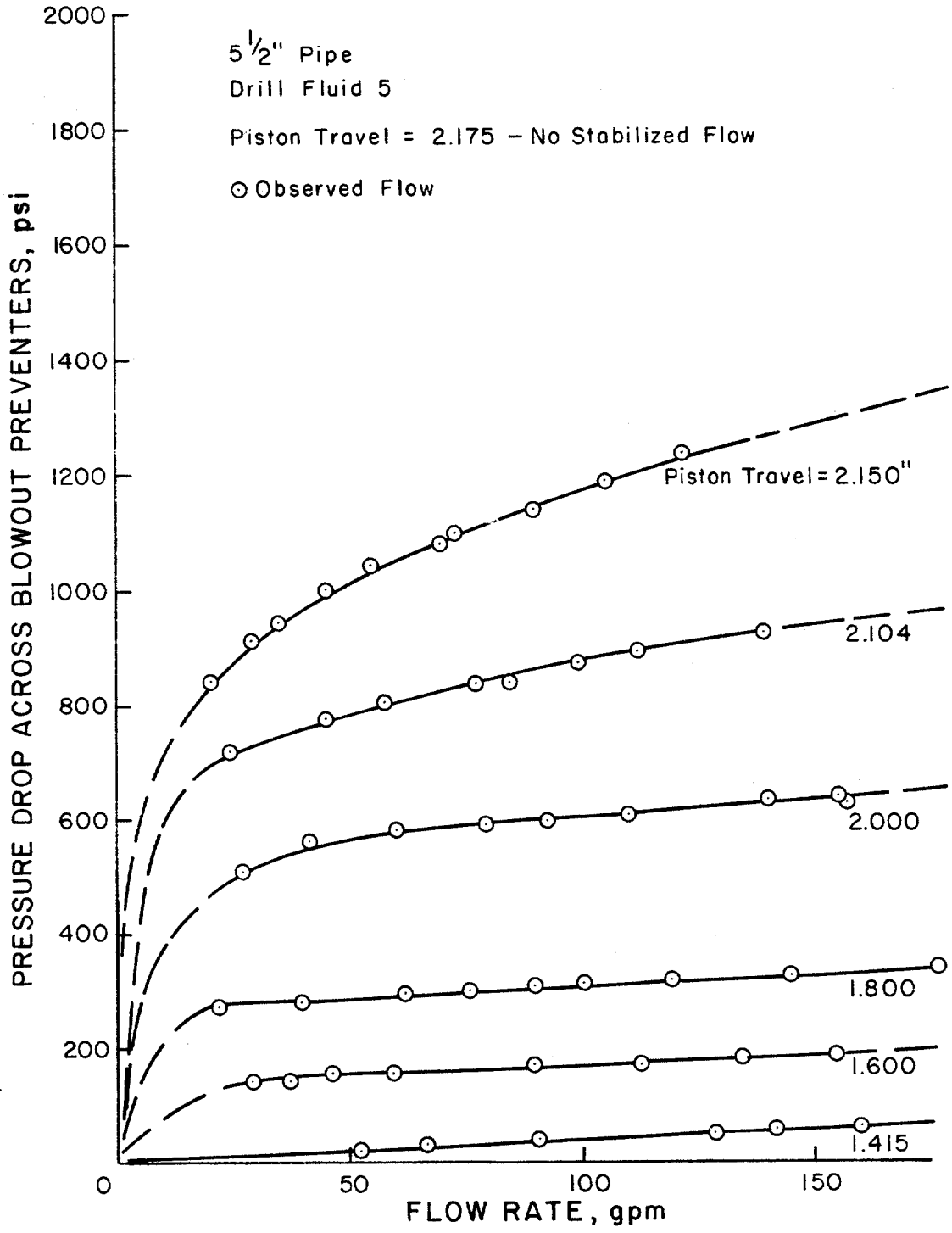

FIGURE 4.11. PRESSURE DROP THROUGH SPHERICAL BLOWOUT PREVENTER FOR VARIOUS POSITIONS OF THE CLOSING PISTON

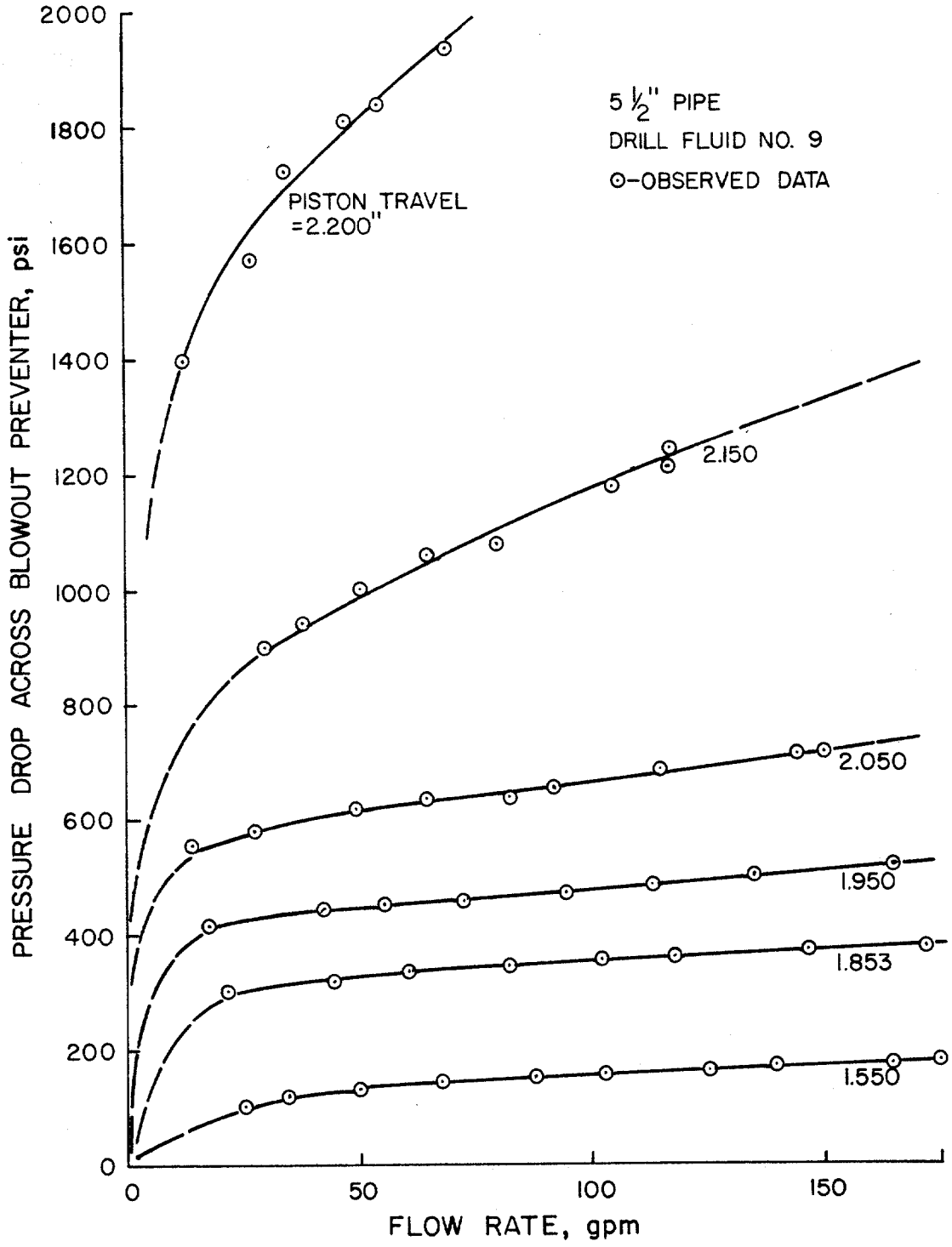

FIGURE 4.12. PRESSURE DROP THROUGH SPHERICAL BLOWOUT PREVENTER FOR VARIOUS POSITIONS OF THE CLOSING PISTON

results for the various annular geometries and drilling fluids. Each figure shows pressure drop across the blowout preventer as a function of flow rate for various positions of the piston in the blowout preventer. As seen in the previous chapter the piston movement can be used as a gage of the degree of closure for the blowout preventer. The data for each figure are also presented in tabular form in the Appendix, with the table numbers corresponding to figure numbers. For instance, Table A.1 represents the same data as Figure 4.1. Several interesting observations can be made concerning the data plots.

The most obvious observation which can be made from the data presented here is that, regardless of fluid type or pipe size in the hole, the flow is essentially unrestricted until a fairly high degree of closure is attained. For instance, in Figure 4.1, the pressure drop across the blowout preventer is negligible until the piston has traveled approximately 2.5 in. In contrast, movement of the piston from 2.583 to 3.803 in., only 22 hundreds of an inch, produces a very large increase in pressure drop. For the conditions in Figure 4.1, the blowout preventer was full closed with a total piston travel of 2.96 in. The piston must travel 85% of its total traverse before any significant restriction of the flow is realized. The actual shut-in can be attributed to the final 15% of total piston

travel.

As shown in Chapter 2, rapid closure of a valve in a pipeline produces a water hammer pressure surge approaching that of instantaneous closure. More gradual closure, where the closure time, t_c, is greater than the time for a pressure wave to be reflected from the upstream end of the system, produces a less intense pressure rise. The above results seem to support the theory that a hard shut-in could produce surge pressures comparable to a rapid valve closure. Even if the total time to close the blowout preventer is long enough to constitute a slow closure, the behavior of the blowout preventer could effectively reduce the actual closing time and produce a rapid closure with a correspondingly higher pressure. This effect in itself is not, however, grounds to disapprove of the hard shut-in since the magnitude and propagation of the pressure surges in the wellbore have yet to be analyzed.

The varying behavior of the rubber sealing elements seems to be a dominant factor in the characteristics of the blowout preventer during closure. The rubber element is deformed as it is forced upward and inward by the piston. The piston position is therefore used to gage the degree of closure of the blowout preventer. However, the data of Figures 4.5 and 4.6 show inconsistent results for measurements made at the same piston positions. For instance, in Figure 4.6, the upper curve

at a piston position of 2.600 was obtained and then the data was remeasured without moving the piston. There is a considerable difference between the two curves. Inconsistencies are also shown by the total travel required to achieve full closure of the preventer. The configuration of the rubber element, and thus the area open to flow, seems to change each time the element is exercised. Therefore, even though the exact piston position can be reproduced, the exact flow restriction can never be duplicated, and some degree of irreproducibility can be expected owing to the deformation characteristics of the rubber element.

The slope of the pressure drop - flow rate curves also seems to be influenced by the behavior of the rubber sealing element. The curves are uncharacteristically flat for certain ranges of piston position between the initial pressure response and the full closed position. Figure 4.1 illustrates this point rather well.

Assuming laminar flow in a closed conduit, if the flow rate is doubled, then the pressure drop through the conduit should also be doubled. Turbulent flow would produce an even larger increase in the pressure drop through the conduit. In the case of an orifice, the pressure drop increase due to an increase in flow rate is much the same as for turbulent flow in a conduit. However, referring to Figure 4.1, for piston positions from approximately 2.70 to 2.77 in., the

increase in pressure drop does not correspond to the increase in flow rate as expected. For a piston position of 2.723 in., the pressure drop increases from 340 psi at 50 gpm to 495 psi at 100 gpm, an increase of only 45%. However, for a piston position of 2.803, the pressure drop increases from 1080 psi at 50 gpm to 2100 psi at 100 gpm (from extrapolation), which is close to the expected behavior for laminar flow. It still, however, is not as large of an increase as would be expected for flow through an orifice.

The response of the rubber element to increases in pressures and flow rates may account for the unexpected behavior above. With the blowout preventer piston stationary, as the flow rate is increased the rubber element seems to deform or "breathe", assuming a different configuration or area open to flow. The pressure drop across the preventer is increased less than for a rigid flow restriction. As the piston approaches the full closed position, the rubber seems to lose its ability to relieve itself or "breathe". This may be due to the higher pressure encountered under these conditions compressing the rubber. Whatever the reason, the slope of the pressure drop - flow rate curves increases as the blowout preventer element approaches full closure and increases in flow rate seem to induce more reasonable increases in pressure drop across the blowout preventer.

4.2 Valve Coefficients for the Spherical Blowout Preventer

The valve industry often uses a valve coefficient, C_v, to characterize the pressure drop across a valve for any flow rate. The parameter is used in this study to characterize flow rate and pressure drop through the 7-1/16 in. spherical blowout preventer. Values of C_v were calculated, using Equation (2.27), for various positions of the piston and various flow rates. Figures 4.13 through 4.24 show C_v plotted as a function of piston position for various flow rates from 25 gpm to 175 gpm.

In dealing with valves, the valve coefficient is often assumed to be constant, regardless of the flow rate or pressure across the valve. It was found from the results of this investigation that, for a constant piston position, the value of C_v is not constant. Instead of a single curve representing C_v as a function of piston position, the results show a family of curves, each representing C_v as a function of piston position for a different flow rate.

Although Figures (4.13) through (4.24) each represent different annular geometries and/or fluid properties, the same general trends are apparent in the curves of C_v. For the blowout preventer in the full open position, the pressure drop across the preventer is negligible and the value of C_v approaches infinity. The value of C_v remains very high until the piston reaches the point where

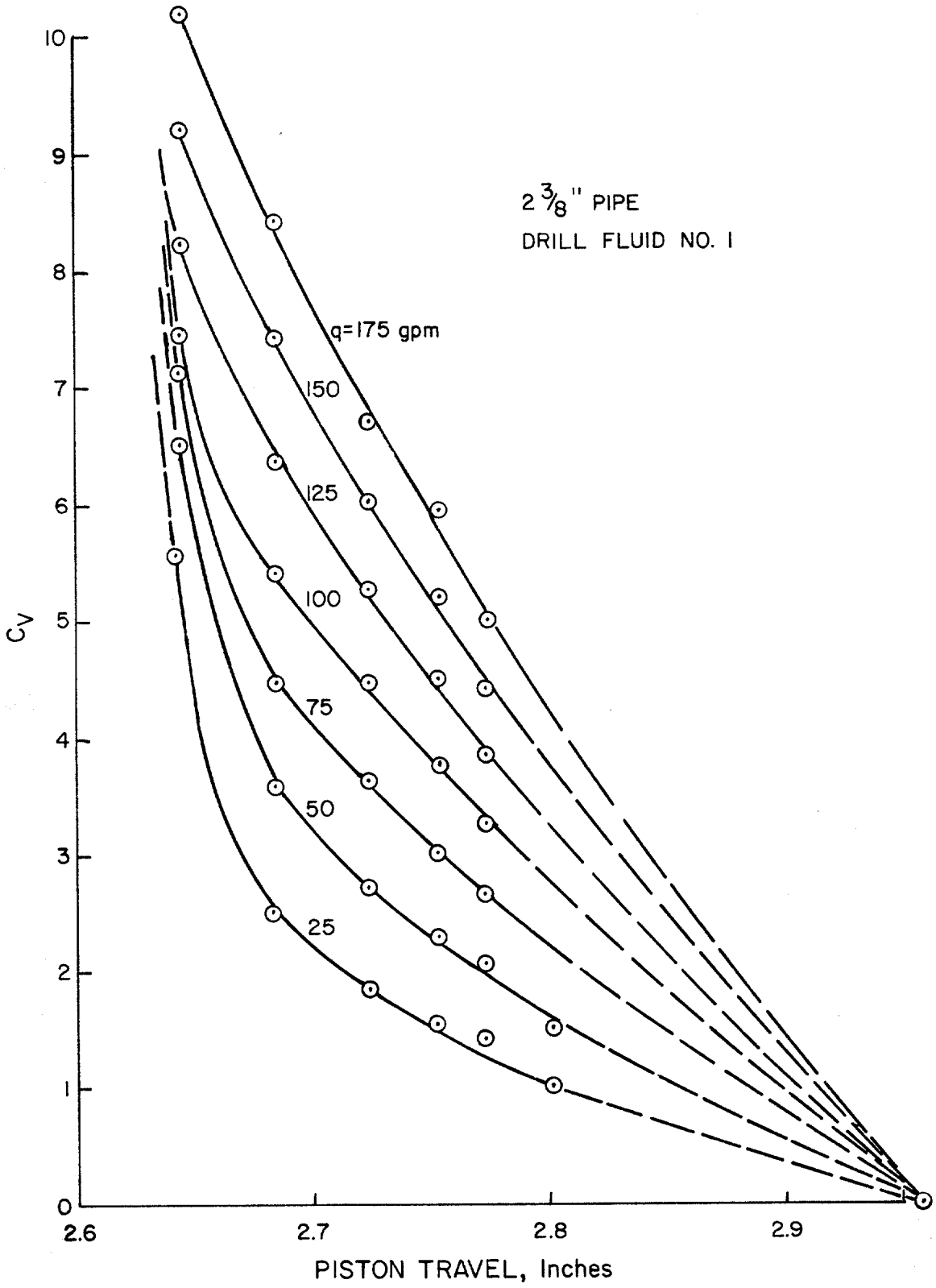

FIGURE 4.13. VALVE COEFFICIENT , C_v, AS A FUNCTION OF PISTON POSITION FOR SPHERICAL BLOWOUT PREVENTER

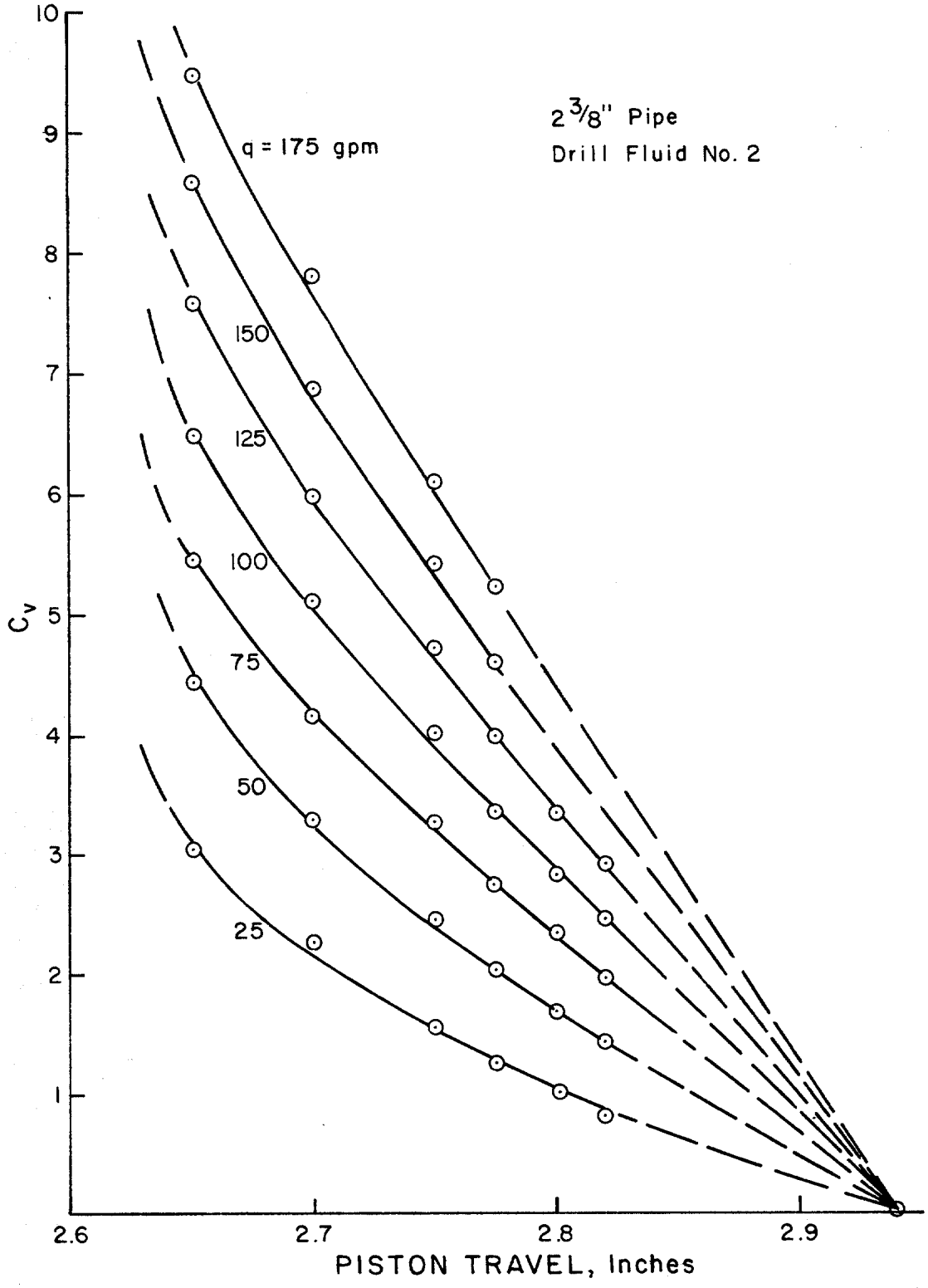

FIGURE 4.14. VALVE COEFFICIENT, C_v, AS A FUNCTION OF PISTON POSITION FOR SPHERICAL BLOWOUT PREVENTER

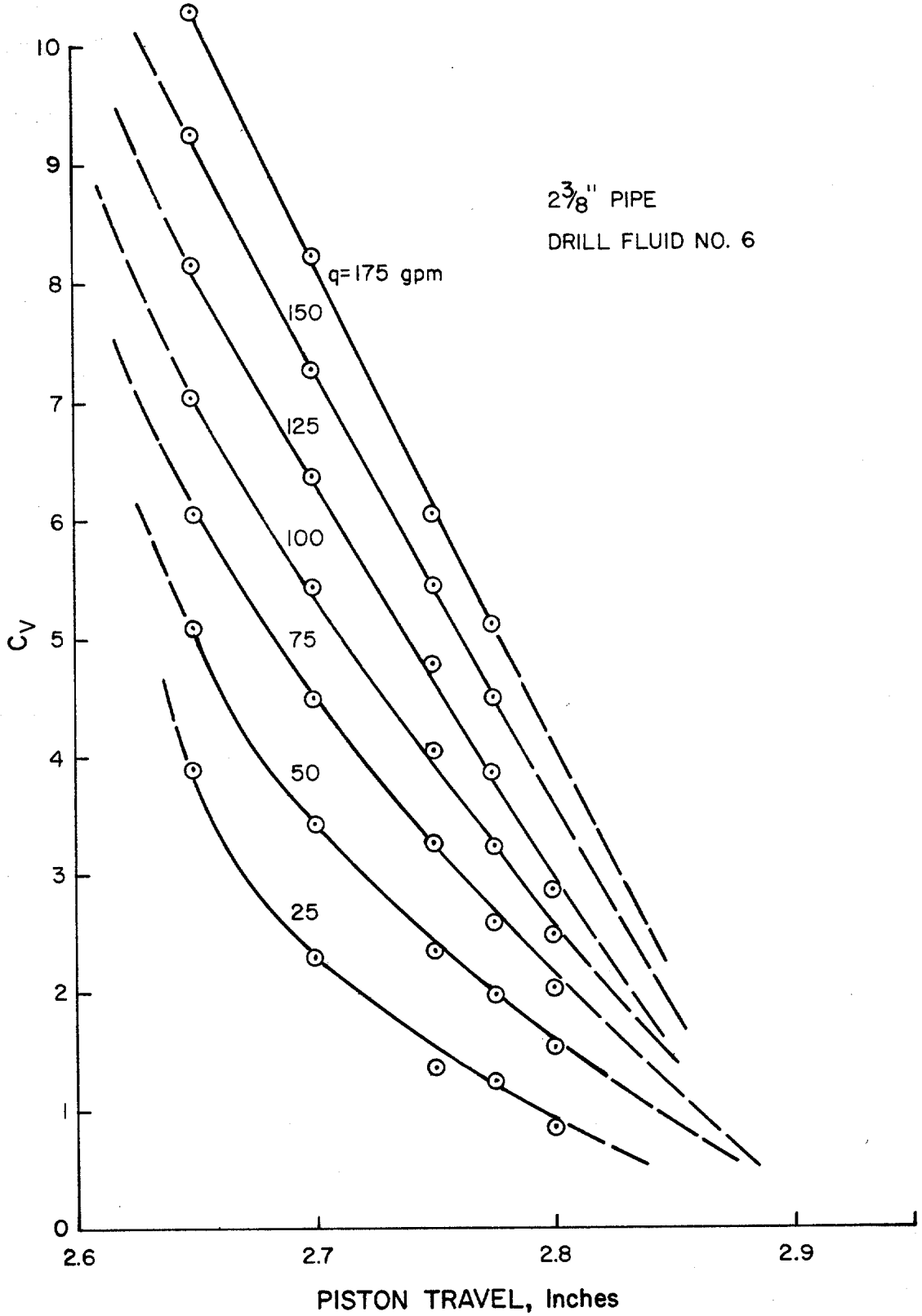

FIGURE 4.15. VALVE COEFFICIENT, C_v, AS A FUNCTION OF PISTON POSITION FOR SPHERICAL BLOWOUT PREVENTER

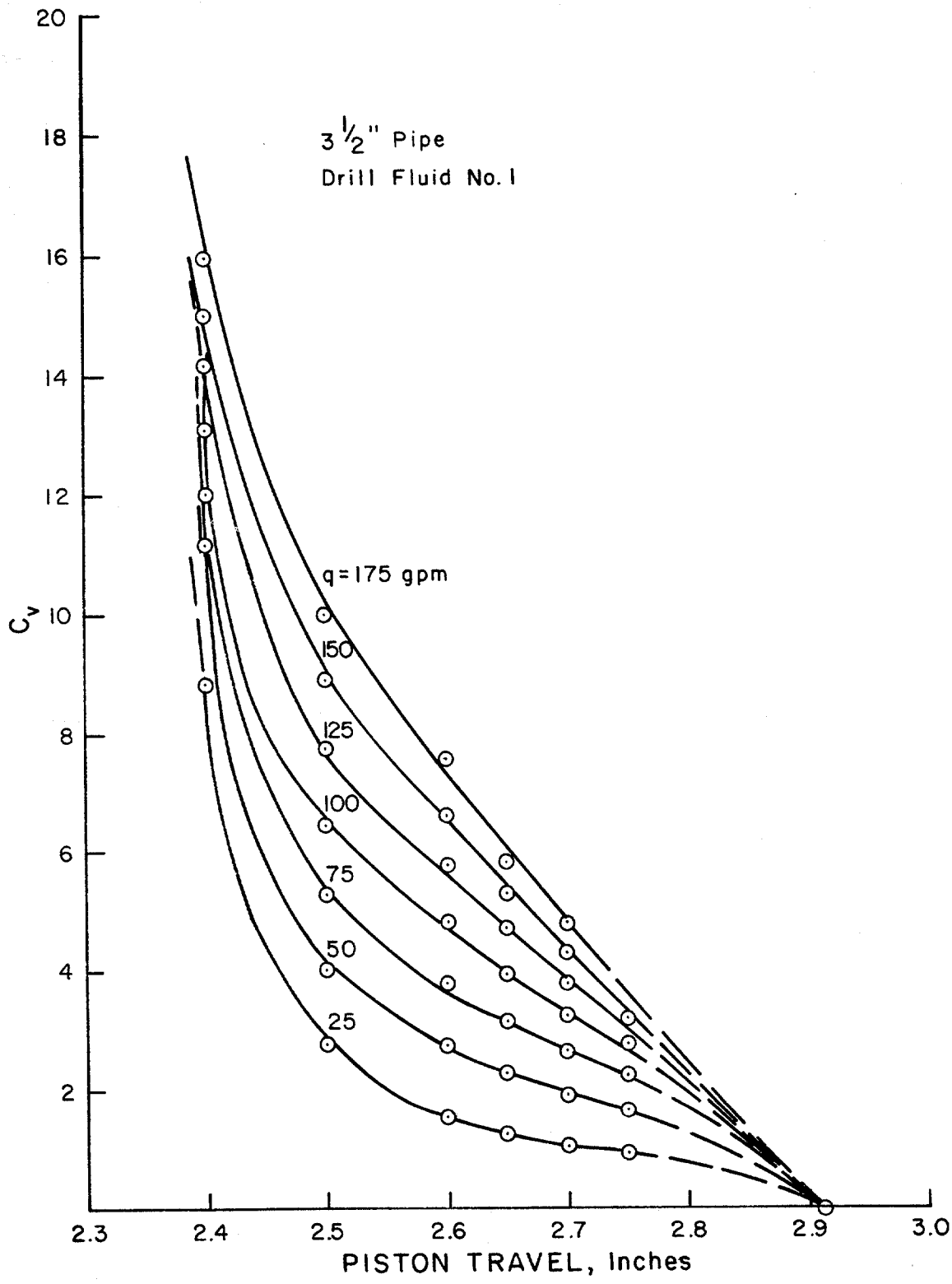

FIGURE 4.16. VALVE COEFFICIENT, C_v, AS A FUNCTION OF PISTON POSITION FOR SPHERICAL BLOWOUT PREVENTER

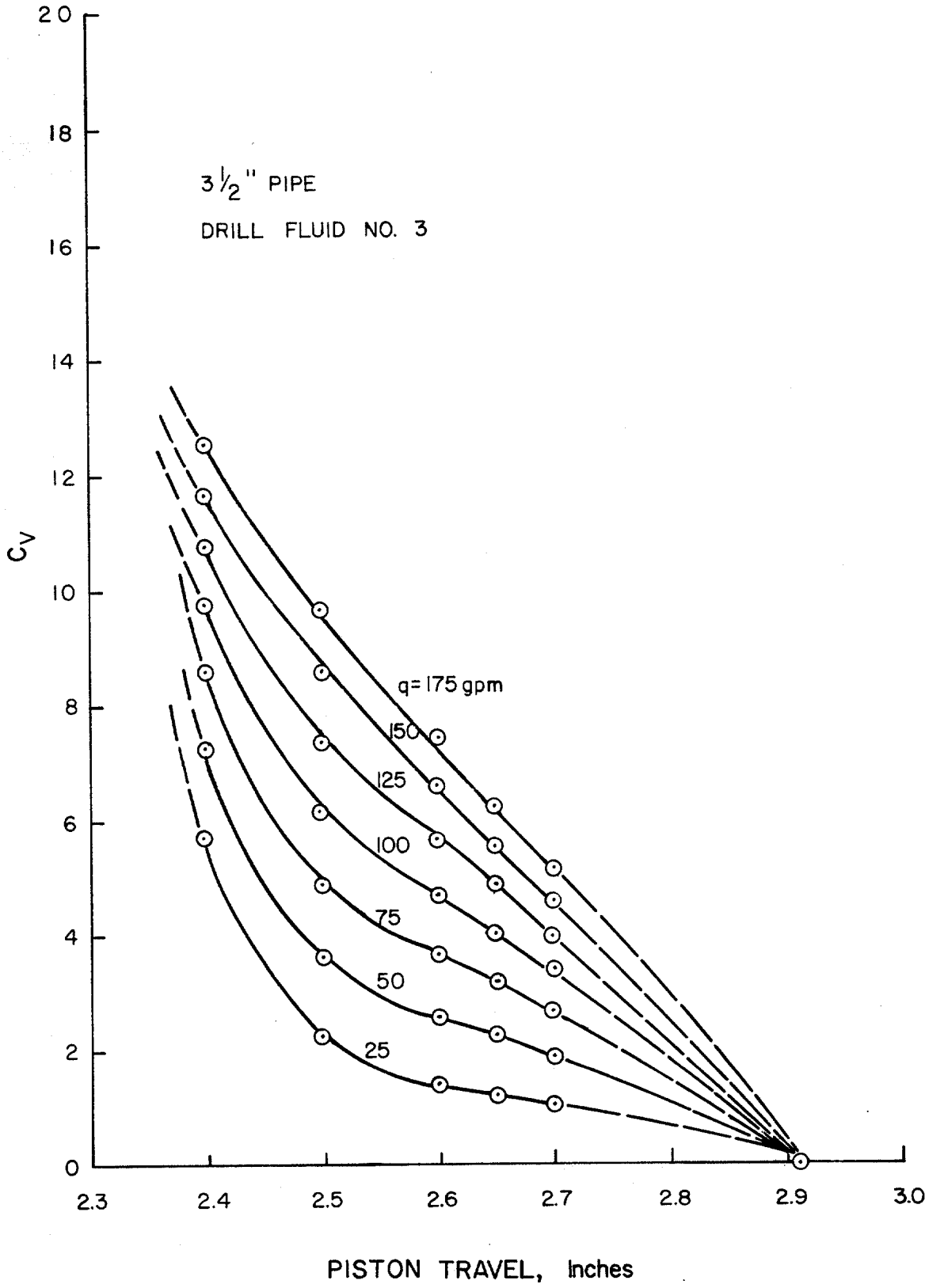

FIGURE 4.17. VALVE COEFFICIENT, C_v, AS A FUNCTION OF PISTON POSITION FOR SPHERICAL BLOWOUT PREVENTER

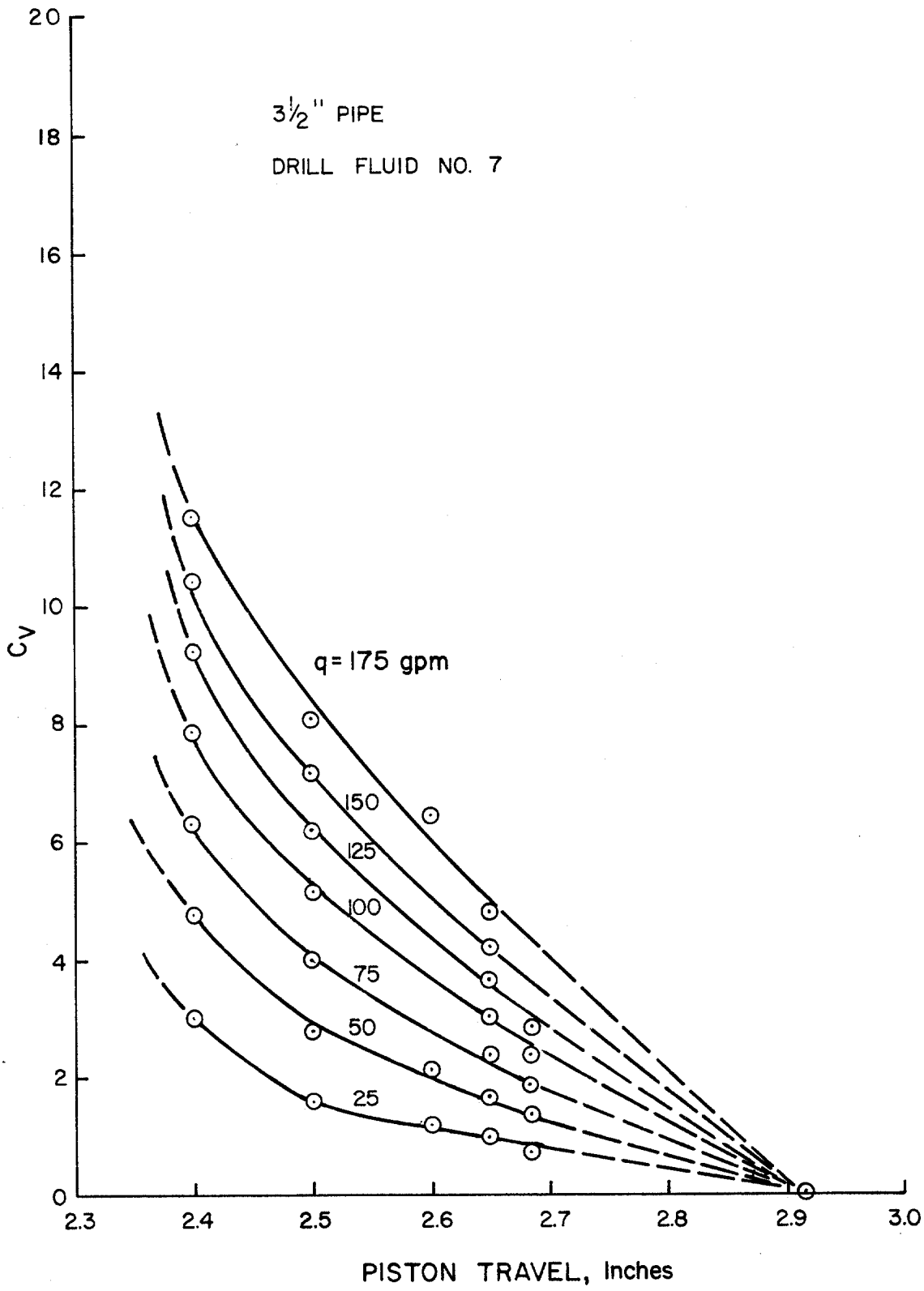

FIGURE 4.18. VALVE COEFFICIENT, C_v, AS A FUNCTION OF PISTON POSITION FOR SPHERICAL BLOWOUT PREVENTER

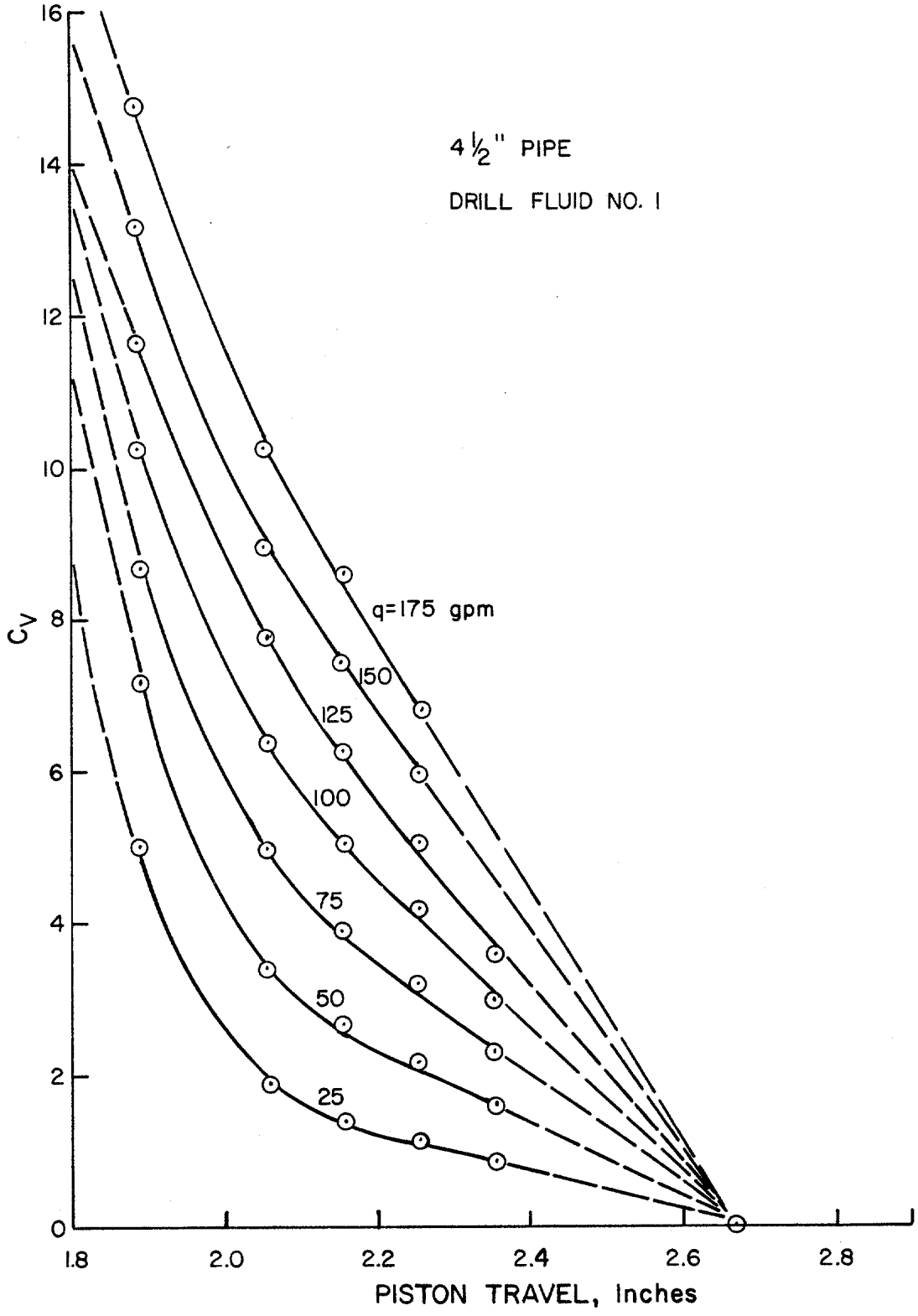

FIGURE 4.19. VALVE COEFFICIENT, C_v, AS A FUNCTION OF PISTON POSITION FOR SPHERICAL BLOWOUT PREVENTER

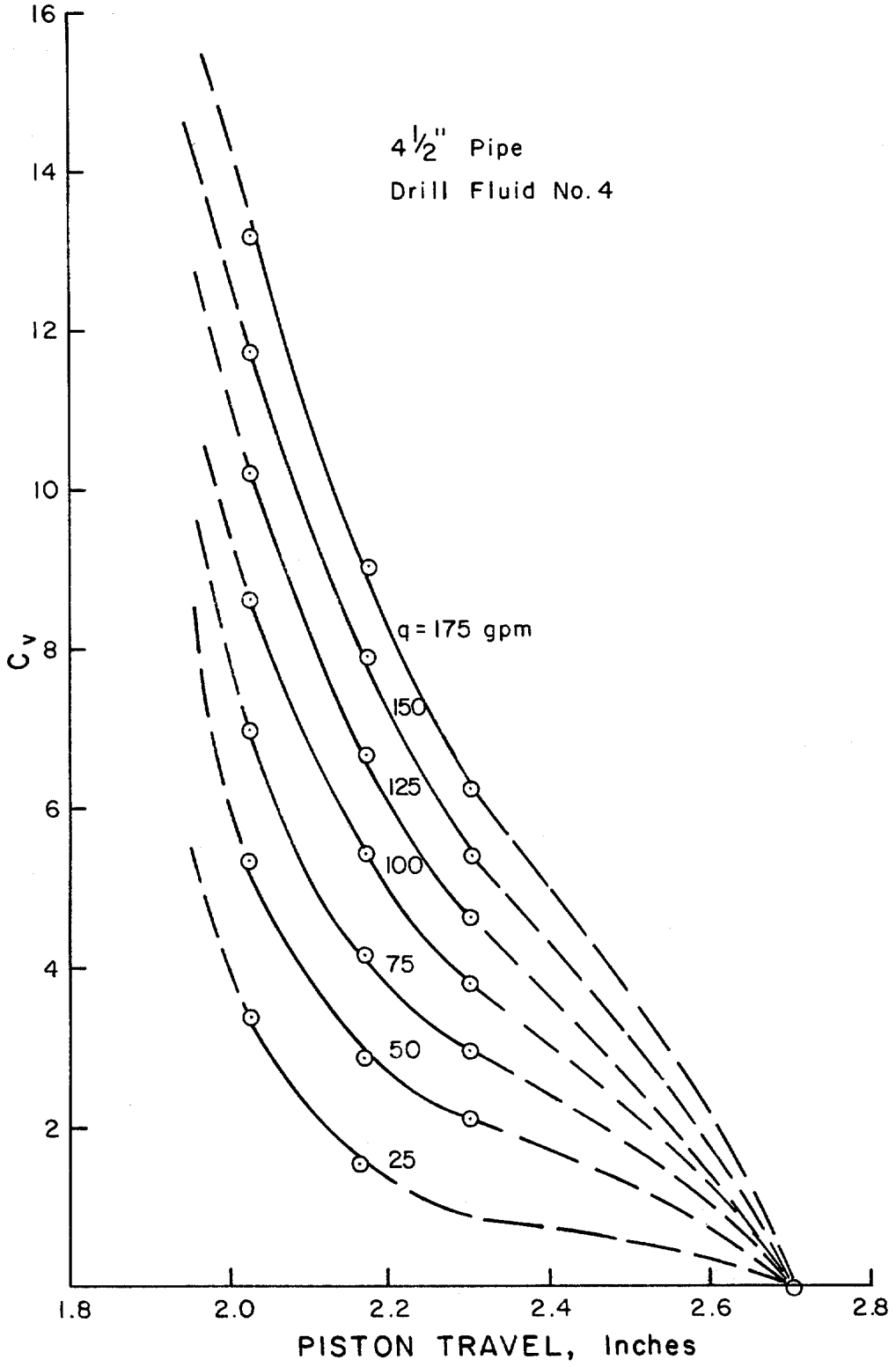

FIGURE 4.20. VALVE COEFFICIENT, C_v, AS A FUNCTION OF PISTON POSITION FOR SPHERICAL BLOWOUT PREVENTION

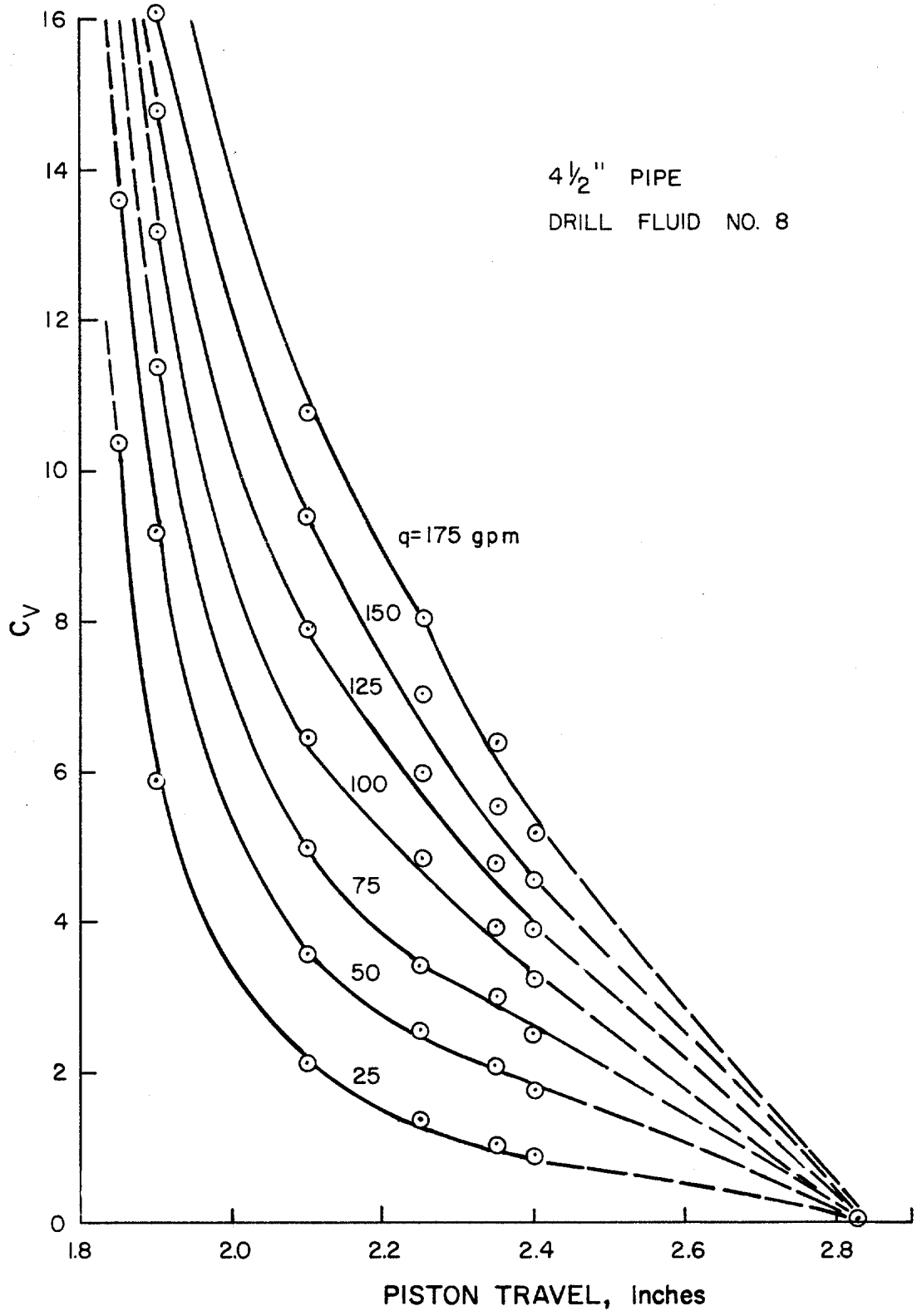

FIGURE 4.21. VALVE COEFFICIENT, C_v, AS A FUNCTION OF PISTON POSITION FOR SPHERICAL BLOWOUT PREVENTER

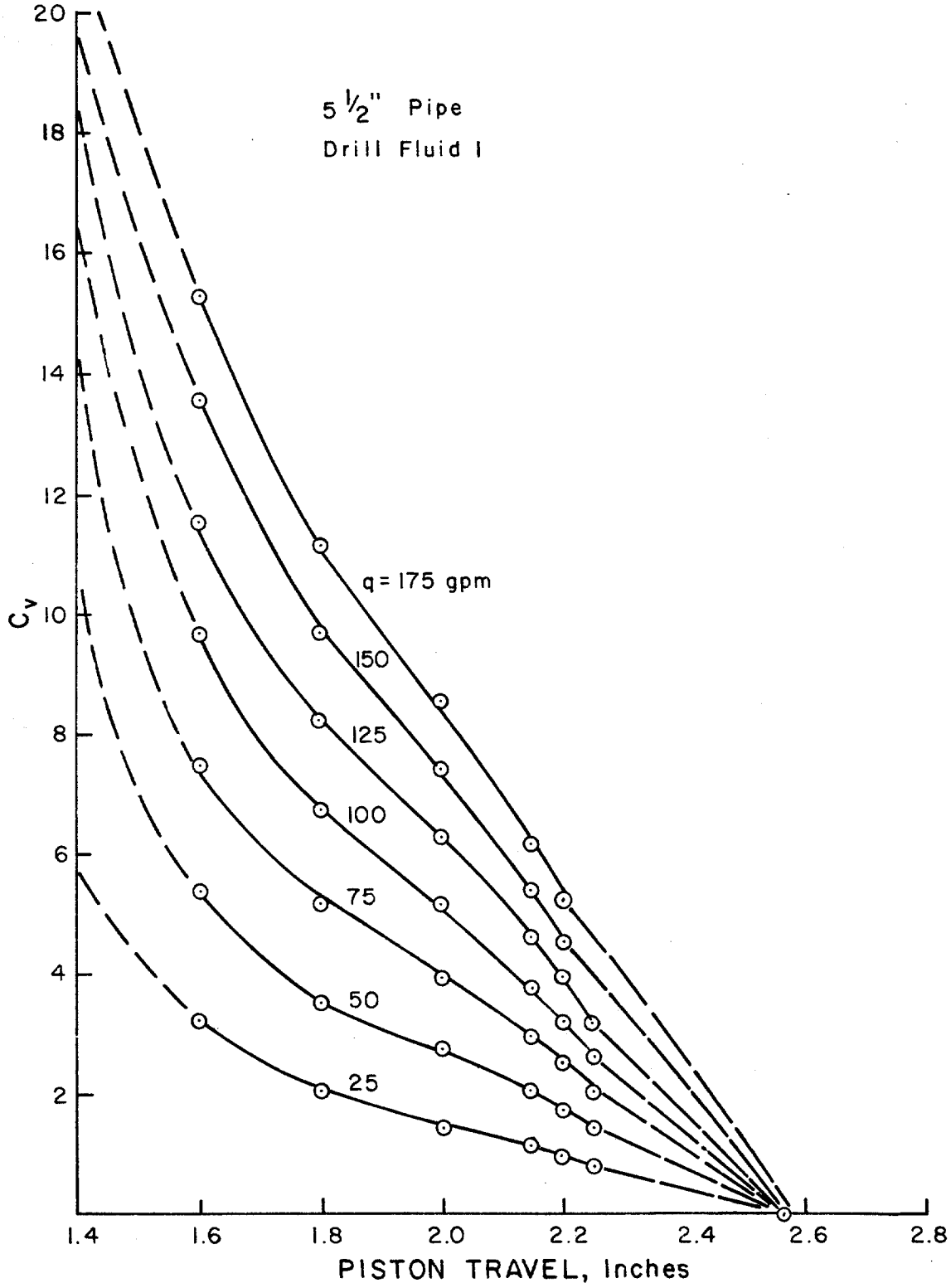

FIGURE 4.22. VALVE COEFFICIENT, C_v, AS A FUNCTION OF PISTON POSITION FOR SPHERICAL BLOWOUT PREVENTER

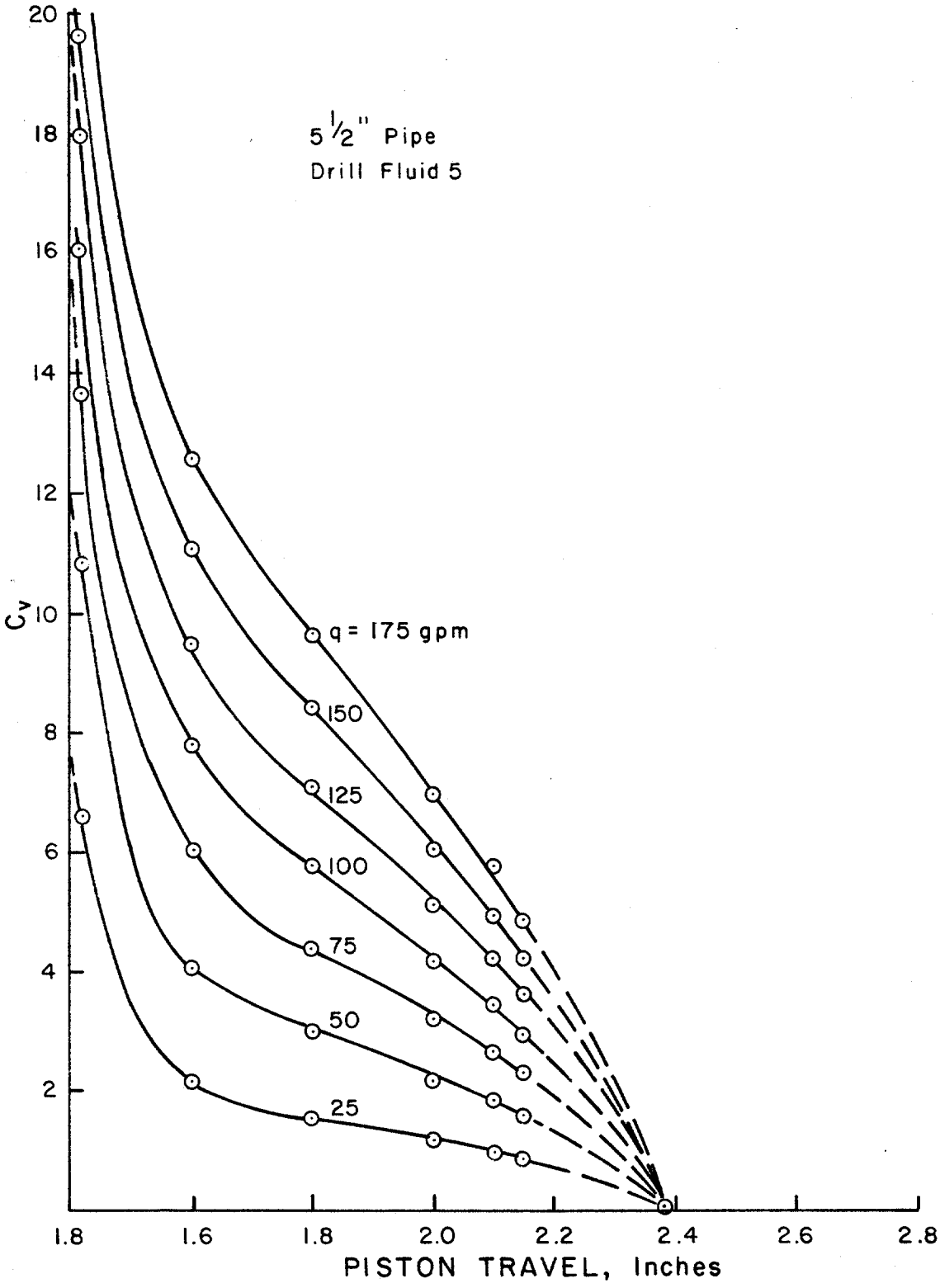

FIGURE 4.23. VALVE COEFFICIENT, C_v, AS A FUNCTION OF PISTON POSITION FOR SPHERICAL BLOWOUT PREVENTER

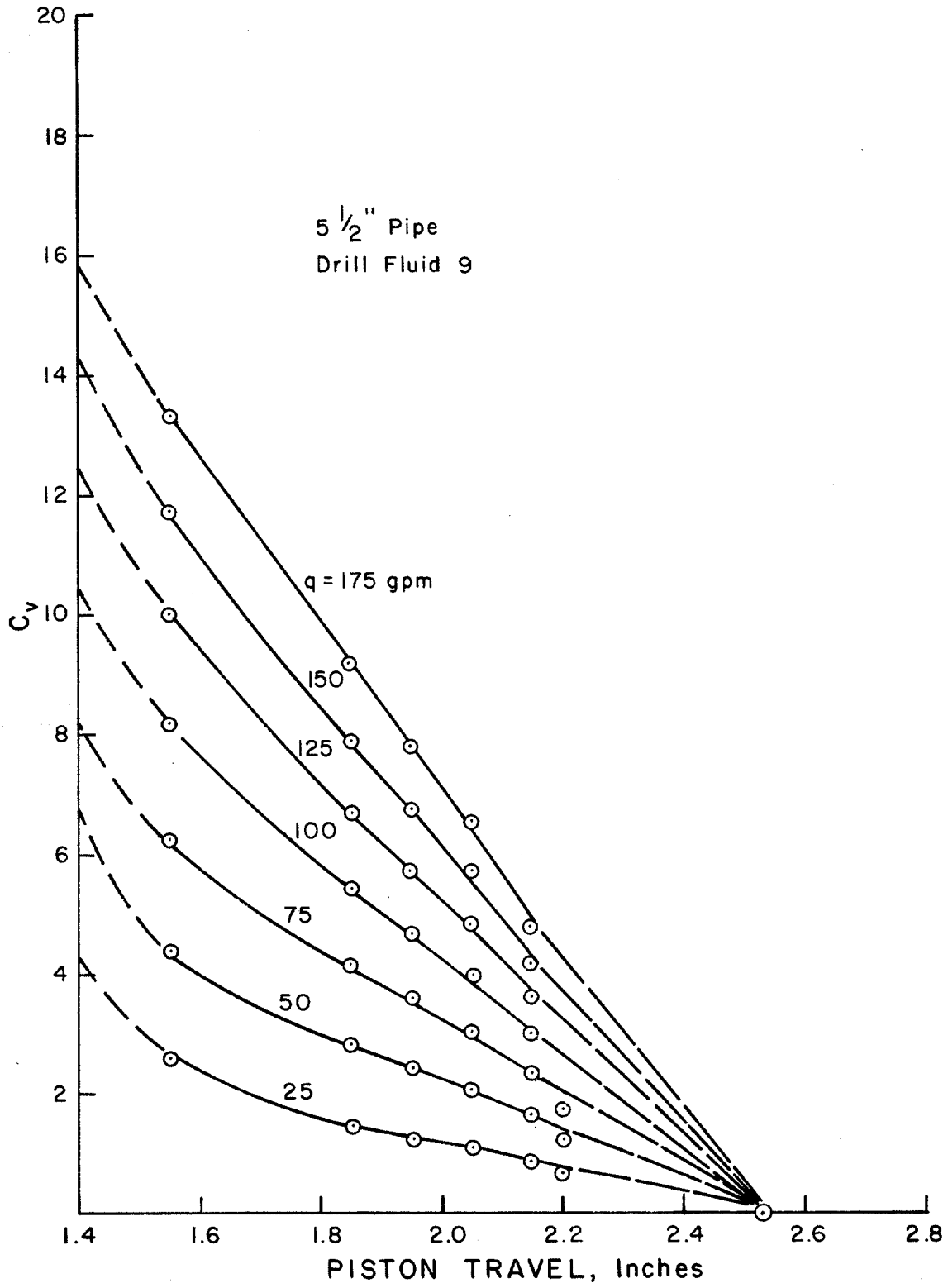

FIGURE 4.24. VALVE COEFFICIENT, C_v, AS A FUNCTION OF PISTON POSITION FOR SPHERICAL BLOWOUT PREVENTER

the initial restriction to flow is felt. Then, if the flow rate remains constant, as the piston moves upward, C_c decreases uniformly until, at full closed, C_v is equal to 0.

It should be noted that Figures (4.13) through (4.24) were obtained under steady-state flow conditions. However, since no acceptable description of the pressure drop - flow rate characteristics of the blowout preventer during closure is available, these curves can provide an approximation of the blowout preventer behavior during closure.

Figure 4.25 is a plot of the volume of accumulator fluid which must be pumped into the closing chamber of the blowout preventer to displace the piston to a given position. Using this figure, C_v can be represented as a function of volume pumped. This is needed if the behavior of the blowout preventer piston is to be combined with the characteristics of the hydraulic accumulator in a mathematical simulation program. The characteristics of the accumulator system is not addressed in this study.

4.3 Anomalous Fluid Viscosity Effects

Some of the data obtained in this study seem to indicate that the viscosity of the fluid affects the pressure drop produced by a given flow rate through the blowout preventer. Figure 4.26 shows pressure drop data For flow through the annular preventer with 3-1/2 in.

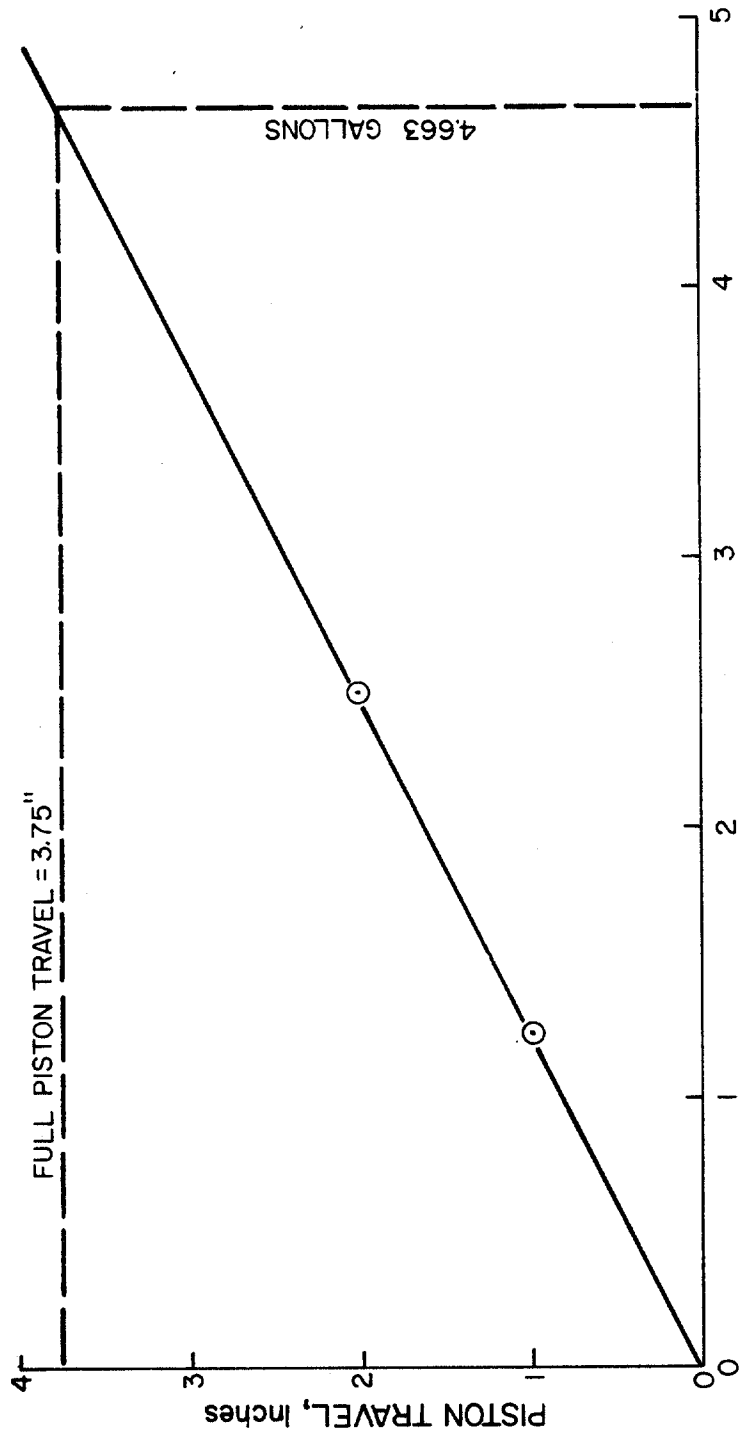

FIGURE 4.25. PISTON TRAVEL AS FUNCTION OF GALLONS OF ACCUMULATOR FLUID APPLIED TO CLOSING CHAMBER

pipe in the hole.

Three fluids of various viscosity are shown. The pressure drop is highest for the highest viscosity fluid and lowest for the lowest viscosity fluid. This seems to suggest that the pressure drop across the preventer is directly related to the viscosity of the fluid.

Referring to Figure 4.27, however, which shows data for 2-3/8 in. pipe in the hole, no evidence is shown to indicate a relation between the fluid viscosity and the pressure drop characteristics of the blowout preventer. In fact pressure losses for the high viscosity mud (6) are lower than for the low viscosity mud (2). Additional data for other geometries and viscosities shows similar results.

In light of the above evidence, the discrepancies between the results for various viscosity fluids can not be totally attributed to viscosity effects. Although viscosity may have a slight effect on the pressure drop characteristics it seems that the unpredictable deformation characteristics of the rubber element has a more dominant effect on the pressure drop across the blowout preventer. In other words, viscosity effects are relatively unimportant in comparison to the effects of the deformation behavior of the rubber element.

4.4 Annular Geometry Effects

The effects of the annular geometry (pipe size in

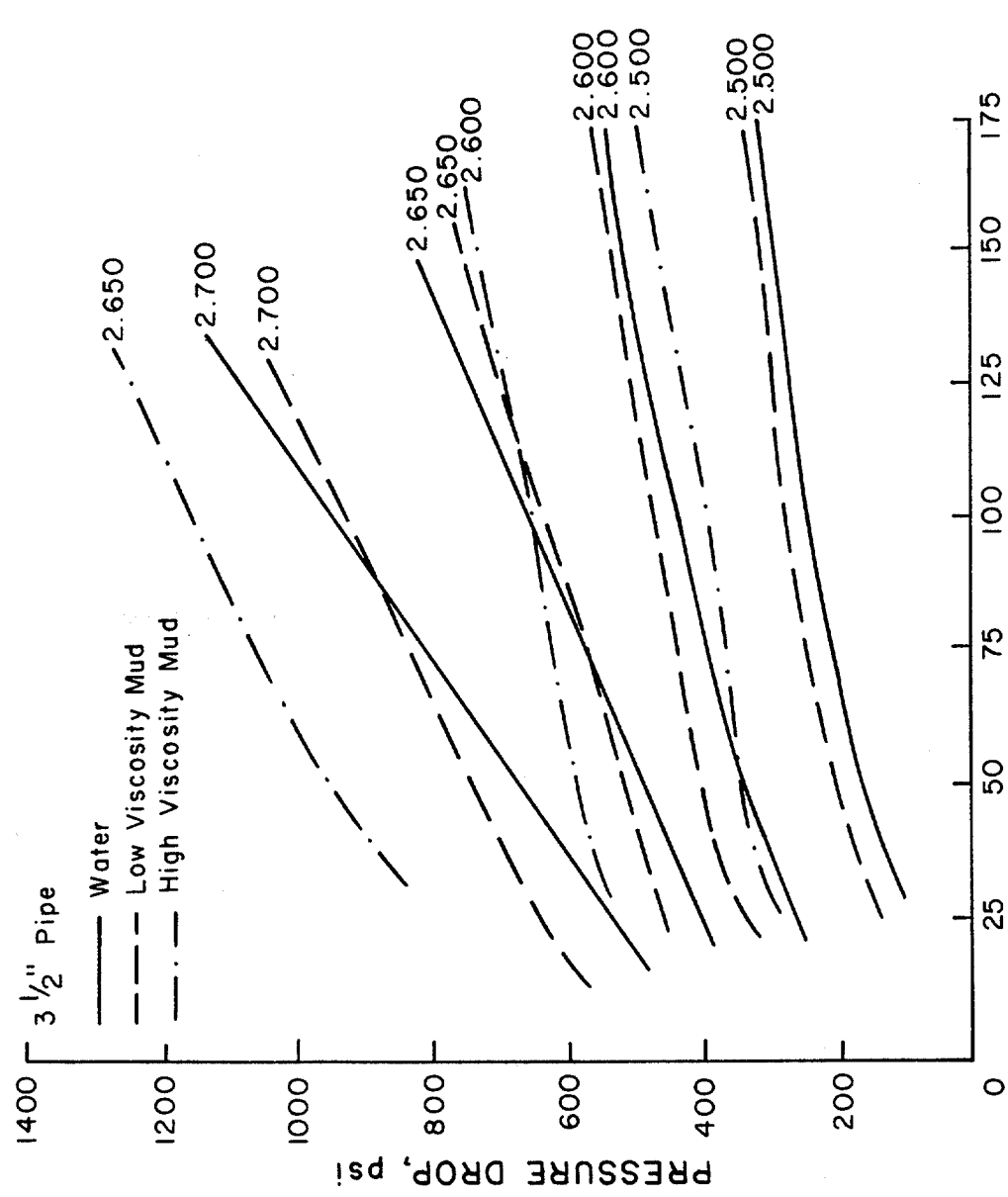

FIGURE 4.26. EFFECT OF VISCOSITY ON PRESSURE DROP–FLOW RATE CHARACTERISTICS OF SPHERICAL BLOWOUT PREVENTER.

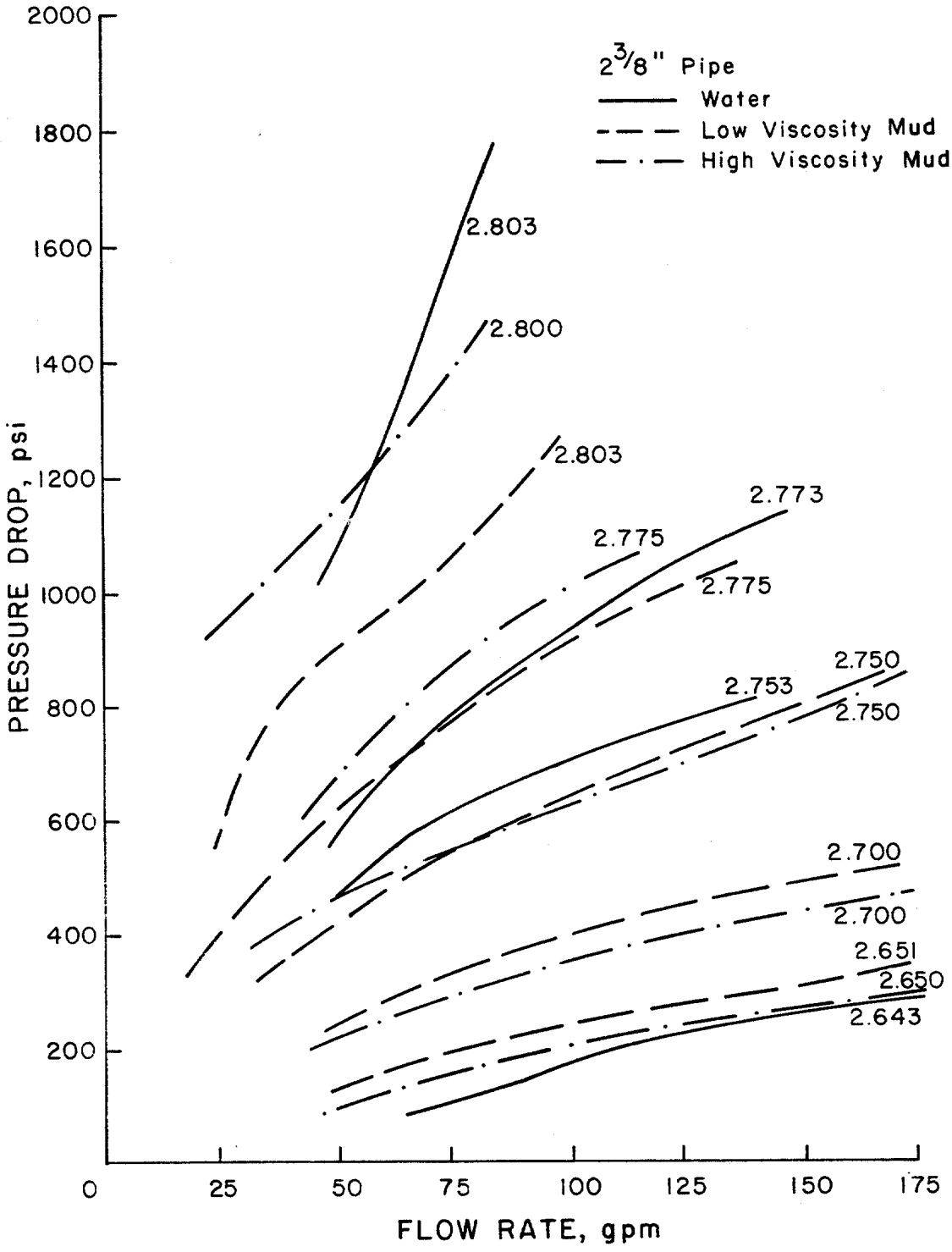

FIGURE 4.27. EFFECT OF VISCOSITY ON PRESSURE DROP–FLOW RATE CHARACTERISTICS OF SPHERICAL BLOWOUT PREVENTER.

hole) on the closing characteristics of the blowout preventer are quite evident from Figure 4.28. The plot shows the piston travel required to achieve the initial restriction to flow and the total piston travel to complete closure around pipes ranging in diameter from 0 to 7-1/16 in., the bore diameter of the blowout preventer.

Obviously the total travel of the piston to achieve full closure is less for the large diameter pipes. However, the plot also indicates that the intial pressure response occurs at a lower piston position for the larger diameter pipes than for the small diameter pipes. The initial response is produced sooner for larger pipe sizes, not only on the basis of actual piston travel, but also on the basis of the percentage of total piston travel. For instance, for closure on 3-3/8 in. pipe, the initial pressure response is shown at a piston position of 2.60 in. or 88% of the total piston travel from full open to full close. For a 4-1/2 in. pipe the initial pressure response occurs at a piston position of 2.00 in.,or 73% of the total piston travel.

Finally, the travel of the piston from the position where the initial pressure response occurs to the full closed position is, in general, longer for larger diameters. For instance the "effective" travel is only 0.4 in. for 2-3/8 in. pipe while for a 4-1/2 in. pipe the "effective" travel is 0.8 in. This response suggests a more gradual closure is achieved with large diameter

pipes in the hole than with small diameter pipes.

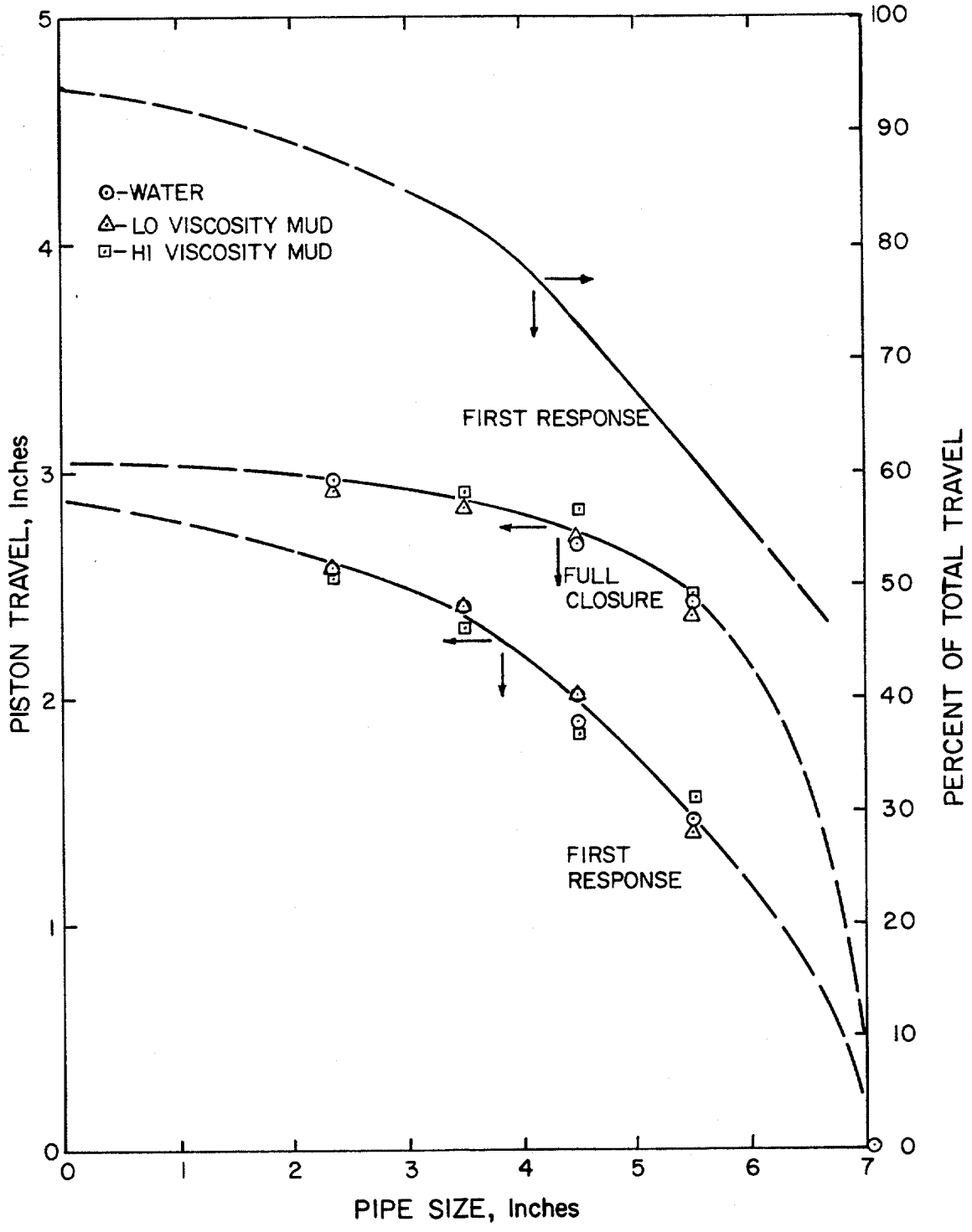

FIGURE 4.28. EFFECT OF PIPE SIZE ON THE CLOSING CHARACTERISTICS OF SPHERICAL BLOWOUT PREVENTER

CHAPTER V

CONCLUSIONS AND RECOMMENDATIONS

Based on the experimental results of this study the following conclusions can be made:

1. The restriction of flow through a spherical-type, annular blowout preventer during closure is negligible until the preventer is very near to being fully closed.
2. The rubber sealing element in the spherical blowout preventer cannot be treated as a rigid orifice for pressure drop - flow rate calculations. For a given piston position, the element deforms to assume the least restrictive configuration for any given flow rate.
3. The rubber sealing element deforms slightly differently each time the element is exercised by opening or closing the blowout preventer.
4. The effect of fluid viscosity on the pressure drop - flow rate characteristics of the blowout preventer is negligible compared to the effects of the deformation characteristics of the rubber element.
5. The "effective" piston travel for the spherical blowout preventer (over which flow is actually restricted) is very short. It is on the order of 1/10 ths of an inch of piston travel.

6. The "effective" piston travel is a function of the size (O.D.) of pipe in the hole. Large diameter pipes show a longer effective piston travel (both in terms of actual inches of travel and in terms of percentage of total piston travel) than small diameter pipes.
7. The valve coefficient, C_v, is not constant for a given partial closure of the blowout preventer (piston position). The valve coefficient, C_v, is also a function of the flow rate.

As stated previously, this work is part of an ongoing research effort to develop improved shut-in procedures for use in deep-sea drilling. In regard to the continuation of the research begun in this study the following recommendations are made:

1. The effect of fluid density on the pressure drop - flow rate characteristics of the spherical blowout preventer should be determined using the same experimental procedures developed for this study.
2. The characteristics of the hydraulic accumulator system, and associated control lines, should be studied in order to fully define the boundary condition at the blowout preventer as a function of time.
3. A computer model should be developed to simulate the transient behavior of a wellbore during shut-in, for use in evaluating various shut-in procedures.

The Methods of Characteristics should be used in the model to solve the differential equations of continuity and motion.

4. Actual measurements of the magnitude and propagation effects of pressure surges produced by shut-in should be made using the L.S.U. Blowout Prevention Training Well.

REFERENCES

1. Allievi, L.: Theory of Water-Hammer, translated by E.E. Halmos, Printed by Riccardo Garoni, Rome, Italy (1925).

2. Beggs, J. P. and Brill, H. D.: Two-Phase Flow in Pipes, 34d ed., The University of Tulsa (1978).

3. Bell, F. S.: "High Pressure Drilling and Blowout Preventers," Oil and Gas Journal (October 14, 1937) 139.

4. BLH Electronics: "5200 Transducer Conditioner - Operating and Service Manual."

5. Bourgoyne, A. T., Jr.: "A Proposal for the Expansion of the LSU-IADC Blowout Prevention Training Center," Louisiana State University, Petroleum Engineering Department (1979).

6. Crane Company: "Flow of Fluids through Valves, Fittings, and Pipes," Technical Paper No. 410 (1970).

7. Daugherty, R. L. and Ingersoll, A. C.: Fluid Mechanics with Engineering Applications, McGraw - Hill Book Company, Inc., New York (1954).

8. Glover, R. E.: "Computation of Water-Hammer in Compound Pipes," Symposium on Waterhammer, ASME - ASCE (1933) 64-71.

9. Halliburton Services, Inc: "Fracrecorder Manual."

10. Halliburton Services, Inc.: Personal Communications.

11. Hise, B. R., et al.: Blowout Prevention, Louisiana State University, Petroleum Engineering Department (1978).

12. Joukovsky, N.: "Water Hammer," translated by O. Simin, Proceedings of American Water Works Association, Vol. 24 (1904) 341-424.

13. McKenzie, M. F.: "Factors Affecting Surface Casing Pressures During Well Control Operations," M. S. Thesis, Louisiana State University, Baton Rouge (1974).

14. Moody, L. F.: "Simplified Derivation of Water-Hammer Formula," Symposium on Waterhammer, ASME - ASCE (1933) 25-28.

15. N. L. Shaffer Company: Personal Communications.

16. N. L. Shaffer Company: "Preventive Maintenance Program for Spherical Blowout Preventers (With 5000 psi and Less Working Pressure)," RP-688S-1M-778.

17. O'Brien, T. B. and Goins, W. C.: "The Mechanics of Blowouts and How to Control Them," API Drilling and Production Practice (1960) 41.

18. Parmakien, J.: Waterhammer Analysis, Prentice - Hall, Inc., New York (1955).

19. Pool, E. B.: "Friction Area and Nozzle Area for Valves and Fittings as New All - Purpose Flow Parameter," Flow Line, Rockwell International.

20. Rich, G. R.: Hydraulic Transients, McGraw - Hill Book Company, Inc., New York (1951).

21. Rucker Shaffer Company: "Spherical Blowout Preventer," RP-1295-5M-871.

22. Streeter, V. L.: Fluid Mechanics, 2nd ed., McGraw - Hill Book Company, Inc., New York (1958).

23. Streeter, V. L. and Wiley, E. B.: Fluid Mechanics, 6th ed., McGraw - Hill Book Company, Inc., New York (1975).

24. Streeter, V. L. and Wiley, E. B.: Hydraulic Transients, McGraw - Hill Book Company, Inc., New York (1967).

25. Teledyne - Taber Company: "Model 2204 Bonded Strain Gage Pressure Transducer," Bulletin 2204-76.

APPENDIX

EXPERIMENTAL DATA

An explanation of the comments used in the data tables in this Appendix is given below.

a. Blowout preventer fully open.

b. Pressure rising and flow rate dropping rapidly - indicates preventer element beginning to seal due to well pressure.

c. Data remeasured for verification.

d. Flow rate not stabilized - beginning to drop.

e. Element sealed to flow.

f. Blowout preventer fully closed with well pressure of about 2000 psi applied below preventer.

g. Blowout preventer fully closed with no well pressure applied.

Table A-1 Experimental Pressure Drop Data

(2 3/8 inch Pipe - Drilling Fluid 1)

Piston Travel, inches	Flow Rate, gpm	Pressure Drop, psi	Comments
0.000	55	2	a
	105	3	
	160	3	
2.496	62	3	
	99	4	
	115	6	
	183	9	
2.593	60	12	
	93	32	
	110	47	
	131	70	
	180	136	
2.643	60	64	
	83	122	
	95	170	
	114	220	
	136	250	
	155	275	
	174	295	
2.683	46	155	
	62	240	
	83	305	
	101	335	
	115	360	
	137	395	
	164	425	
2.723	37	270	
	48	340	
	64	405	
	83	450	
	99	500	
	118	520	
	128	545	
	143	600	
	149	615	

Table A-1 (Continued)

Piston Travel, inches	Flow Rate, gpm	Pressure Drop, psi	Comments
2.753	49	470	
	62	565	
	80	625	
	98	700	
	115	730	
	127	760	
	142	810	
2.773	47	545	
	63	700	
	79	805	
	97	920	
	113	1000	
	126	1060	
2.803	49	1080	
	58	1225	
	68	1490	
	79	1640	
2.888	-	-	e
2.961	-	-	g

Table A-2 Experimental Pressure Drop Data

(2 3/8 inch Pipe - Drilling Fluid 2)

Piston Travel, inches	Flow Rate, gpm	Pressure Drop, psi	Comments
2.571	74	24	
	80	29	
	98	45	
	107	55	
	120	67	
	131	77	
	147	92	
	160	105	
	173	124	
	182	131	
2.651	62	155	
	70	190	
	82	205	
	91	228	
	107	253	
	133	265	
	144	310	
	152	325	
	168	345	
2.700	54	260	
	64	300	
	75	330	
	91	370	
	107	410	
	118	435	
	130	455	
	136	465	
	144	480	
	163	505	
2.750	35	335	
	41	380	
	53	440	
	66	510	
	80	510	
	98	635	
	115	685	
	128	735	
	143	780	
	147	785	

Table A-2 (Continued)

Piston Travel, inches	Flow Rate, gpm	Pressure Drop, psi	Comments
2.775	25	435	
	27	420	
	40	445	
	51	630	
	64	720	
	80	810	
	90	870	
	106	940	
	115	965	
	131	1030	
2.830	27	640	
	38	820	
	50	900	
	64	990	
	66	1005	
	80	1110	
	83	1150	
	96	1240	b,d
	34	785	c
	37	815	c
	51	910	c
	75	1025	c
2.820	38	1150	
	48	1235	
	58	1330	b,d
	59	1350	b,d
	80	1545	b,d
2.909	-	-	e
2.939	-	-	f

Table A-3 Experimental Pressure Drop Data

(2 3/8 inch Pipe - Drilling Fluid 6)

Piston Travel, inches	Flow Rate, gpm	Pressure Drop, psi	Comments
2.543	50	12	
	80	18	
	100	22	
	120	30	
	143	38	
	170	50	
	205	65	
2.650	50	98	
	58	125	
	68	158	
	83	184	
	115	226	
	140	264	
	177	300	
	192	325	
2.700	47	215	
	66	280	
	84	325	
	97	350	
	112	370	
	122	390	
	135	410	
	148	435	
	173	475	
	190	500	
2.750	54	475	
	63	515	
	73	560	
	95	620	
	114	670	
	134	725	
	148	760	
	161	810	
	173	860	
2.775	50	680	
	54	725	
	64	800	
	77	880	
	92	975	
	100	1000	
	107	1125	b,d

Table A-3 (Continued)

Piston Travel, inches	Flow Rate, gpm	Pressure Drop, psi	Comments
2.800	28	955	
	34	1015	
	40	1060	
	48	1115	
	56	1240	b,d
2.825	31	1450	d
	36	1495	d
	41	1610	b,d
	50	1800	b,d

Table A-4 Experimental Pressure Drop Data

(3 1/2 inch Pipe - Drilling Fluid 1)

Piston Travel, inches	Flow Rate, gpm	Pressure Drop, psi	Comments
0.000	0	0	a
	56	0	
	110	1	
	168	2	
	196	2	
2.300	53	1	
	98	5	
	116	6	
	123	7	
	127	8	
	133	9	
	146	11	
	158	13	
	183	17	
	195	19	
2.400	32	4	
	40	7	
	46	10	
	62	19	
	87	45	
	101	60	
	121	80	
	152	105	
	189	140	
2.500	31	105	
	42	145	
	52	170	
	64	190	
	76	210	
	91	225	
	124	260	
	140	280	
	171	305	
	180	310	
2.600	23	250	
	43	305	
	73	390	
	87	410	
	101	435	
	115	450	

Table A-4 (Continued)

Piston Travel, inches	Flow Rate, gpm	Pressure Drop, psi	Comments
2.600	141	495	
	159	525	
	168	530	
2.650	21	370	
	26	395	
	32	420	
	43	460	
	56	485	
	77	565	
	94	590	
	109	655	
	127	740	
	149	815	
2.700	17	480	
	28	545	
	34	570	
	46	625	
	62	705	
	74	790	
	85	860	
	102	935	
	125	1085	
	129	1155	
2.755	13	580	
	20	640	
	22	660	
	32	740	
	43	820	
	51	880	
	62	985	b,d
	72	1130	b,d
	77	1260	b,d
	83	1500	b,d
	96	1765	b,d
2.800	-	-	d
2.869	-	-	e
2.914	-	-	f

Table A-5 Experimental Pressure Drop Data

(3 1/2 inch Pipe - Drilling Fluid 3)

Piston Travel, inches	Flow Rate, gpm	Pressure Drop, psi	Comments
0.000	54	0	a
	112	1	
	155	2	
	197	2	
2.300	54	3	
	106	10	
	122	15	
	147	25	
	159	35	
	180	45	
	195	50	
2.400	31	20	
	40	35	
	56	50	
	69	70	
	80	90	
	113	130	
	120	140	
	140	165	
	150	180	
	168	190	
	189	195	
2.500	28	140	
	35	165	
	40	170	
	50	195	
	60	220	
	77	245	
	97	265	
	100	275	
	120	295	
	139	310	
	165	325	
	178	340	
2.600	22	330	
	30	350	
	41	385	
	50	400	
	60	415	
	75	440	

Table A-5 (Continued)

Piston Travel, inches	Flow Rate, gpm	Pressure Drop, psi	Comments
2.600	87	455	
	103	480	
	125	505	
	150	530	
	164	555	
2.650	16	430	
	23	465	
	40	495	
	60	535	
	80	570	
	91	605	
	107	640	
	125	695	
	141	735	
	152	770	
2.700	12	560	
	17	600	
	25	635	
	37	685	
	45	710	
	50	730	
	62	775	
	82	815	
	90	885	
	105	1140	b,d
	47	780	c
	80	825	c
	100	930	c
2.750	79	1450	b,d
2.845	-	-	e
2.910	-	-	f
3.126	-	-	g

Table A-6 Experimental Pressure Drop Data

(3 1/2 inch Pipe - Drilling Fluid 7)

Piston Travel, inches	Flow Rate, gpm	Pressure Drop, psi	Comments
0.000	20	0	a
	47	1	
	87	1	
	119	2	
	161	2	
	187	3	
2.250	37	2	
	59	3	
	73	4	
	86	6	
	117	10	
	151	18	
	175	30	
	184	40	
2.400	39	65	
	52	113	
	64	133	
	83	155	
	106	175	
	118	195	
	139	200	
	160	220	
	178	235	
2.500	24	255	
	41	335	
	52	340	
	71	350	
	87	380	
	105	390	
	127	425	
	139	440	
	167	470	
	138	460	c
	105	420	c
2.600	16	560	
	33	615	
	45	650	
	61	675	
	88	735	
	118	835	
	133	925	

Table A-6 (Continued)

Piston Travel, inches	Flow Rate, gpm	Pressure Drop, psi	Comments
2.600	138	960	
	151	735	c
	137	715	c
	119	680	c
	88	640	c
	62	600	c
	43	570	c
2.650	33	840	
	49	915	
	62	990	
	83	1080	
	98	1150	
	98	1135	c
	118	1215	
	102	1095	c
	83	1020	c
	56	890	c
	122	1200	c
2.685	35	1400	
	48	1500	
	60	1580	
	70	1640	
	85	1760	b,d
2.710	-	-	d
2.745	-	-	e
2.914	-	-	f
3.075	-	-	g

Table A-7 Experimental Pressure Drop Data

(4 1/2 inch Pipe - Drilling Fluid 1)

Piston Travel, inches	Flow Rate, gpm	Pressure Drop, psi	Comments
0.000	0	2	a
	64	4	
	106	3	
	129	5	
	140	5	
1.886	54	60	
	95	95	
	119	115	
	143	130	
	183	145	
2.058	40	210	
	79	240	
	110	255	
	142	265	
	176	285	
2.256	15	490	
	37	515	
	81	570	
	113	605	
	145	625	
	157	630	
2.356	36	880	
	39	925	
	63	1040	
	83	1195	
	95	1230	
	104	-	b,d
2.669	-	-	g

Table A-8 Experimental Pressure Drop Data

(4 1/2 inch Pipe - Drilling Fluid 4)

Piston Travel, inches	Flow Rate, gpm	Pressure Drop, psi	Comments
0.000	0	0	a
	64	1	
	137	3	
	174	6	
1.621	64	1	
	126	3	
	173	6	
1.894	65	2	
	117	7	
	160	13	
2.026	66	110	
	97	138	
	126	153	
	160	168	
2.162	31	278	
	61	318	
	97	338	
	133	353	
	160	375	
2.298	51	563	
	65	628	
	97	692	
	120	736	
	146	773	
2.701	-	-	g

Table A-9 Experimental Pressure Drop Data

(4 1/2 inch Pipe - Drilling Fluid 8)

Piston Travel, inches	Flow Rate, gpm	Pressure Drop, psi	Comments
0.000	91	1	a
	120	1	
	161	2	
	211	2	
1.850	45	8	
	88	25	
	116	32	
	138	44	
	161	47	
	170	57	
	191	66	
	210	72	
1.900	50	30	
	85	49	
	104	62	
	123	72	
	138	85	
	160	96	
	174	107	
	205	122	
2.100	46	196	
	51	209	
	66	222	
	80	232	
	99	253	
	128	255	
	147	260	
	174	275	
	180	280	
2.250	23	360	
	41	390	
	60	410	
	80	425	
	88	430	
	117	450	
	133	465	
	155	475	
	168	485	

Table A-9 (Continued)

Piston Travel, inches	Flow Rate, gpm	Pressure Drop, psi	Comments
2.350	16	560	
	38	595	
	55	625	
	68	640	
	100	680	
	110	695	
	127	718	
	144	745	
	152	760	
2.400	14	770	
	32	820	
	46	865	
	63	900	
	77	940	
	42	805	c
	86	955	
	107	1020	
	131	1090	
2.450	-	-	b,d
2.460	-	-	e
2.829	-	-	f

Table A-10 Experimental Pressure Drop Data

(5 1/2 inch Pipe - Drilling Fluid 1)

Piston Travel, inches	Flow Rate, gpm	Pressure Drop, psi	Comments
0.000	0	0	a
	48	1	
	88	1	
	119	1	
	151	2	
	186	3	
1.450	0	1	
	50	4	
	75	10	
	94	15	
	123	25	
	136	30	
	163	35	
	188	45	
1.600	40	80	
	78	100	
	90	110	
	103	110	
	126	120	
	147	125	
	166	130	
	185	135	
1.804	31	170	
	39	185	
	81	210	
	110	220	
	127	230	
	155	235	
	176	245	
2.004	24	285	
	40	315	
	57	340	
	82	360	
	102	375	
	120	390	
	144	405	
	170	415	

Table A-10 (Continued)

Piston Travel, inches	Flow Rate, gpm	Pressure Drop, psi	Comments
2.150	17	485	
	37	545	
	44	560	
	62	605	
	83	650	
	101	680	
	137	745	
	147	765	
2.200	25	645	
	32	695	
	51	770	
	71	870	
	77	875	
	90	930	
	107	985	
	115	1010	
	131	1040	
2.250	15	850	
	23	960	
	28	1030	
	36	1095	
	48	1165	
	60	1265	
	71	1315	
	87	1390	
	101	1520	b,d
2.451	-	-	e
2.551	-	-	g

Table A-11 Experimental Pressure Drop Data

(5 1/2 inch Pipe - Drilling Fluid 5)

Piston Travel, inches	Flow Rate, gpm	Pressure Drop, psi	Comments
0.000	0	0	a
	57	1	
	80	2	
	124	3	
	151	4	
	195	5	
1.415	0	1	
	53	25	
	67	30	
	91	40	
	129	50	
	142	60	
	159	65	
	189	70	
1.600	29	140	
	37	145	
	47	155	
	59	160	
	90	170	
	113	175	
	134	185	
	155	190	
	186	195	
1.800	22	270	
	40	280	
	62	295	
	76	300	
	90	310	
	101	315	
	120	320	
	146	330	
	168	340	
	178	342	
2.200	-	380	
	27	510	
	42	560	
	61	580	
	79	590	
	93	600	
	111	610	

Table A-11 (Continued)

Piston Travel, inches	Flow Rate, gpm	Pressure Drop, psi	Comments
2.200	141	635	
	156	640	
	158	630	
2.104	-	570	
	24	715	
	45	770	
	58	805	
	78	840	
	85	840	
	100	875	
	113	895	
	140	930	
2.150	20	840	
	29	910	
	35	945	
	45	1000	
	55	1040	
	70	1080	
	73	1095	
	90	1140	
	106	1190	
	122	1235	
2.175	-	-	b,c,d
2.384	-	-	f

Table A-12 Experimental Pressure Drop Data

(5 1/2 inch Pipe - Drilling Fluid 9)

Piston Travel, inches	Flow Rate, gpm	Pressure Drop, psi	Comments
0.000	0	2	a
	48	5	
	61	7	
	95	8	
	133	9	
	156	9	
	189	11	
1.550	26	100	
	34	120	
	50	130	
	68	145	
	88	155	
	103	160	
	125	165	
	140	170	
	165	175	
	175	180	
1.853	22	300	
	44	325	
	61	335	
	82	350	
	102	360	
	118	365	
	147	375	
	172	380	
1.950	18	415	
	42	445	
	56	455	
	72	460	
	94	475	
	113	490	
	135	505	
	164	520	
2.050	14	555	
	28	575	
	49	615	
	64	635	
	83	640	
	92	660	
	115	690	

Table A-12 (Continued)

Piston Travel, inches	Flow Rate, gpm	Pressure Drop, psi	Comments
2.050	144	715	
	150	720	
2.150	-	760	
	30	900	
	38	940	
	51	1000	
	65	1060	
	80	1075	
	105	1185	
	117	1210	
	118	1250	
2.200	-	1150	
	13	1395	
	27	1570	
	34	1725	
	48	1810	
	54	1840	
	69	1940	b,d
2.250	-	1504	b,d
2.507	-	-	g

VITA

Raymond Scott Doyle was born on October 2, 1957 in Baton Rouge, Louisiana. He attended Catholic High School in Baton Rouge, and graduated from there in May of 1975. In August of the same year, Scott entered Louisiana State University, and received a Bachelor of Science degree in Petroleum Engineering in December of 1979. He immediately entered the Graduate School at Louisiana State University and is now a candidate for the Master of Science degree in Petroleum Engineering. Scott is married to the former Kimberly Anne Thomas, a native of New Orleans, Louisiana.